TRANSPORTATION RESEARCH BOARD
NATIONAL RESEARCH COUNCIL

IDEA

Innovations Deserving Exploratory Analysis Project

NATIONAL COOPERATIVE HIGHWAY RESEARCH PROGRAM

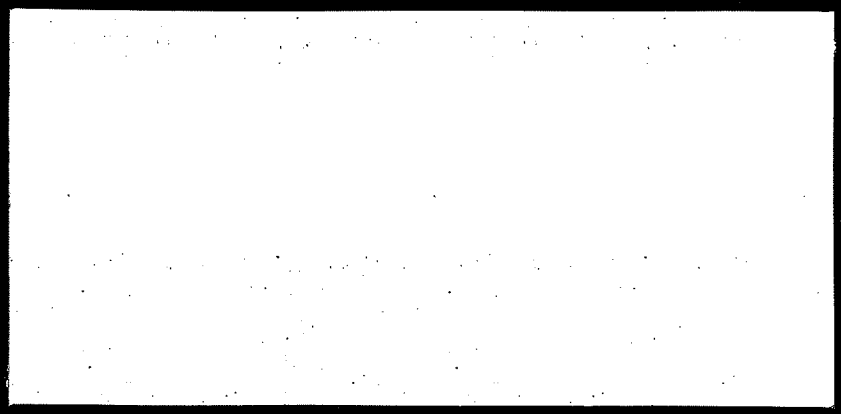

Report of Investigation

IDEA PROJECT FINAL REPORT

Contract NCHRP-33

IDEA Program
Transportation Research Board
National Research Council

June 1999

EVALUATION OF A NEW REHABILITATION TECHNOLOGY FOR BRIDGE PIERS WITH COMPOSITE MATERIALS

Prepared by:
Roberto Lopez-Anido, Rakesh Gupta, Hota V.S. Gangarao, Udaya B. Halabe, Sachin Kshirsagar and Reynold Franklin
West Virginia University

INNOVATIONS DESERVING EXPLORATORY ANALYSIS (IDEA) PROGRAMS
MANAGED BY THE TRANSPORTATION RESEARCH BOARD (TRB)

This NCHRP-IDEA investigation was completed as part of the National Cooperative Highway Research Program (NCHRP). The NCHRP-IDEA program is one of the four IDEA programs managed by the Transportation Research Board (TRB) to foster innovations in highway and intermodal surface transportation systems. The other three IDEA program areas are Transit-IDEA, which focuses on products and results for transit practice, in support of the Transit Cooperative Research Program (TCRP), Safety-IDEA, which focuses on motor carrier safety practice, in support of the Federal Motor Carrier Safety Administration and Federal Railroad Administration, and High Speed Rail-IDEA (HSR), which focuses on products and results for high speed rail practice, in support of the Federal Railroad Administration. The four IDEA program areas are integrated to promote the development and testing of nontraditional and innovative concepts, methods, and technologies for surface transportation systems.

For information on the IDEA Program contact IDEA Program, Transportation Research Board, 500 5th Street, N.W., Washington, D.C. 20001 (phone: 202/334-1461, fax: 202/334-3471, http://www.nationalacademies.org/trb/idea)

ACKNOWLEDGEMENTS

The work presented in this Report was conducted by the authors through the Constructed Facilities Center, College of Engineering and Mineral Resources, at West Virginia University.

The authors are grateful to Mr. Samer Petro, Ms. Sharon Santos and Ms. Eleanor Nevera for their technical and administrative assistance during the project. The authors are thankful to Mr. Paul Frum, Mr. David Turner, Mr. Dana Henderson and Mr. Jim Hall for their assistance in setting up the laboratory experiments. The authors are also thankful to Dr. Ever Barbero for facilitating access to the servo-hydraulic testing frame utilized to conduct the fiber composite coupon tensile experiments.

The authors want to thank the valuable suggestions from the panel of experts that have advised this project: Dr. Ravi Devalapura, Mr. Jack Justice and Mr. Robert Smith.

Finally, the authors want to acknowledge the active participation of West Virginia Department of Transportation, Division of Highways in the Pond Creek Bridge repair demonstration project.

TABLE OF CONTENTS

EXECUTIVE SUMMARY

Idea Product and Concept

An innovative repair method for deteriorated highway bridge piers has been under evaluation in order to establish long-term environmental protection, concrete confinement, and interfacial bond integrity. This repair method uses high-strength, non-corrosive fiber reinforced polymer composites bonded to concrete. Pier columns of a highway bridge that were in need of repair were rehabilitated using this fiber composite wrap system.

This IDEA Project aimed at examining the process and possible causes of damage due to harsh environmental conditions of concrete pier columns wrapped externally with glass/aramid fiber composites. Major emphasis was on evaluating long-term performance and durability of such a wrap system. The durability of a fiber composite wrap system, and the bond between the composite material and concrete were studied in order to establish the protection levels and confinement of concrete under harsh environments, freeze-thaw effects, and moisture seepage. A non-destructive evaluation (NDE) method using an ultrasonic pulse generator was applied to concrete cylinders to detect delaminations and property degradation of the fiber composite wrap system. The basic concept of the IDEA Project was to go from an "innovative repairing art" into sound engineering science and practice. The IDEA Project has potential to lead to a viable rehabilitation method that will provide a durable and economic alternative to conventional repair.

Project Results

The objective of this research was to investigate the durability of glass/aramid-epoxy composite material for rehabilitation of concrete bridge piers. Standard concrete cylinders wrapped with glass/polyaramid woven fabric wetted with an epoxy resin matrix were utilized as experimental specimens. The wet lay-up method was used to wrap the concrete cylinders, where the epoxy resin served the dual purpose of adhesive for bonding to the concrete substrate and matrix binder for the reinforcing fibers. Specimens were subjected to six different accelerated aging conditions: (1) pH 9.4, 73°F; (2) pH 12.4, 73°F; (3) pH 12.4, 150°F; (4) pH 7.0, 150°F; (5) Dry Heat at 150°F; and (6) Extended Freeze-thaw Cycles with 100% RH. Compression experiments of concrete wrapped specimens were conducted to establish changes in ultimate strength and ultimate strain after exposure to 1000, 3000 and 8000 hrs of accelerated aging. Compression experiments were also conducted using concrete cylinders wrapped with different number of reinforcing layers to evaluate the confining effects of higher wrap thickness on the strength and ultimate strains. Tension experiments of fiber composite coupons after accelerated aging were conducted to establish degradation in mechanical properties. Dynamic mechanical thermal analysis (DMTA) was also conducted to evaluate the effect of accelerated aging on properties such as the glass transition temperature and the modulus.

A bi-linear stress-strain model was developed to predict the ultimate strength and ultimate strain of standard wrapped concrete cylinders under compression. The bi-linear model was further extended to incorporate changes in properties of the composite wrap after aging. The damage model thus obtained attempted to estimate the residual strength and ductility of the wrapped concrete cylinders after aging based on the properties obtained from the fiber composite material tension experiments. Estimated values from the stress-strain model were correlated with the experimental results.

Aging studies on wrapped cylinders indicated that the ultimate strength and ultimate strain of the specimens were considerably reduced when exposed to pH 12.4 solution at 150°F and water at 150°F after 1000 hrs of aging. Specimens exposed to extended freeze-thaw cycles also experienced similar reduction in strength and ductility after 3000 hrs of aging. The tensile strength of the fiber composite coupons was significantly reduced when aged in pH 12.4 solution at 150 F for 1500 hrs; this suggested that the composite became brittle upon aging. As a result of moisture absorption, a split in tan δ curve was indicated for the DMTA test specimens during the temperature sweep experiments.

It was found that the fiber composite wrap enhanced the strength and ductility of concrete specimens. These properties were retained throughout the aging period when exposed to dry heat or moisture at ambient temperature suggesting that the composite material did not degrade under these conditions. However, exposure to moisture at high temperature was the most critical factor in reducing the compressive strength of the concrete specimens. The reason for this decrease in compressive strength was explained mainly due to degradation in tensile strength of the composite wrap.

An ultrasonic testing method capable of assessing structural integrity of FRP wrapped concrete compression members was developed. This ultrasonic testing methodology identified regions of material degradation based on simple parameters such as peak magnitude, area, and third moment of the power spectral density (PSD) curve. Logarithmic regression analysis showed that the area under PSD curve is directly related to the member behavior. Good correlation was obtained between the ultrasonic signal energy and the ultimate compressive strength and hoop strain. A model was proposed to predict the ultimate compressive stress and ultimate hoop strain from the received ultrasonic signal energy. The proposed methodology can be used for long-term performance monitoring of FRP bonded systems in the field. It should be noted that uniformity in testing condition and equipment is of utmost importance for consistent ultrasonic signal energy measurements. Also, field monitoring may impose additional difficulties such as larger dimensions and presence of steel reinforcement.

Product Payoff

The concrete repair system evaluated consist of a fiber composite wrap applied by wet lay-up, which is commercialized by Fyfe Co. L.L.C. of San Diego, CA with the trade name Fibrwrap™ system. In this system, the fiber sheet (fabric) is presaturated in a specially formulated epoxy resin, and then is wrapped around a concrete column like applying wall paper. The system can be applied in the following rehabilitation situations: seismic retrofit, repair, defects in design, defects in workmanship, and environmental protection. The system has been used to repair concrete bridge pier columns, pier caps, pier walls, beams, and piles. The fiber material is a hybrid of E-glass and aramid called SEH-51 (Knytex). The fibers are supplied as a woven fabric sheet. The fiber reinforcement is mainly placed around the column in the hoop direction. The resin material is a two-part epoxy called Tyfo S. The installation process is simple and fast, and does not require expensive equipment. The advantages of this process are resin cure at ambient temperature, flexibility of the wrap system and ease to use in restricted areas. The main issues of concern in this repair system are quality control of the resin mix, wet-out of the fabric, uniformity of the resin distribution, compaction and fiber wrinkling, and control of resin cure. The fiber composite wrap system has the following cost benefits: (1) reduction in installation time as compared to conventional repair methods; (2) increase in shear/flexural strength and ductility of piers and columns; (3) long service life; and reduction in maintenance cost.

Product Transfer

A bridge in need of column repair was selected by West Virginia Department of Transportation, Division of Highways (WVDOT-DOH) to demonstrate the IDEA Product. The subject bridge is the Pond Creek Road Overpass Bridge carrying Interstate Route 77 in Wood County, West Virginia. According to the WVDOT-DOH Condition Report, six columns of two piers had vertical hairline cracking. These cracks resulted from a previous unsuccessful repair with a concrete layer after the columns were subjected to fire and the original concrete cover was lost. Three columns of the Pier 2 of the Bridge Northbound were repaired in July 1998 with the fiber composite wrap system evaluated through the IDEA Project. The other three columns were repaired with an alternative rehabilitation method using prefabricated composite cylindrical shells. The field performance of the repaired concrete columns was monitored during the first year after installation and the results were satisfactory.

Application of fiber composite wrap in Pond Creek Bridge

Pier concrete column after wrapping

CHAPTER 1 - IDEA PRODUCT

BACKGROUND

Structural engineers are faced with problems of repairing deteriorated highway bridges. In the United States, the need to repair the Civil Infrastructure is well documented. The Federal Highway Administration has recently reported that nearly 32% of the Nation's 581,942 bridges need to be repaired or replaced. The U.S. Navy is another example of an organization with a substantial need of concrete structures repair. According to a survey, conducted by the U.S. Naval Facilities Engineering Services Center (NFESC) in Port Hueneme, CA, as cited by Busel and Barno (1996), 75% of its 582 concrete waterfront piers and wharves will require some form of repair or remediation over the next 5 to 8 years. It is also stated that upgrade of 50 % of these piers with fiber reinforced polymer (FRP) composites would represent $200 million worth of concrete repair for the Navy alone.

Composite materials mostly applied in the aviation industry, are now finding other industrial applications including civil infrastructure renewal. FRP material systems composed of continuous fibers embedded in a polymeric matrix exhibit physico-mechanical properties that are desirable for use as structural reinforcement for concrete. FRP composites have directional properties, e.g. high tensile strength in the fiber direction, that can be tailored for specific concrete repair applications. For example, proper external wrapping of a concrete column with fiber reinforcement in a resin matrix would provide external confinement leading to strength and ductile increases. Also fiber reinforced composites provide a cost-effective alternative towards the rehabilitation and maintenance of bridges, because of their non-corrosiveness, high strength-to-weight ratio and ease of installation. However, lack of understanding of durability of composites under harsh environments is a major concern.

Traditional Methods of Concrete Repair

Rehabilitation of concrete piers supporting bridge decks may be carried out by external application of concrete over the deteriorated surface. The concrete may be kept in place using steel reinforcement, which is normally in the form of a wire mesh. Deterioration of concrete and exposure of the steel reinforcement to moisture, which in turn causes corrosion, is a major concern in the application of this technique.

Another method of concrete repair is bonding a steel plate to the tension flange of the beam, thereby increasing both strength and stiffness (Karbhari and Engineer, 1996). Influence of several factors such as plate thickness, type of adhesive, and the anchoring conditions on the performance of such a system have been investigated. The primary disadvantage of steel plate bonding has being installation difficulties due to self-weight. The length restriction often necessitates the use of joints, which need special attention in design since field welding may lead to deterioration of the bond to the concrete substrate. Moreover, corrosion of steel plates may lead to debonding at the interface of steel and concrete. Some of these limitations of steel plates/jackets based rehabilitation techniques have led for alternative techniques such as rehabilitation with fiber composite encasing.

Fiber Composite Wrapping

In the rehabilitation method proposed, concrete piers were externally wrapped with glass-aramid fabric wet in an epoxy resin matrix. In the presence of a vertical compressive load, the concrete column tends to expand in the lateral direction. In the case of wrapped concrete columns, confinement actually helps the concrete column to sustain higher loads since the fibers in the hoop direction prevent this expansion of the concrete.

Improvement of mechanical properties due to externally bonded reinforced composite stems from the development of a triaxial stress field within the confined concrete through the restraint of transverse dilation. This type of repair is has been proposed to enhance the seismic resistance of bridge columns. The matrix serves a dual purpose of protecting both the concrete and the fibers from direct environmental attack, and it also acts as an adhesive that forms a bond between the concrete and the fiber reinforcement.

Current Efforts Using Composites for Concrete Repair

A number of qualification programs have focused on understanding the technical needs and cost-related issues of using FRP composites for rehabilitation of concrete. The Composites Institute (CI) and the U.S. Army Corps of Engineers Construction Engineering Research Laboratories (USACERL), Champaign, IL, cooperated on a Construction Productivity Advancement Research (CPAR) project to develop and demonstrate FRP composite materials systems for the repair of reinforced concrete structures. The CPAR project was involved in investigating different methods of concrete repair with various composite materials systems that were available. The emphasis was in designing and defining a specific FRP composite system for a particular repair or upgrade (Busel and Barno, 1996).

In an another initiative, the State of California's Department of Transportation (CALTRANS) has been working with the Society of Advanced Materials and Process Engineers (SAMPE) and the Aerospace Corporation to qualify composite materials systems for seismic retrofit of reinforced concrete structures, including bridge columns (Hawkins et al., 1998). CALTRANS effort has been to set-up materials performance specifications and design recommendations that would apply to concrete column retrofit with fiber composites (Busel and Barno, 1996).

IDEA PRODUCT

The IDEA product presented herein studied a novel application of composite materials technology for the rehabilitation of bridge columns. Lack of understanding of durability of fiber composite wraps over concrete does not allow ready acceptance of this rehabilitation method

The aims of this IDEA product are to answer the following questions:

1. *How efficient is the fiber composite rehabilitation technology to repair concrete columns?*
2. *How to evaluate the long-term performance (durability) of composite wraps with concrete substrate under harsh environments?*
3. *What degradation mechanisms developed in concrete elements wrapped with fiber composites in the presence of harsh environments?*
4. *How to model the non-linear stress-strain response of FRP wrapped concrete elements under compression loading?*
5. *What time-dependent factors govern the column compression response under harsh environments?*
6. *How to monitor the health of the fiber composite wrap bonded to concrete using non-destructive evaluation methods?*

Through this IDEA project, this rehabilitation technique was applied to repair three columns of a bridge in West Virginia. West Virginia Division of Highways (WVDOH) selected the Pond Creek Road Overpass Bridge (near Parkersburg, WV) for this purpose.

CHAPTER 2 – CONCEPT AND INNOVATION

MATERIALS SELECTION

The constituents of a composite material consist of two or more distinct phases, one of which, the fibers are embedded in a continuous matrix phase. Fiber reinforced composites contains filaments made of glass, aramid, or carbon embedded in a resin matrix. The fibers are the primary load carrying elements within the composite. The matrix binds the fibers together and transfers load between fibers. The matrix also protects the fibers from environmental attack and damage due to handling. The fibers have a strong influence on the mechanical properties of the composite, such as strength, elastic modulus and deformation properties.

Fibers

Fibers are the principal constituent in a fiber-reinforced composite. They bear most of the load acting on a composite. Proper selection of the type, amount and orientation of the fibers is very important, since it influences the following characteristics of a composite:

- Specific gravity
- Tensile strength and modulus
- Compressive strength and modulus
- Shear strength and modulus.
- Fatigue strength as well as fatigue failure mechanisms
- Electrical and thermal conductivity
- Cost

Glass, carbon and aramid fibers are commonly used in fiber reinforced polymer composites. The following discussion gives a brief description of all the three listing out the major advantages and disadvantages of the various types, which will help in selecting the proper type.

Glass fibers

Glass fibers are the most common of all the reinforcing fibers for polymer matrix composites. Principal advantages of the glass fibers are low cost, high strength, good chemical resistance and insulating properties. Fiberglass fabric is among the various forms of glass fibers that are commercially available, and it is very versatile for seismic retrofit applications. Major disadvantages are low tensile modulus, relatively high specific gravity, sensitivity to abrasion with handling, relatively low fatigue resistance and high hardness (which causes excessive wear on molding dies and cutting tools). Two types of glass fibers commonly used in the fiber-reinforced plastics industry are E-glass and S-glass. E-glass has the lowest cost of all the commercially available reinforcing fibers, which is the main reason for its widespread use in the FRP industry. S-glass was originally developed for aircraft components and missile casings for their highest tensile strength among all fibers in use (Mallick, 1993).

Carbon fibers

Two general sources for the commercial production of carbon fibers are synthetic fibers, similar to those used for making textiles, and pitch, which is obtained by the destructive distillation of coal or petroleum. The textile fiber polyacrylonitrile (PAN) is a synthetic polymer that is spun as a bundle of continuous filaments. In the process, the fibers are stretched so that their molecular chains are aligned parallel to the fiber axis. It is essential that this parallel orientation be preserved throughout the carbonization process. Carbon fibers are commercially available with a variety of tensile moduli ranging from 3×10^7 psi to 1.5×10^8 psi. Generally, the low-modulus fibers have lower specific gravity, lower cost, higher tensile and compressive strength and higher tensile strains-to-failure than the high modulus fibers. Among the advantages of carbon fibers are their exceptionally high tensile strength-to-weight as well as tensile modulus-to-weight ratios, very low coefficient of linear thermal expansion and high fatigue strengths. Principal disadvantages are their low impact resistance and high electrical conductivity, which may cause "shorting" in unprotected electrical machinery and high cost. Because of the cost factor, carbon fibers have been limited from widespread commercial applications. They are used mostly in the aerospace industry, where weight savings is considered more critical than cost (Mallick, 1993).

Aramid fiber

Aramid is short for aromatic amide; the DuPont trade name for the polymer is "Kevlar". In addition to the Kevlar^R used in the rubber industry, two variations of the fiber are manufactured for special applications. These are Kevlar 29^R and Kevlar 49^R. Kevlar 29^R is mainly used in woven and twisted forms for personnel protection, friction materials and woven fabrics for ropes and cables. This fabric is not suitable for reinforcement purposes, as the surface treatment applied is not compatible with most of the resin systems. As a reinforcement, Kevlar 49^R fibers are being used in many marine and aerospace applications where light weight, high tensile strength and resistance to impact damage are important. The major disadvantages of aramid fiber-reinforced composites are their low compressive strengths and difficulty in cutting or machining. They are also quite sensitive to UV light. Prolonged direct exposure to sunlight causes discoloration and significant loss in tensile strength. Besides, Kevlar 49^R fibers are hygroscopic and can absorb up to 6% moisture at 100% relative humidity (RH) and 23°C. The equilibrium moisture content is directly proportional to the RH and is attained in 16-36 hours. At high moisture content, the fibers tend to crack internally at pre existing microvoids and produce longitudinal splitting (Mallick, 1993). Typical mechanical properties of the various fibers are reported in Table 2.1 (Hollaway, 1990).

Table 2.1 Mechanical Properties of Fibers

PROPERTIES	E-GLASS	CARBON	KEVLAR
Density g/cc	2.56	1.95	1.45
Tensile strength, GPa (ksi)	1.5-2.5 (218-363 ksi)	2.0 (290 ksi)	2.7-3.5 (392-507 ksi)
Strain to failure (%)	1.8-3.0	0.5	2.0-2.7
Tensile modulus, GPa (psi)	70 (10 x 10^6 psi)	380 (55 x 10^6 psi)	120 (17 x 10^6 psi)
Coefficient of thermal expansion: 10^{-6}/ ^{0}C	5.0	-0.6 to –1.3	-2.0

Resins

All the component materials and their method of combination play an important role in determining the performance of a polymer composite. The contribution of the resin system is the most important factor in relation to the durability of the composite. The adverse effect of the environment on the fibers can be significantly decreased by application of a proper resin system. The resin serves as a medium for holding the fibers together, as a basis for shear load transfer and also as a protective binder for the fibers. Important resin systems used for composites: Polyesters, Epoxies, Vinyl Esters, Polyurethanes and Phenolics. Herein, we only discussed epoxy resins because they have been successfully used for concrete repair with fiber composites.

Epoxy Resins

A common starting material is Diglycidyl ether of bisphenol A (DGEBA), which contains two epoxide groups (3-membered rings of one oxygen atom and 2 carbon atoms), one at each end of the molecule. The polymerization reaction to transform the liquid resin to the solid state is initiated by adding small amounts of a reactive curing agent just prior to incorporating fibers into the liquid mix. One such curing agent is diehtylenetriamine (DETA). Curing time and temperature to complete the polymerization reaction depends on the type and amount of curing agent. With some curing agents, the curing reaction initiates and proceeds at room temperature, but with others, elevated temperatures are required. Epoxy matrix has the following advantages over the other thermoset matrices:

- Wide variety of properties because of availability of large number of starting materials, curing agents and modifiers.
- Absence of volatile matter during cure.
- Low shrinkage during cure.
- Excellent resistance to chemicals and solvents.
- Excellent adhesion to a wide variety of fillers, fibers and other substrates.

Principal disadvantages are its relatively high cost and long curing time (Mallick, 1993). Typical mechanical properties of resins are reported in Table 2.2 (Hollaway, 1990).

Table 2.2 Mechanical Properties of Resins

PROPERTIES	POLYESTER RESIN	EPOXY RESIN	PHENOLIC RESIN
Density (g/cc)	1.2 – 1.4	1.1 – 1.35	1.35 – 1.75
Tensile strength, MPa (ksi)	45–90 (6.5-13.0)	40–100 (5.8-14.5)	45 – 65 (6.5-9.4)
Compression strength, MPa (ksi)	100 – 250 (14.5-36.2)	100 – 200 (14.5-29.0)	
Modulus of Elasticity, Tension GPa, (ksi)	2.5 – 4.0 (362.5-580.1)	3.0 – 5.5 (435.1-797.7)	5.5 – 8.0 (797.7-1160.2)
Poisson's ratio	0.37 – 0.4	0.38 – 0.4	0.37 – 0.4
Coeff. of thermal expansion $10^{-6}/{}^0C$	100 – 120	45 – 65	30 - 45
Shrinkage on curing (%)	5 – 8	1 – 2	
Water absorption, 24hrs at 20 ^0C (%)	0.15 – 0.2	0.1 – 0.35	

LITERATURE REVIEW

The literature survey is organized into three parts. One aspect examines the performance of concrete columns wrapped with FRP composites, the second, looks at the effects of aging on such a structure, and the third, reviews the methods of composite repair. There are four separate regions to consider in evaluating the performance of these wrapped concrete columns when exposed to various environmental conditions. They are:

- Concrete substrate
- Concrete - FRP interface
- Fiber - matrix bond
- Fiber reinforced composite system

Performance of Wrapped Concrete Columns

Flexural behavior of earthquake damaged reinforced concrete columns when repaired with prefabricated fiber reinforced plastic wraps has been studied by others; the damaged column specimens were repaired with FRP composite wraps using unidirectional E-glass fibers in the form of a fabric saturated with a polyester resin matrix. This was done for circular as well as rectangular bridge columns. The specimens were tested to failure under simulated earthquake loading conditions, e.g., reversed inelastic cyclic loading, (Saadatmanesh et al., 1997). In an another study (Saadatmanesh et al., 1994), analytical work was performed on concrete columns strengthened with composite straps to illustrate the effectiveness of this method for rehabilitation.

Effects of wrapping concrete cylinders with composite materials were studied on concrete cylinders with dimensions 3" x 6", 4" x 8", and 6" x 12" diameter by height (Bavarian et al., 1996). Two different fiber/matrix systems were used in this experiment: S-glass embedded in polyester resin and Kevlar-29^R embedded in epoxy resin. The ultimate strength of the concrete cylinders without reinforcement was measured to be about 3.6 - 4.2 ksi with a strain of 0.5 - 0.6% at failure. It is interesting to note that the ultimate stress increased by nearly a factor of three when four layers of Kevlar-29^R were applied. The ductility was increased by a factor of five to six resulting in an ultimate strain of 3.5 - 4.0 % at failure. A compression test was also conducted on a previously failed 4" by 8" specimen wrapped again with two layers of fabric. This test revealed that the failed specimen had almost as much strength and more ductility than a fresh unwrapped sample. A composite column was proposed in which a filament-wound tubular shell served as a protective jacket and a confining member for concrete cylinders (Mirmiran et al., 1996). The composite tube was a multi-layer FRP shell consisting of two plies of FRP. This work concentrated on developing a new confinement model to explain the behavior of this system

under a compressive load. Compression tests conducted on 6" x 12" concrete cylinders confined inside a FRP tube showed that using a 3 mm thick jacket around the concrete could almost triple the strength of the cylinder. An increase in the axial strength of the column was observed as the jacket thickness increased, but this increase was not linearly proportional to the jacket thickness. Tests that were conducted to examine the effect of the winding angle suggested that the pure axial strength of the section decreased as the winding angle increased. This rate of decrease was less for smaller winding angles (0 to 15 degrees) and more for larger winding angles (45 to 60 degrees), which may be attributed to an inefficient confining pressure provided by the fibers with larger winding angles.

Aging Effects

This section examines the aging effects on the four possible regions mentioned earlier.

Concrete Substrate

The disintegration effects caused due to the following potential reasons markedly reduce the useful life of concrete (Troxell et al., 1968): weathering, reactive aggregates, sulfate waters, chemical corrosion and mechanical wear or abrasion. In severe climates, weathering is an important consideration. The most common accelerated aging test conducted to simulate the weathering effect is a freeze-thaw test. Deterioration of concrete upon freezing is caused by hydraulic pressure developed by the expansion of water when converted to ice, this expansion being about 9%. Thus, it is obvious that the higher the amount of water in the concrete the fewer the cycles of freezing and thawing required to disintegrate the mass.

Several types of aggregates such as opaline silica and siliceous limestones are known to react with high-alkali cement. Because of an increase in volume followed by this reaction (expansive reaction), random cracking and disintegration of concrete has been observed in many structures. These reactive aggregates in combination with high-alkali cement cause deterioration of concrete, hence weakening of the structure. The sulfates of sodium, potassium and magnesium present in alkali soils and waters are known to have caused deterioration of many concrete structures. The sulfates react chemically with the hydrated lime and hydrated calcium aluminate in the cement paste to form calcium aluminate, calcium sulfate and calcium sulfoaluminate respectively. These reactions are accompanied by a considerable expansion that causes disruption of concrete. The deposition of sulfate crystals on the pores of concrete also tends to disintegrate concrete. Concrete exposed to farm silage, animal wastes, and organic solids from various industries is sometimes damaged by surface corrosion.

The wear resistance of concrete is of importance in various types of concrete construction. For floors, pavements, and hydraulic structures as tunnels and dam spillways, the concrete should withstand destructive wearing forces that may include abrasion and impact. Cavitation effects especially have caused severe damage to several hydraulic structures. Under certain conditions of hydraulic flow where disturbances develop, a cavity will occur in the moving water, which eventually becomes severely pitted with continuous exposure to moving water.

Concrete - FRP Interface

Durability of the concrete-composite bond and the performance of the composite when exposed to different aging conditions have been investigated (Karbhari and Engineer, 1996). Experimental specimens consisting of composite plates adhered to concrete beams of dimensions 13" x 2" x 1" using a wet lay-up type procedure were used for this purpose. Two different resins were employed in the research to form the matrix for the composite, and their performance was compared. The specimens were tested in four point loading with composite plates on the tensile surface. The composite plates were subjected to different aging conditions where they were exposed to water at ambient temperature, sea-water, temperature of 4 ^{0}F, and a freeze-thaw cycle. Performance of the samples was analyzed on the basis of failure loads, deflection and flexural stiffness. Maximum deterioration was seen after immersion in fresh water and sea-water but there was very little change resulting from exposure to 4 ^{0}F. Debonding was observed at the concrete-resin interface and some damage to the bulk resin due to exposure to aqueous solutions. These tests added to Dynamic Mechanical Analysis conducted on neat resin suggested that the composite employing a resin with a higher glass transition temperature performed better than the one having a lower value.

A modified peel test was employed to investigate the durability of the bond between the concrete and the composite under different environmental exposure regimes (Karbhari et al., 1997). Concrete blocks of dimensions 9" x 6" x 1" were used over which the composite was laid using a wet lay-up procedure. Individual peel strips had a length of 12" and were 1" wide. E-glass and carbon fiber reinforcements were used in unidirectional form. The interfacial fracture energy, G,

and the phase angle of loading Ψ, characterized the fracture and crack propagation at the bi-material interface (concrete and the resin-composite system). It was reported that the effect of exposure to water resulted in a decrease in levels of peel force and also the interfacial fracture energy.

Fiber - Matrix Bond

Strength and failure mechanism of E-glass/epoxy laminates subjected to uniaxial and in-plane biaxial compression loading was studied (Wang and Socie, 1993). Unidirectional and cross-ply laminates were employed for both uniaxial and biaxial compressive strengths. Three distinct compressive failure modes were observed in this study. A material failure mode, which included matrix shear failure and fiber failure due to either microshear or bending; delamination was a separate failure mode caused by interlaminar stresses that are related to the stacking sequence of the laminate; and global buckling that was a failure mode of the laminate caused by an instability and is related to the stiffness and unsupported length. The study also suggested that smaller specimens failed in material failure modes that included matrix shear and fiber kinking, whereas large specimens failed by delamination.

Fiber reinforced composite system

Another aspect that was taken into account was the aging of the resin itself. Diffusion of water through the epoxy, for example, can be considered as a main criterion for the weakening of glass fibers, which in turn is responsible for the reduction in strength of the wrapped cylinder. Karbhari and Seible (1997) gave high importance to the selection of materials for the wrapping system. They have tried to explain the problem of diffusion through the glass/epoxy composite by means of the following diagram.

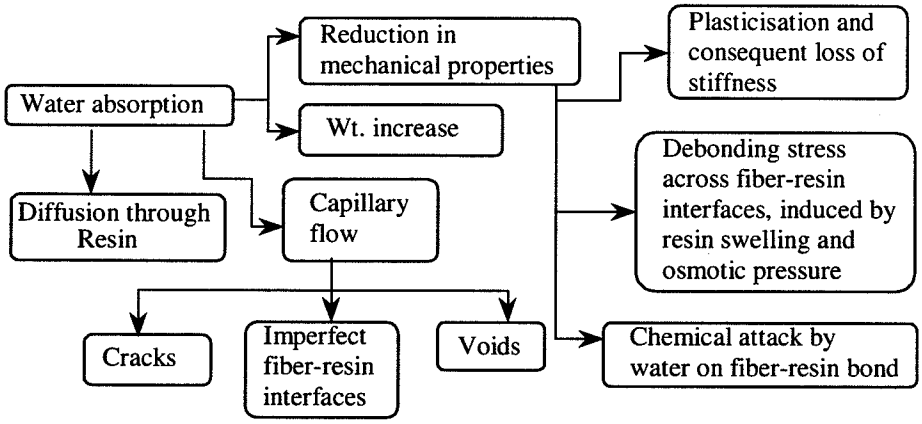

Figure 2.1 Effect of Water Absorption on the Performance of Glass/Epoxy Composite (Karbhari and Seible 1997)

Weight gain experiments were conducted on epoxy resin matrix composites to understand the diffusion phenomenon (Aminabhavi, 1988). These composites were exposed to distilled water and salt solution at different temperatures. The main objective was to investigate the diffusion mechanism in these composites. It was observed that the maximum absorptivity depended on the type of filler that was used in the composite. It was also observed that the diffusion rate of distilled water was higher than that of the salt solution, whereas in general, the activation energy for diffusion was higher in the latter. This increase in activation energy for the salt solution was attributed to an increased penetrant size of sodium and chloride ions.

In an attempt to evaluate the aging effects on an epoxy adhesive, the polymer was exposed to a high temperature and high relative humidity (De Neve and Shanahan, 1993). This research was mainly conducted to evaluate the durability of the epoxy as a structural adhesive since it is widely used in the aerospace and automotive industries. Both weight gain experiments and Dynamic Mechanical Analysis indicated significant water absorption at 70°C and 100 % RH. It was observed that as the aging period increases, the loss tangent curve shifts towards lower temperatures, which is mainly due to the plasticization of the polymer. From the gravimetric experiments conducted on the adhesive, the researchers concluded that the absorption phenomenon is mainly Fickian.

The combined effects of load, temperature and moisture on the performance of E-Glass/Vinyl ester composite materials were studied (Buck et al., 1997). The durability was estimated in terms of the ultimate strength of the composite

after it had been subjected to as many as 3000 hrs. of conditioning. The aging resulted in a decrease in the ultimate strength of the composite. A more severe deteriorating effect was observed when the samples were loaded. This clearly suggests that a combination of moisture and sustained load at a high temperature causes a significant decrease in the ultimate tensile strength making the material less durable.

A unique observation was reported when experiments were conducted to study the diffusion mechanism in epoxy resin/glass composite systems (Marzi et al., 1989). Experiments conducted on neat resin and the composite revealed that the amount of water absorbed by the composite was initially less than that of neat resin but later the situation was reversed. The authors suggested that this might be because of the presence of additional water located at the interface between the glass and the epoxy. With dynamic mechanical measurements the researchers tried to distinguish between the location of water at the resin-glass interface, water present in micro-cracks or voids in the resin and the water which was dissolved in the bulk polymer.

Diffusion experiments were conducted on fiber-reinforced epoxy composites by immersing them in salt-water solution and distilled water (Soulier et al., 1988). The researchers analyzed the data using two diffusion coefficients in their computations, one, parallel to the fiber direction and the other perpendicular. Kinetics of the sorption process calculated using Fick's law were compared with the sorption data obtained from the experiment. Viscoelastic experiments showed a broadening of tan δ curve and a split in the glass transition relaxation peak. Researchers Jenny et al. (1996) attempted to come up with a model that explains the dynamic response of continuous fiber/matrix composites. With torsional dynamic mechanical analysis, they have tried to analyze the properties of viscoelastic materials. Their results indicate that the magnitude of dynamic properties increases with the fiber volume fraction. A micro-mechanical model developed to predict the torsional dynamic response of the composite shows that there is a significant effect of fiber volume fraction on the dynamic response properties of the composites.

Methods of Concrete Repair with Composites

Karbhari and Seible (1997) have listed seven different methods that are commonly used to strengthen and confine concrete columns with the use of composite wraps especially for seismic retrofit. These are: wet winding of tows, winding of prepreg tow/tape, wet lay-up of fabric, lay-up of tape, adhesive bonding of prefabricated shells, in situ resin infusion of jacket, and, use of composite cables wrapped around a concrete core. Table 2.3 outlines various methods used for the wrapping of concrete elements.

Table 2.3 Methods of Concrete Repair with Composites (Karbhari and Seible 1997)

TECHNIQUE	ASPECTS	ISSUES/CONCERNS
Wet winding	Use of dry tows impregnated in a wet bath. Use of continuous fiber. Fiber tension assists consolidation. Ambient cure	Quality control of mix. Wet-out Non-uniform resin distribution. Control of cure Environmental issues
Prepreg winding	Automated winding of prepreg tow. Control of incoming material Use of continuous fiber Elevated temperature cure Control of tension	Prepegging cost and shelf life Use of machines Space limitations
Wet Lay-up	Use of wet bath or impregnator Manual or semi-automated process Ambient cure Flexible Ease of use in restricted areas	Quality control of mix Wet-out Non-uniform resin distribution Compaction and fiber wrinkling Control of cure Environmental issues
Lay up of tape	Similar to the wet lay-up method, except that smaller widths of tape are used that are wetted and then applied onto the column.	
Adhesive bonding of shells	Use of prefabricated sections Adhesive bonding in the field Rapid procedure Ease of fabrication	Lack of fiber continuity Shear lag effect Durability of the adhesive Increase in overall thickness
In-situ resin infusion	Placement of dry fabric followed by infusion under vacuum Fills cracks Non-uniform geometry	Wet-out Excessive resin use Appearance Non-uniform and low tension Difficulty of holding vacuum
Composite cables	Anchorage at top and bottom Rapid procedure	Non-uniform coverage Overall durability Very little data

CHAPTER 3 – EXPERIMENTAL INVESTIGATION

DESIGN OF EXPERIMENTS

This section describes the design of experiments employed by the authors to evaluate changes in the properties of the composite after exposing to severe environmental conditions. As the composite is likely to be exposed to various environmental conditions over a period of time, suitable aging conditions have to be selected to simulate in-service life of the structure. Also, experiments carried out in the laboratory need to be relevant to the problem at hand and should represent the actual field situation.

Materials

The materials selected for the experimental investigation are presented.

Concrete

Ready mixed concrete of 4500 psi strength, commonly used for highway applications, was used to prepare the experimental specimens. Smaller size gravel (commonly called p-gravel, size approximately 1cm) than that typically used in highway applications was employed to obtain consistency among the specimens. These materials were supplied by a local company, Hoy Ready-Mix Concrete.

Fiber reinforcement

The fiber material was a hybrid of E-glass and polyaramid called SEH-51 manufactured by Fyfe Co. This reinforcement was used in the form of a woven fabric sheet for easy application to the concrete surface. The reinforcing fiber in the hoop direction was E-glass amounting to almost 93% of the total weight of the fabric. Both E-glass and polyaramid were present in the fill (axial) direction constituting 4% and 3% of the total weight respectively. Cost was a major factor in choosing glass as a reinforcing material for the composite.

Resin Matrix

Epoxy resin marketed under the trade name TYFO S^R, also manufactured by Fyfe Co., was considered suitable for this application because of the following reasons:

- Appropriate viscosity: This helped in good penetration of the epoxy in between the crevices of the fabric that resulted in excellent wet out of the fibers.
- Workability: With a reasonable pot life of around 3-4 hours there was no sudden increase in viscosity of the epoxy, which allowed considerable time to work with it.
- Low glass transition temperature: The glass transition temperature of this epoxy when fully cured was approximately 82 ^{0}C which made it less brittle on lowering the temperature.

Characteristic properties of the composite and fibers are discussed in more detail in Appendix A. The thickness of a single layer of wrap around the cylinder was approximately 0.039 inches; this resulted in a fiber volume fraction of approximately 38 %.

Experimental Specimens

To evaluate the performance of the fiber-reinforced polymer composite in harsh environments, experiments were conducted on FRP-concrete components and FRP coupon specimens.

At the component level, compression experiments were conducted on concrete cylinders, 4" in diameter and 8" in height, wrapped with glass-aramid fabric saturated in epoxy resin matrix. These specimens were prepared using the wet lay-up method where the epoxy resin used in the preparation of the wrapped cylinders also served as an adhesive binding the concrete and the FRP. Since the rehabilitation of concrete structures is mainly focussed upon the repair of concrete bridge piers, cylinders were considered a suitable geometry for the test specimens. Compression tests were conducted according to the ASTM C-39 Standard.

Tensile experiments of rectangular strips of FRP material having dimensions of 8" x 1" x 0.055" were conducted based on the ASTM D-3039 Standard. These experiments were used to evaluate tensile strength, ultimate strain and elastic modulus in the main fiber direction (corresponding to the hoop direction of the cylindrical specimens). Dynamic mechanical thermal analysis was conducted on small thin rectangular coupons of FRP material having dimensions of 35mm x 12mm x 1.5mm.

Aging Conditions

Durability of the composite wrap when exposed to severe environmental conditions over a long period of time can be estimated in a laboratory by exposing the wrapped cylinders to accelerated aging conditions for a short period of time. Among many aging conditions that were possible, only those that were thought more relevant to the case at hand were carefully chosen. The accelerated aging conditions were the following:

1. Exposure to alkaline solution of pH 9.4 and temperature 73 ^{0}F
2. Exposure to alkaline solution of pH 12.4 and temperature 73 ^{0}F
3. Exposure to alkaline solution of pH 12.4 and temperature 150 ^{0}F
4. Exposure to water of neutral pH and temperature 150 ^{0}F
5. Exposure to dry heat at a temperature of 150 ^{0}F
6. Exposure to extended freeze-thaw cycles with a relative humidity of 100%

Only alkaline solutions were considered, as this is the more likely environment at the concrete-FRP interface. Hydration of Portland cement results in a pore solution containing calcium, sodium and potassium hydroxides. The pH of this pore solution in concrete, prepared using low alkali cement is observed to vary from 12.7 to 13.1. On the other hand, in the case of high alkali cement this range is between 13.5 to 13.9 (Hobbs, 1988). Note that the hydroxyl ion concentration in a saturated solution of calcium hydroxide is 0.04 molar that results in a pH of 12.6. Exposing the composite to an alkaline solution having a pH as high as 12.4 simulates a situation where its performance is of a concern when fresh concrete is poured into a pre-fabricated FRP jacket.

Different temperature and pH levels allowed investigation of the effect of different solution strengths on the wrap, while acquiring information on the role of temperature in accelerating the rate of degradation. Exposure to dry heat was important as it would allow differentiation between the damage caused as a result of chemical reaction initiated by the alkali and that caused by exposure to high temperature alone. The extended freeze-thaw cycle adopted had a duration of 5 days with maximum temperature of 49 C and minimum temperature of –29 C. The relative humidity for the specimens subjected to extended freeze-thaw cycles was 100% as they were immersed in water. Specimens were aged in the mentioned accelerated aging conditions for a period of 1000, 3000 and 8000 hrs. These environmental exposures were adopted based on recommendations from the FRP material qualification programs of CALTRANS and the Highway Innovative Technology Evaluation Center (HITEC) of the Civil Engineering Research Foundation (CERF).

Test Procedures

Compression Tests of Concrete Wrapped with FRP

Concrete cylinders were tested for their ultimate compressive strength and tensile strain. Using a composite wrap provides confinement to the cylinder and increases its ultimate strength and ductility. In order to keep the research effort manageable only cylinders of size 4" x 8" wrapped with one layer of FRP were tested for reduction in compressive strength after aging. On the other hand, plain concrete cylinders of the same dimensions were also subjected to similar aging conditions to provide an estimate of the magnitude of damage caused to concrete alone. Specimens were also wrapped with two and three layers of wrap to find the effect of an increase in the magnitude of confinement.

Tension Tests on FRP Material

Unidirectional glass-fabric reinforced epoxy composite samples were evaluated experimentally (ASTM D-3039) for their tensile strength before and after exposure to accelerated aging conditions. Monitored properties like the modulus of elasticity and the ultimate tensile stress and strain to failure would indicate the extent of degradation that was caused in the composite. The evaluated properties were also used in the development of a model for the stress-strain curve for the wrapped cylinder. Reduction in the ultimate tensile stress and the strain to failure is a good indication that the composite

has become brittle when aged and this may have a significant contribution towards lowering the ultimate strength of the wrapped cylinders.

Dynamic Mechanical Thermal Analysis

Dynamic mechanical thermal analysis (DMTA) was conducted on small rectangular strips of FRP material. These tests were at a coupon level. The aim behind conducting these tests was to identify property changes in the composite alone that may have been brought about by exposure to the aging conditions. Coupons were exposed to same aging conditions as the wrapped concrete cylinders. Virgin samples not exposed to any of the aging conditions acted as control specimens. DMTA basically consists of measuring a sinusoidal stress response when a sinusoidal strain is imposed on the sample. Two different tests can be conducted (i) imposing a constant sinusoidal strain as a function of temperature at a fixed frequency (called temperature sweep) and (ii) similar experiment with the values obtained as a function of frequency at a series of temperatures (called frequency-temperature sweep). Dividing the stress amplitude in-phase with the strain by the strain amplitude gives the storage modulus (G') whereas the stress-amplitude that is out-of-phase with the strain when divided by the strain amplitude gives the loss modulus (G").

A plot of G"/G' in the temperature sweep experiment vs. temperature is commonly called the tan δ curve. The peak of this curve represents the glass transition temperature of the composite, T_g. As a composite experiences sudden reduction in modulus beyond its glass transition temperature, T_g normally sets an upper limit for its operative temperature. Note that as a consequence of plasticization of the polymer during aging, a widening or splitting of tan δ peak is generally observed. Curves of storage modulus obtained at different temperatures as a function of frequency in a frequency-temperature sweep can be superimposed to form a single curve at a specific temperature called the reference temperature. This curve is referred to as the master curve. Major advantage in obtaining such a curve is that it provides information regarding the variation of G' over an extended frequency range which could not be obtained in a short period of time. On the other hand, master curves obtained for aged and unaged specimen can be compared to determine if any change in the modulus of the composite has taken place. Since the storage modulus is analogous to the Young's modulus, its measurement provides a technique to identify any damage that may have been caused to the composite in the process of aging. Monitoring the physical properties of the composite such as T_g and modulus would indicate a possible progressive decline in its ability to provide necessary confinement to the cylinder. Chemical reactions within the polymer and moisture ingress are likely to be responsible for any changes in strength of the composite.

EXPERIMENTAL RESULTS

Results from Compression Tests on Wrapped Concrete Cylinders

Cylinders of 4" x 8" wrapped with one layer of FRP were the major experimental specimens. Concrete cylinders that were 6" x 12" in dimensions were also tested to find the ultimate stress of the concrete, which was in turn used to calculate its modulus of elasticity. Also, 4" x 8" cylinders wrapped with 2 and 3 layers of FRP were tested to obtain an estimate of the increase in strength with an increase in confinement. Stress-strain curves were obtained with the help of strain gages that were affixed to the FRP surface and connected to a data acquisition system. Gages were affixed in the hoop and axial directions to record the tensile and axial strain during testing. All the cylinders were tested on a Baldwin machine having a maximum load capacity of 200,000 lbs.

Control Specimens

Figure 3.1 illustrates the stress-strain curves obtained for typical unaged specimens that acted as controls. These include stress-strain curves for plain concrete cylinders and concrete cylinders wrapped with 1, 2 and 3 layers of fabric. Positive values of strain represent the hoop or the tensile strain in the composite wrap measured by the strain gage affixed in the horizontal direction. On the other hand, a strain gage affixed in the vertical direction recorded the axial or the compressive strain in the composite. It is apparent from these graphs that the load carrying capacity of a plain concrete cylinder was very much increased when confined by the FRP. Also, when compared to the plain concrete cylinder, ultimate tensile strain to failure for the wrapped cylinder was much higher. This indicates that the use of composite wrap improves the column ductility. This aspect is particularly useful in field applications since it reduces the chances of a catastrophic failure.

Stress-strain behavior of the wrapped cylinder under the influence of a compressive load shows a bi-linear relationship, where the initial linear region of the curve closely matches with the curve obtained for the plain concrete cylinder.

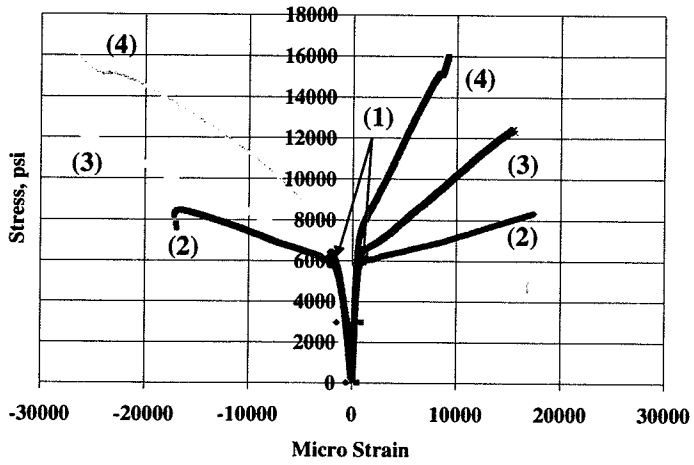

(1 Micro Strain = 10^{-6} Strain)

(1) Plain Concrete Cylinder
(2) 1 Layer of Wrap
(3) 2 Layers of Wrap
(4) 3 Layers of Wrap

Figure 3.1 Stress-Strain Behavior for Plain Concrete and Wrapped Cylinders

The failure of wrapped cylinders was initiated by a tensile failure in the wrap that was indicated by the wrap torn in the hoop direction. Inspection of failed specimens revealed that the composite remained attached to the concrete at most of the locations. This indicates a good bond between the concrete and FRP.

Load Cycles during Compression Tests

To determine the elastic limits of the wrapped cylinder when tested in compression, loading and unloading cycles were carried out during the two stages of the bi-linear curve. When load was removed from the specimen during the first straight line portion of the bi-linear curve, the curve almost retraced its path to zero whereas when the load was removed from the specimen during the second straight line stage, it did not return to zero leaving a residual strain in the FRP. This is illustrated in Fig. 3.2. Thus, it is apparent that during the initial stages of loading, the wrapped cylinder is still within the elastic limit. In the second linear region, the stress-strain relationship continues on its original path rejoining the curve at the end of the unloading cycle.

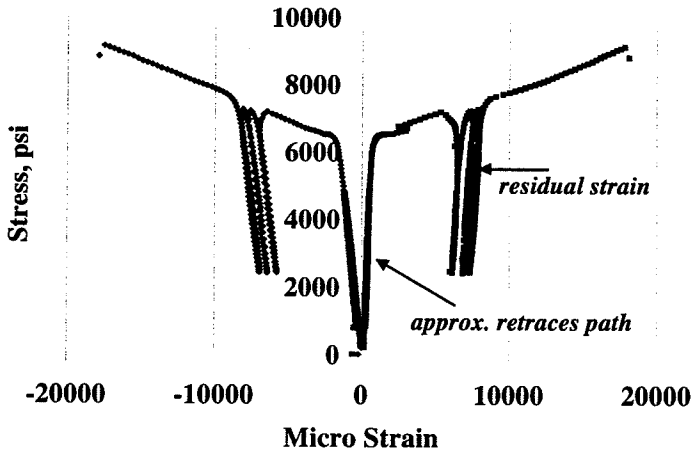

Figure 3.2 Stress-Strain Behavior of Wrapped Cylinder During Loading and Unloading Cycles

Aged Specimens

Concrete cylinders of dimensions 4" x 8" wrapped with one layer of FRP were exposed to the various accelerated aging conditions mentioned in a previous section. These cylinders were then tested for their compressive strength after 1000, 3000 and 8000 hrs of aging. These results are presented in the following sections.

Tests After 1000 hrs of Aging

Although the stress-strain curves for all the aged specimens were affected by aging, they still depict a bi-linear relationship. In Fig. 3.3, stress-strain curves for the samples experiencing minimum damage are compared with the stress-strain curve for a control sample. Particularly for specimens experiencing the maximum damage, a change in slope occurred earlier than that obtained for the control specimen. This is illustrated in Fig. 3.4. This could result due to the property changes in either the concrete (ultimate strength) or the wrap (ability to provide confinement) or both. Subjecting plain concrete cylinders to similar aging conditions could identify possible deterioration in concrete affecting its ultimate strength.

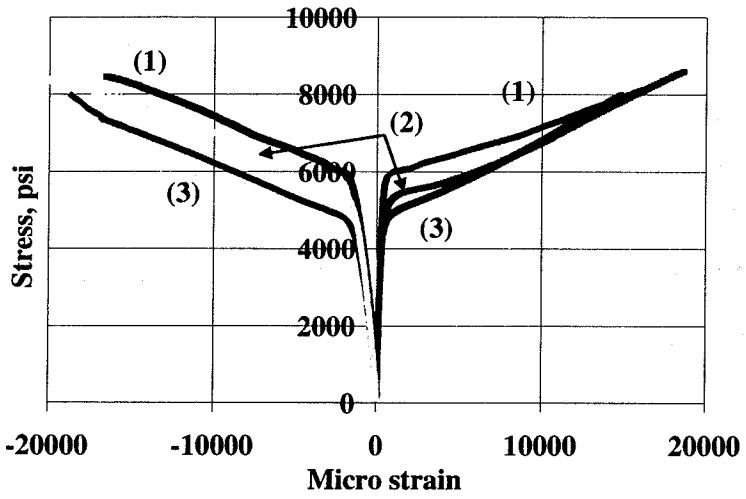

(1) Control Sample (2) pH 12.4, 73 ^{0}F (3) Dry Heat, 150 ^{0}F

Figure 3.3 Specimens Experiencing Minimum Damage (1000 hrs Aging)

The average ultimate strength and tensile strain values for the plain concrete cylinders and wrapped cylinders aged for 1000 hrs are reported in Table 3.1. Axial strain and hoop strains are represented by symbols "z" and "θ" respectively. As reported in this table, specimens aged in water at 150 ^{0}F and alkaline solution of pH 12.4 at 150 ^{0}F indicated a major reduction in the ultimate strength and strain. On the other hand, practically no change in the ultimate strength resulted for wrapped cylinders aged in alkaline solutions at 73 ^{0}F, extended freeze-thaw cycles or dry heat at 150 ^{0}F.

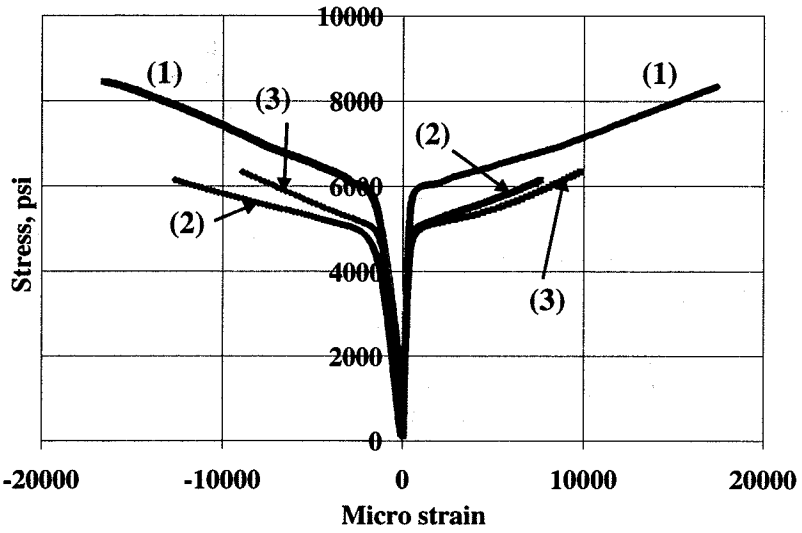

(1) Control Sample (2) Water (pH 7.0), 150 ^{0}F (3) pH 12.4, 150 ^{0}F

Figure 3.4 Specimen Experiencing Maximum Damage (1000 hrs of Aging)

Table 3.1 Ultimate Strength and Ultimate Strain Values for Control and Aged Specimens after 1000 hrs of Aging

Control	Ultimate Strength, psi	% Reduction in Strength	Ultimate Strain, z	Ultimate Strain, θ
Plain Concrete	5505		0.0022	0.0011
Cylinder With 1 Layer of Wrap	8270		0.0173	0.0174
AGED SPECIMEN (Wrapped Cylinder)				
pH 9.4, 73 ^{0}F	8370	-1.21	0.0271	0.0180
pH 12.4, 73 ^{0}F	8411	-1.69	0.0206	0.0183
pH 12.4, 150 ^{0}F	6150	25.65	0.0088	0.0089
pH 7.0, 150 ^{0}F	6087	26.41	0.0118	0.0090
Dry Heat, 150 ^{0}F	8077	2.34	0.0196	0.0163
Freeze-thaw	8051	2.65	0.0159	0.0144
AGED SPECIMEN (Plain Concrete)				
pH 12.4, 73 ^{0}F	5729	-4.07	-	-
pH 12.4, 150 ^{0}F	5562	-1.04	-	-
Freeze-thaw	5788	-5.14	-	-

It was also observed that exposure of plain concrete cylinders to aging did not result in any change in their ultimate strength. This suggested that only the FRP wrap or the concrete-matrix interface was affected during aging. It is apparent after 1000 hrs of aging that moisture at high temperature was critical in reducing the strength and ductility of the wrapped cylinder. This effect was independent of the pH of liquid media.

Tests After 3000 hrs of Aging

Since the properties of concrete as well as the composite are expected to change with time, a control sample with one layer of wrap was tested again after 3000 hrs of aging to obtain an exact comparison of strengths and hence, the state of the aged specimen after the same time period. Average ultimate strength of the control sample with one layer of wrap after 3000 hrs (Refer to Table 3.2) was approximately 10% higher than that previously observed (Table 3.1). At this stage, further reduction in the strength of wrapped cylinders was observed when these specimens had been exposed for 3000 hrs to moisture coupled with high temperature i.e., the same aging conditions identified to be the most critical at the end of 1000 hrs. Fig. 3.5 illustrates this. A significant change in the ultimate strength for samples subjected to extended freeze-thaw cycles was also observed after 3000 hrs of aging (25 cycles). A minor change in ultimate strength resulted for specimens exposed to dry heat at 150 ^{0}F. Fig. 3.6 illustrates typical stress-strain curves obtained for dry heat and extended freeze-thaw aged specimens; these are compared with the control sample. Similar to the situation that was reported at the end of 1000 hrs, exposure to alkaline solutions at 73 ^{0}F had virtually no effect in reducing the strength of the wrapped cylinder. This is illustrated in Fig. 3.7. Average ultimate strength and ultimate strain values for the cylinders at the end of 3000 hrs of aging are reported in Table 3.2.

Table 3.2 Ultimate Strength and Ultimate Strain Values for Control and Aged Specimens after 3000 hrs of Aging.

Control	Ultimate Strength, psi	% Reduction in Strength	Ultimate Strain, z	Ultimate Strain, θ
Plain	5715		-	-
Cylinder With 1 Layer of Wrap	9151		0.0160	0.0207
AGED SPECIMEN (Wrapped Cylinder)				
pH 9.4, 73 ^{0}F	8895	2.90	0.0143	0.0199
pH 12.4, 73 ^{0}F	8917	2.56	0.0220	0.0194
pH 12.4, 150 ^{0}F	6235	31.88	0.0112	0.0077
pH 7.0, 150 ^{0}F	6052	33.87	0.0091	0.0063
Dry Heat, 150 ^{0}F	8159	10.85	0.0167	0.0169
Freeze-thaw	7179	21.57	0.0126	0.0098
AGED SPECIMEN (Plain Concrete)				
pH 12.4, 73 ^{0}F	5607	1.89	-	-
pH 12.4, 150 ^{0}F	5730	-0.26	-	-
Freeze-thaw	5687	0.49	-	-

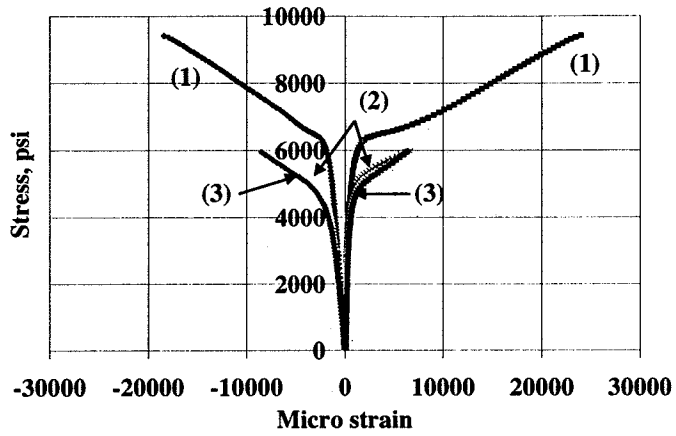

1) Control Sample (2) Water (pH 7.0), 150 ^{0}F (3) pH 12.4, 150 ^{0}F

Figure 3.5 Samples Experiencing Maximum Damage (3000 hrs of Aging)

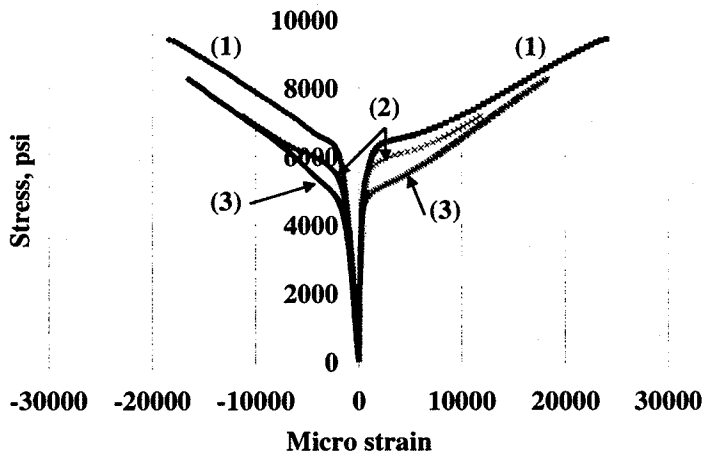

(1) Control Sample (2) Freeze-thaw (3) Dry Heat, 150 ^{0}F

Figure 3.6 Stress-Strain Curves for Freeze-thaw and Dry Heat Aging (3000 hrs)

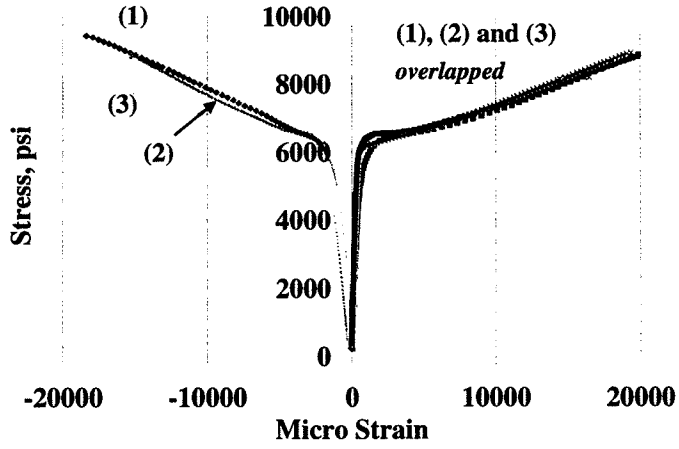

(1) Control Sample (2) pH 9.4, 73 ^{0}F (3) pH 12.4, 73 ^{0}F

Figure 3.7 Samples Experiencing Minimum Damage (3000 hrs of Aging)

Compression tests on the aged plain concrete cylinders indicate no change in their ultimate strength value. This result confirms that plain concrete is unaffected by the aging conditions. Therefore the only possibilities that could be associated with the reduction in the ultimate strength of the aged wrapped cylinders are degradation of the composite wrap or delamination at the interface or both. It is understood that elevated temperature probably enhances moisture diffusion through the composite diminishing its strength and directly influencing the concrete-FRP bond.

Tests After 8000 hrs of Aging

At the end of 8000 hrs of aging, there was no further significant reduction in the ultimate strength of the cylinders for high temperature/moisture aging conditions that had proved to be the most severe so far. The ultimate strength values approached that of plain concrete cylinder. This probably suggests that the composite is no longer useful in enhancing the ultimate strength of the cylinder. Typical stress-strain curves obtained for these specimens are shown in Fig. 3.8. Although the load carrying capacity of the wrapped cylinder has been significantly reduced, the ultimate strain to failure of the composite is much higher than that of plain concrete. Thus, the wrapped column still maintains a much higher ductility when compared to plain concrete.

At the end of 8000 hrs, a slight reduction in the ultimate strength for specimens exposed to liquid media at low temperature was observed (illustrated in Fig. 3.9). Freeze-thaw aging had a similar effect with a reduction that was found intermediate to that of low and high temperature aging. There was also practically no reduction in the strength of specimens exposed to dry heat. Typical stress-strain curves obtained for specimens aged in freeze-thaw cycles and dry heat are illustrated in Fig. 3.10. The results at the end of 8000 hrs of aging are reported in Table 3.3.

Table 3.3 Ultimate Strength and Ultimate Strain Values for Control and Aged Specimens after 8000 hrs of Aging

Control	Ultimate Strength, psi	% Reduction in Strength	Ultimate Strain, z	Ultimate Strain, θ
Plain concrete	5735		-	-
Cylinder With 1 Layer of Wrap	8766		0.0179	0.0189
AGED SPECIMEN (Wrapped Cylinder)				
pH 9.4, 73 ^{0}F	8186	6.63	0.0142	0.0166
pH 12.4, 73 ^{0}F	8119	7.38	0.0179	0.0164
pH 12.4, 150 ^{0}F	6108	30.33	0.0068	0.0047
pH 7.0, 150 ^{0}F	5635	35.72	0.0058	0.0057
Dry Heat, 150 ^{0}F	8924	-1.80	0.0186	0.0216
Freeze-thaw	6797	22.47	0.012	0.0076

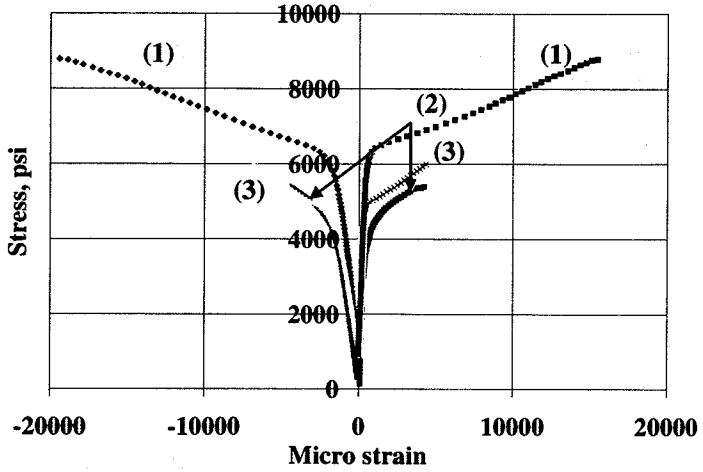

(1) Control Sample (2) Water (pH 7.0), 150 ^{0}F (3) pH 12.4, 150 ^{0}F

Figure 3.8 Samples Experiencing Maximum Damage (8000 hrs of Aging)

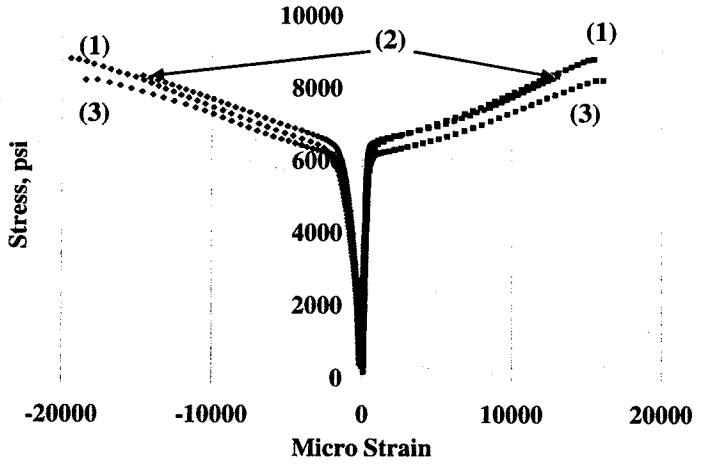

(1) Control Sample (2) pH 9.4, 73 ^{0}F (3) pH 12.4, 73 ^{0}F

Figure 3.9 Samples Experiencing Minimum Damage (8000 hrs of Aging)

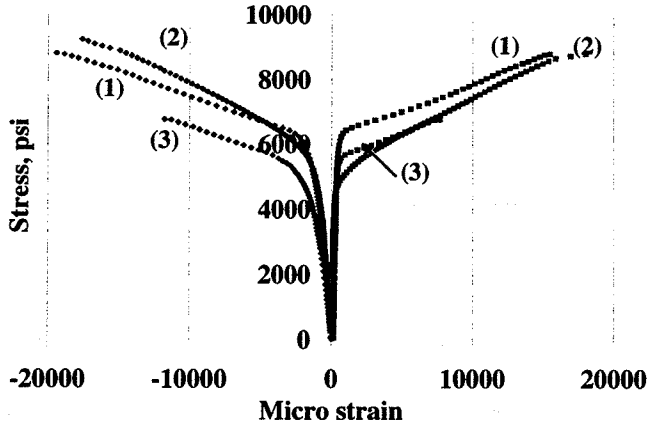

(1) Control Sample (2) Dry Heat, 150 ^{0}F (3) Freeze-Thaw Cycle

Figure 3.10 Samples Aged in Freeze-thaw and Dry Heat (8000 hrs of Aging)

Discussion of Experimental Results from the Compression Tests of Wrapped Cylinders

It was observed that the composite wrap enhances the strength and ductility of the plain concrete cylinder by providing external confinement. Compression test results on the aged specimens identified the following accelerated aging conditions to be the most critical for reducing the strength and ductility of the wrapped cylinder

1. Alkaline Solution of pH 12.4, 150 ^{0}F
2. Water of pH 7.0 at 150 ^{0}F
3. Extended freeze-thaw Cycles

Plain concrete cylinders when exposed to similar aging conditions did not indicate any change in the ultimate strength. Further, wrapped cylinders when exposed to the following aging conditions retained their properties

1. pH 9.4, 73 ^{0}F
2. pH 12.4, 73 ^{0}F
3. Dry Heat, 150 ^{0}F

It is apparent that a combination of moisture and high temperature resulted in a significant reduction in the cylinder strength, which is independent of the pH of the solution. It could be concluded that the composite or the interfacial bond was responsible for the decrease in strength of the wrapped cylinders. In either case, the system indicated that it was fairly durable when exposed to liquid media at ambient temperature or in the case of exposure to dry heat at an elevated temperature.

Linear Regression on the Stress-Strain Curves

A linear regression analysis was carried out on the two linear regions of the bilinear stress-strain curve to determine the parameters that best describe its nature. Fig. 3.11 represents the stress-strain curve for the wrapped cylinder. As illustrated in the figure, m_1 and m_2 indicate the slopes of initial and latter stages of the bi-linear curve respectively. The axial direction is represented by "z" and the hoop direction by "θ". The stress value at the point where there is a step change in the slope of the curve is identified as the cracking stress of the concrete ($f'_{z,cr}$ and $f'_{\theta,cr}$); and the strain at the same point is called the cracking strain ($\varepsilon^c_{z,cr}$ and $\varepsilon^c_{\theta,cr}$). Strains denoted by $\varepsilon^c_{z,u}$ and $\varepsilon^w_{\theta,u}$ represent ultimate strain in concrete and wrap respectively. Ultimate stress to failure of the concrete is denoted by f'_{cu}. The cracking point is given by the intersection of the two straight lines representing the bi-linear curve obtained by a linear regression analysis carried out on the curves separately.

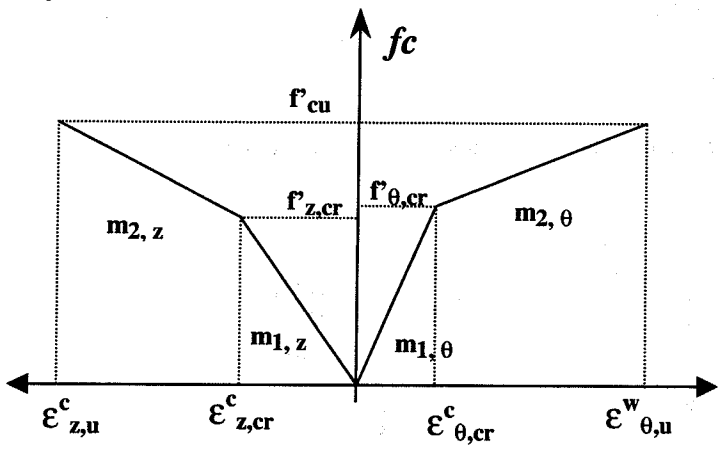

Fig. 3.11 Bi-Linear Stress-Strain Curve for the Wrapped Cylinder

In Table 3.4 are tabulated the average ratio of slopes (m_2/m_1) obtained for concrete cylinders wrapped with 1,2 and 3 layers of wrap, in the hoop (θ) and axial (z) directions. It is observed that both $(m_2/m_1)_z$ and $(m_2/m_1)_\theta$ increase with the no. of layers of wrap around the concrete cylinder. This response is expected due to the increase in confinement provided by the higher jacket thickness around the concrete. Estimated values of $(m_2/m_1)_z$ are used in the development of theoretical model presented in a following chapter.

Table 3.4 Ratio of Slopes of the two Linear Regions of the Bi-Linear Curve for Wrapped Specimens

WRAPPED SPECIMEN	$(m_2/m_1)_z$	$(m_2/m_1)_\theta$
1 layer	0.0438	0.0094
2 layers	0.0908	0.041
3 layers	0.1	0.0542

Results from DMTA Tests

DMTA was conducted on strips of FRP having a size of the order 35mm x 12mm x 1.5mm. Glass fabric used as the reinforcing material for preparing these specimens was the same as that used for the composite wrap. Only one layer of the glass fabric was used in the preparation of these samples. Properties such as storage modulus and the glass transition temperature of the composite were monitored before and after the samples were exposed to same aging conditions as the wrapped cylinders. Also, these coupons were tested at the same intervals as the cylinders.

Control Specimen

Data from a typical temperature sweep experiment for the composite are illustrated in Fig. 3.12. The experiment was conducted at a frequency of 1 rad/s. The graph depicts the variation in the storage modulus (G') and the loss modulus (G") at this frequency as a function of temperature. It is observed that the storage modulus remains constant till a particular temperature after which it falls to another plateau. This occurs at the glass transition temperature of the composite commonly denoted as t_g. The glass transition temperature is more accurately determined by plotting the tanδ curve with respect to temperature. The peak value of the tanδ curve gives the glass transition temperature of the composite as explained earlier.

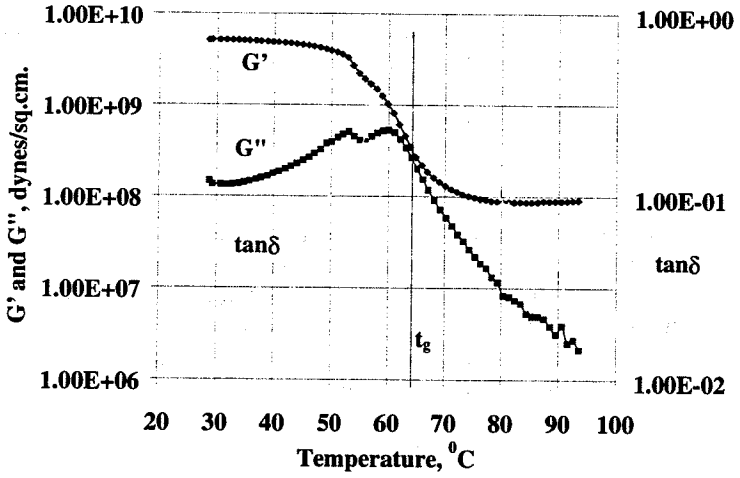

Figure 3.12 Temperature Sweep for Control Sample Indicating T_g.

As shown in Fig. 3.12, the value of T_g estimated for the control sample was around 64 ^{0}C (147 ^{0}F). It should be noted that the wrapped cylinders that were exposed to moisture at a temperature of 150 ^{0}F experienced maximum damage. Since the specimens were subjected to a temperature that was close to the glass transition temperature of the composite, the polymer chains were relatively mobile. On the one hand, this allows for the possibility of a chemical reaction within the composite, while on the other hand it also facilitates moisture diffusion into the polymer. This probably explains why the specimens subjected to high temperature/moisture conditions experienced maximum damage compared to the dry heat environment.

Typical frequency-temperature sweep data for the composite are shown in Fig. 3.13. In this experiment, the storage modulus of the composite was measured while the frequency varied from 0.1 to 100 rad/s, at temperatures ranging from

40 ^{0}C to 80 ^{0}C at equal intervals of 5 ^{0}C. A master curve is obtained by superposition of all these curves into one single curve at a reference temperature, also shown in the same figure. The lowest value of the storage modulus as given by the master curve should be taken as the design value for all the applications of composite materials at that temperature.

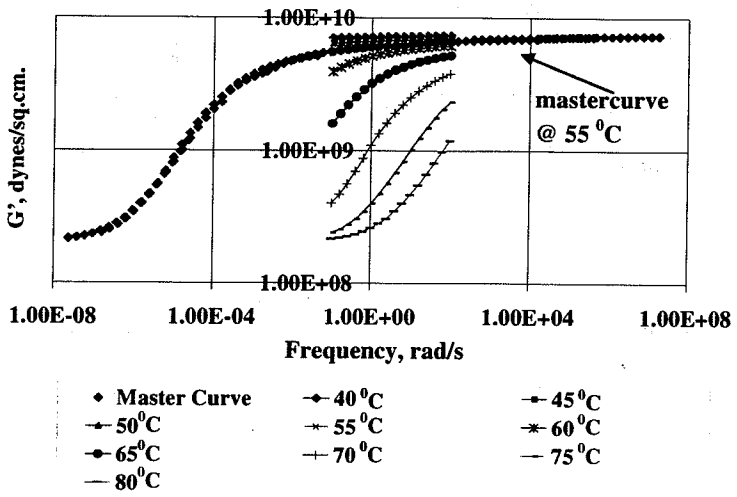

Figure 3.13 Frequency – Temperature Sweep for Control Specimen and Master Curve

Aged Specimens

Temperature sweep data for the aged specimens were compared with those obtained for the control samples. As indicated in the previous section, important properties to be investigated for the aged composite are its glass transition temperature and variation in the storage modulus. These data provide valuable information regarding the state of the composite after aging.

Comparison of master curves for the aged and unaged specimens did not indicate any loss in the modulus of the composite due to aging. The samples aged in liquid media were allowed to dry in ambient temperature for a period of 6-8 hrs before they were tested. The same specimen was used for the temperature sweep and the frequency-temperature sweep; the former was carried out first on each sample. The minimum duration maintained between the temperature sweep and the frequency-temperature sweep for all the specimens was 5 hrs.

Tests after 1000 hrs of Aging

As shown in Fig. 3.12 the temperature sweep conducted on the control specimen indicated a glass transition temperature of around 64 ^{0}C. At the end of 1000 hrs of aging, the aged specimens indicated a value of t_g which was higher than that obtained for the control sample. Typically for the samples aged at high temperature, the glass transition temperature was around 90 ^{0}C. Also, the storage modulus for these specimens was higher than that of the control specimen. This is illustrated in the Fig. 3.14. Since the glass transition temperature and the storage modulus depend on the cross-link density of the polymer, it could be said that as the composite was being exposed to high temperature, it underwent curing. Clearly, an elevated temperature increased the chemical reaction rate within the resin, enhancing the cross-link density of the polymer. This is also evident when master curves for the aged and control specimen are compared; this is illustrated in Fig. 3.15.

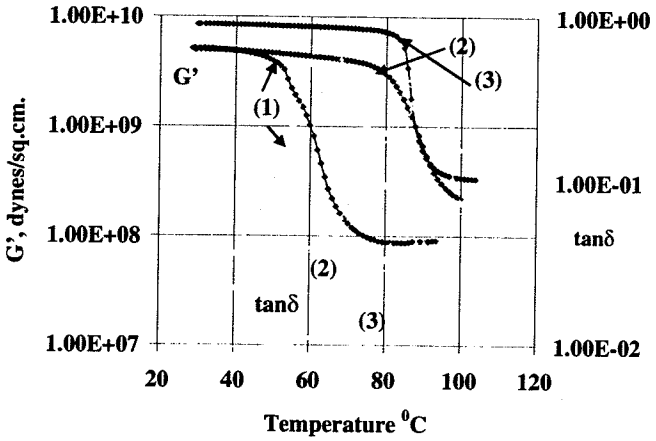

(1) Control Sample (2) Water (pH 7.0), 150 °F (3) Dry Heat, 150 °F

Figure 3.14 Increase in T_g With Exposure to Elevated Temperature (1000 hrs)

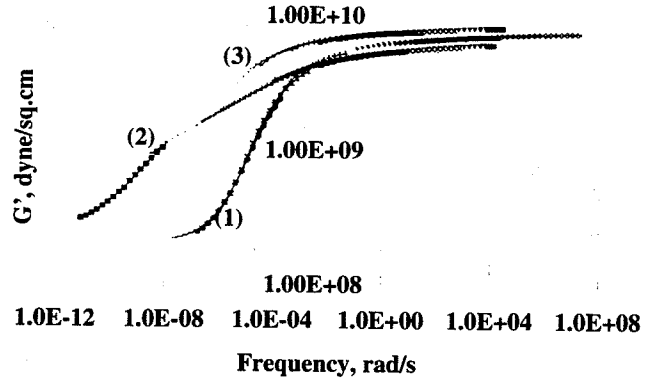

(1) Control Sample (2) Water (pH 7.0), 150 °F (3) Dry Heat, 150 °F

Figure 3.15 Increase in Modulus as Shown by the Master Curve

Tests after 1000 hrs of aging indicated that the composite gained in stiffness and had a higher value of T_g compared to the control sample. But it was observed that wrapped cylinders subjected to high temperature/moisture conditions experienced maximum damage. A possible explanation as to why the DMTA failed to recognize the damage in the composite could be that the DMTA measures the small strain properties of the composite whereas compression tests represent a large strain property. Since the behavior of the composite in these cases could be entirely different it could be difficult to obtain a direct correlation between the two tests. Moreover, DMTA on the aged specimens only indicated that the stiffness of the composite was increased when subjected to high temperature. This result was not sufficient to estimate the strength of the composite.

Results after 3000 hrs of Aging

Results from the temperature sweep experiment conducted on the control sample aged for 3000 hrs indicates a value of T_g around 80 °C. This is illustrated in the Fig. 3.16. On the other hand, specimen aged in dry heat at 150 °F depicts no further increase in its T_g (Fig. 3.17). Thus, it is confirmed that the increase in T_g for aged specimens that was seen at the end of 1000 hrs was nothing but the effect of a progressive chemical reaction taking place within the composite leading to an increase in the cross link density of the polymer. The chemical reaction was complete for specimens exposed to high temperature. But, a different situation resulted for all other aging conditions involving exposure to liquid media (higher or lower temperature). For these specimens, a split in the peak of the tan δ curve was observed indicating a possible plasticization of the polymer during the aging process. A typical curve is illustrated in Fig. 3.18 where the tan δ curve and the storage modulus curve obtained for a sample aged in water at 150 °F are compared with those for the control specimen. Similar results were obtained for all other aging conditions except exposure to dry heat.

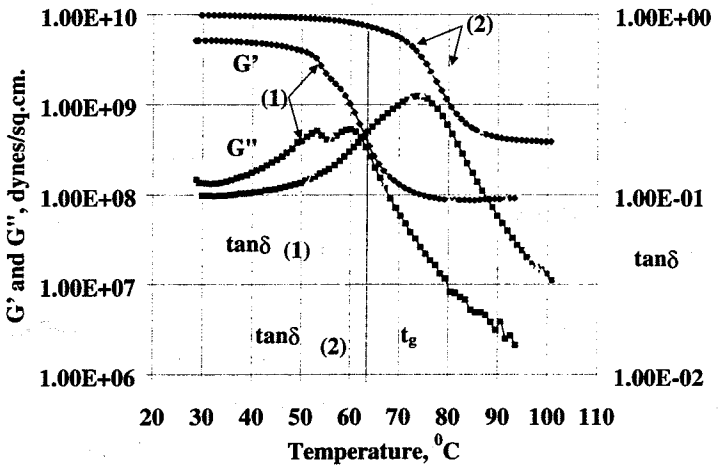

(1) Control Sample

(2) Control Sample at end of 3000 hrs

Figure 3.16 Shift in tan δ for Control Specimen

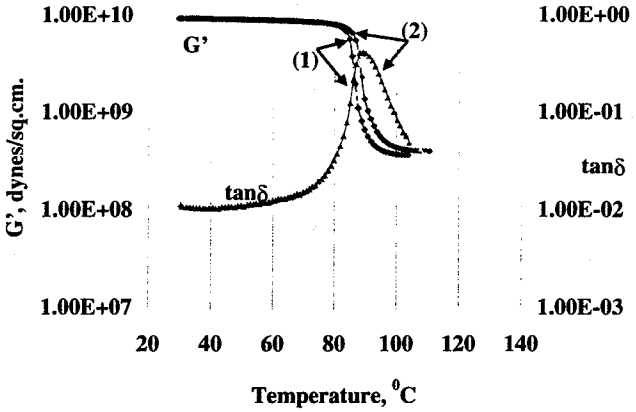

(1) After 1000 hrs

(2) After 3000 hrs

Figure 3.17 No change in T_g observed for specimen aged in Dry Heat at 150 ^{0}F

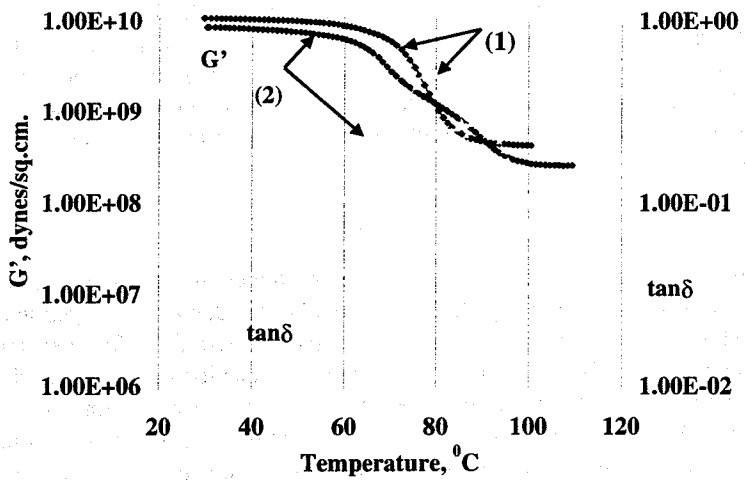

(1) Control Sample at 3000 hrs

(2) Water (pH 7.0), 150 ^{0}F after 3000 hrs

Figure 3.18 Split in tan δ Curve and Reduction in G'

A comparison of master curves for the sample aged at high temperature and the control sample still indicates that the curves for samples aged at higher temperature lie above the control specimen. This is illustrated in Fig. 3.19 with dry heat at 150 ^{0}F and alkaline solution of pH 12.4 at 150 ^{0}F as examples. Besides, the master curve obtained for the same specimen aged for 3000 hrs in an alkaline solution at a lower temperature closely matches with the control specimen (Refer to Fig. 3.20). This again shows that the composite had gained modulus with time, which is a consequence of chemical reaction still probably incomplete even at the end of this time period.

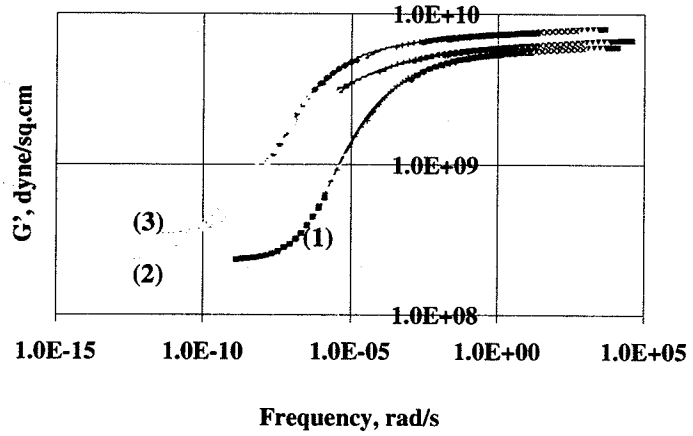

(1) Control Sample (2) pH 12.4, 150 ^{0}F (3) Dry Heat, 150 ^{0}F

Figure 3.19 Comparison of Master Curves Aged in Higher Temperature with Control Sample after 3000 hrs.

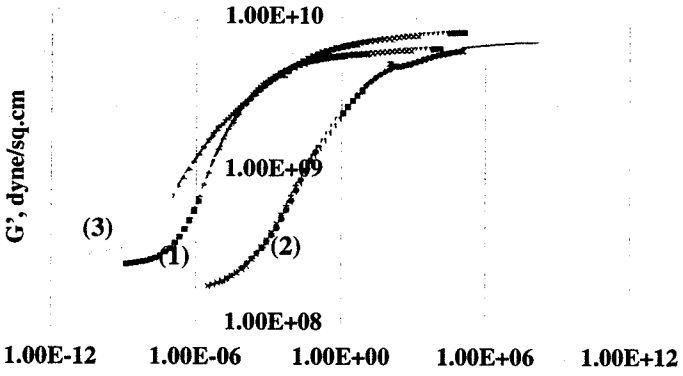

(1) Control Sample after 3000 hrs (2) pH 12.4, 73 ^{0}F after 1000 hrs (3) pH 12.4, 73 ^{0}F after 3000 hrs

Figure 3.20 Control Sample at 3000 hrs vs. Specimen Aged at a Lower Temperature after 1000 and 3000 hrs

Results after 6000 hrs of Aging

Results from the temperature sweep experiments conducted on the aged and the control specimens were similar to those obtained after 3000 hrs. As observed after 3000 hrs of aging a split in the tan δ curve resulted for specimen aged in liquid media irrespective of exposure to higher or ambient temperature. Typical plot obtained is shown in the Fig. 3.21. The storage modulus curve for the aged specimen lies under the curve for the control specimen for all the aging conditions. This is also illustrated in Fig. 3.21.

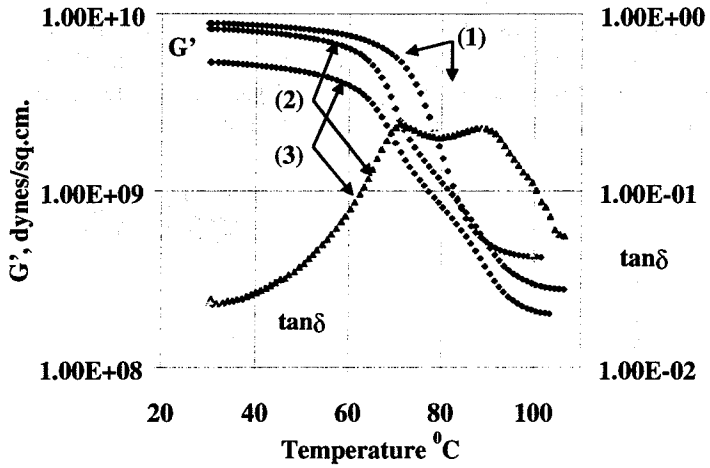

(1) Control Specimen after 6000 hrs (2) Water (pH 7.0), 150 ^{0}F after 6000 hrs (3) pH 12.4, 150 ^{0}F after 6000 hrs

Figure 3.21 Temperature Sweep Indicating Split in tan δ After 6000 hrs of Aging

Discussion of Results from the DMTA Experiments

It is definite from the temperature sweep experiments conducted on the aged FRP coupons (after 3000 and 6000 hrs) that the composite has experienced some damage. This is particularly true for aging in liquid media whether low or high temperature; indicated by a split in the tan δ curve. FRP coupons subjected to dry heat at 150 ^{0}F did not experience any deterioration in their properties. Instead, exposure to elevated temperature enhanced the chemical reaction within the polymer increasing the cross-link density thereby enhancing the stiffness of the composite. Similar to the compression test results on the aged specimens, DMTA also identified the moisture ingress as a fundamental cause of deterioration in the composite. Exact correlation between the DMTA and the compression test results could not be obtained since the former only illustrated an infinitesimal strain behavior of the composite upon aging. The damage being identified only on a qualitative basis, DMTA could not quantify the exact magnitude of deterioration experienced by the composite in each of the aging conditions.

Tensile Tests of FRP Specimens

Control Specimen

Unidirectional glass-fiber epoxy composite specimens were tested in tension to obtain the modulus and the ultimate strain to failure. The samples used for this test had the dimensions of the order of 8″ x 1″ x 0.055″, and were tested according to ASTM D3039 Standard. FRP tabs of thickness 3/16″ and length 2.5″ were used at the ends and both sides of the specimen, and this resulted in a gage length of about 3″. Epoxy resin, Devcon^R 5 Minute^R Epoxy, having a shear strength value of 1300 psi (obtained from the manufacturer) and a setting time of 5 minutes was used to bond FRP tabs to the tensile specimens. A typical stress-strain curve obtained during such a tensile test for the unaged specimen is shown in Fig. 3.22. It can be observed from the figure that the stress-strain relationship followed by the composite is linear until its failure. Table 3.5 reports average values for the quantities obtained from the tensile test and these are also compared with the design values (obtained from the manufacturer).

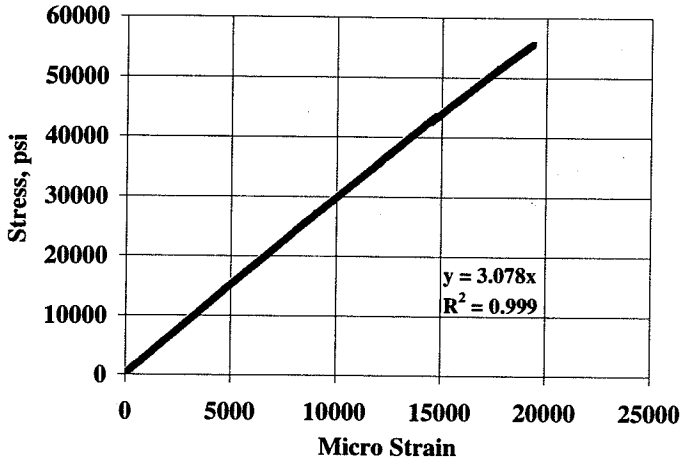

Fig. 3.22 Tensile Test on Control Sample

Table 3.5 Comparison of Experimental and Design Values for the Tensile Test Specimens

	DESIGN VALUES	EXPERIMENTAL COUPONS
Thickness (in)	0.051	0.056
Ultimate Tensile Strain, micro strain	0.0200	0.0196
Modulus of Elasticity (hoop), psi	3.00E6	2.89E6
Breaking Strength (hoop), psi	60000	52665
Breaking Strength (axial), psi	-	4369

Aged Specimens

The FRP specimens were aged for a period of about 1500 hrs. These were then tested for their tensile strength. Unlike DMTA, the tension test results represent both the small and large strain property behavior of the composite. Response of the FRP coupon subjected to a tension test is similar to the response of the composite wrap around the concrete cylinder in the hoop direction when tested under compression. This test is therefore important since it is likely to provide a reason for the reduction in strength of the wrapped cylinders aged in similar conditions. To limit the number of specimens to be tested only the following aging conditions were used. These provided an overall idea of the effect of different environmental conditions on the composite material:

1. Dry Heat, 150 ^{0}F
2. Alkaline Solution pH 12.4, 150 ^{0}F
3. Alkaline Solution pH 12.4, 73 ^{0}F
4. Extended Freeze-thaw cycles

Results from the Tensile Tests

Similar to the results obtained from the compression tests on the cylinders, the tensile strength of the FRP samples was considerably reduced for the samples exposed to a combination of high temperature and moisture conditions. Properties of the composite were altered in two ways: where extended freeze-thaw cycles seemed to have reduced the modulus of the FRP, exposure to alkaline solution of pH of 12.4 at 150 ^{0}F had a considerable impact on the ultimate strain to failure. Comparison of the stress-strain curves for the specimens experiencing minimum damage with the control sample is illustrated in Fig. 3.23. Fig. 3.24 compares the stress-strain curve for the specimen with maximum damage with the control specimen.

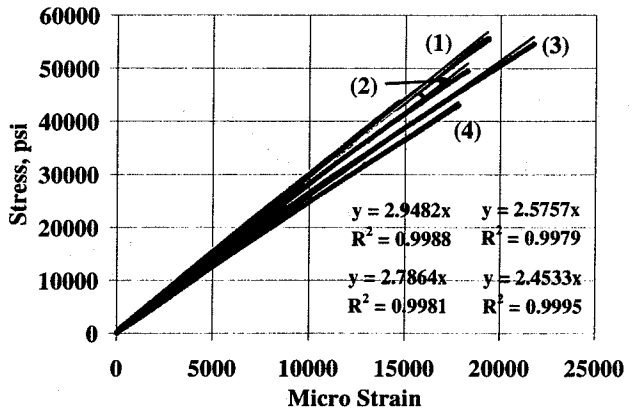

(1) Control Sample
(2) pH 12.4, 73 ^{0}F
(3) Dry Heat, 150 ^{0}F
(4) Freeze-thaw

Figure 3.23 Tensile Tests on Aged Specimen with Minimum Damage & Modulus in the Order of Decreasing Slopes

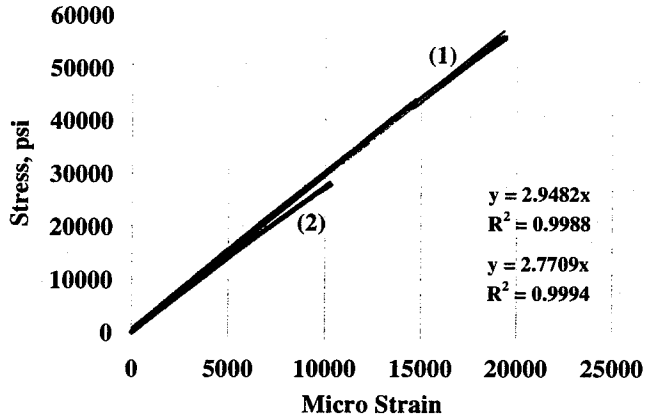

(1) Control Sample
(2) pH 12.4, 150 ^{0}F

Figure 3.24 Tensile Test on Specimen with Maximum Damage and Modulus

Ultimate strength, ultimate strain and the modulus of elasticity obtained for the aged specimens are reported in the following Table.

Table 3.6 Results from the Tension Tests on Aged Specimens

SPECIMEN TYPE	Thickness (in.)	ULTIMATE STRENGTH, psi	ULTIMATE STRAIN	YOUNG'S MODULUS, msi
Control	0.056	52665	0.0196	2.89
Dry Heat, 150 ^{0}F	0.061	55184	0.0216	2.78
pH 12.4, 73 ^{0}F	0.059	50333	0.0196	2.75
pH 12.4, 150 ^{0}F	0.057	30074	0.0113	2.73
Freeze-thaw	0.060	44502	0.0181	2.48

Discussion of Results from the Tension Tests

It can be concluded from the tensile tests that the aging conditions affected the properties of the composite wrap by reducing its tensile strength. Exposure to high temperature and alkaline solution had a serious impact on the tensile strength of the composite. FRP specimens subjected to pH 12.4 at 73 ^{0}F or dry heat at 150 ^{0}F did not result in any change in their properties. A significant reduction in the modulus, though, was observed only in the case of extended freeze-thaw cycles.

Therefore it is understood that a combined exposure to high temperature and liquid media rendered a reduction in FRP tensile strength, which was in turn responsible for lowering the compressive strength of the wrapped cylinders exposed to similar conditions.

Comparison of Elastic Modulus from Tension Test and DMTA

Young's modulus of elasticity for the composite from the tensile test and the shear modulus (G') evaluated from the DMTA when tested in torsion were compared.

- Tension Test (Table 3.5): E = 2.89E+06 psi = 20,000 MPa
- From DMTA Torsion Tests: G' = 8E+09 dynes/sq.cm. = 116,030 psi = 800 MPa

Then, the following elastic parameter for the fiber composite wrap was computed as $\sqrt{(E/G')} = 5.1$, which seems to be within acceptable ranges. Lopez-Anido (1995) reported that $\sqrt{(E/G')}$ is approximately 2.5 for unidirectional pultruded glass-vinyl ester sections with typical fiber contents between 30 and 50 %. Furthermore, for isotropic steel $\sqrt{(E/G')} = 1.61$. This parameter controls the shear lag properties of the FRP composite material. A high value of $\sqrt{(E/G')}$ indicates a material that may have pronounced shear lag effects, and therefore may be prone to shear and warping deformation.

CHAPTER 4 - STRESS-STRAIN MODEL FOR FRP WRAPPED CONCRETE ACCOUNTING FOR ENVIRONMENTAL AGING

INTRODUCTION

Typical stress-strain curves under compression loading for a wrapped cylinder (one layer of wrap) are illustrated in Fig. 4.1. Stress-strain data for a plain concrete cylinder (without wrapping) are also shown in the same figure. It is apparent from this figure that the stress-strain curve for the wrapped cylinder follows a bi-linear relationship, where a sudden change in the slope is observed after a particular point. This point is close to the point of failure of the plain concrete cylinder. Stress-strain curves that are similar in nature were also obtained when the compression test was carried out on cylinders wrapped with 2 and 3 layers of FRP. This is illustrated in Fig. 4.2.

The present chapter attempts to explain theoretically this particular behavior of wrapped concrete column, when acted upon by an axial load. For the same reason, a bi-linear stress-strain model is proposed that will assist in interpreting the nature of curves obtained experimentally in terms of theoretical equations. This model also attempts to assign a meaning to the experimentally observed stress-stain curve by proposing a likely phenomenon that takes place during the whole process of compression test on the wrapped cylinder.

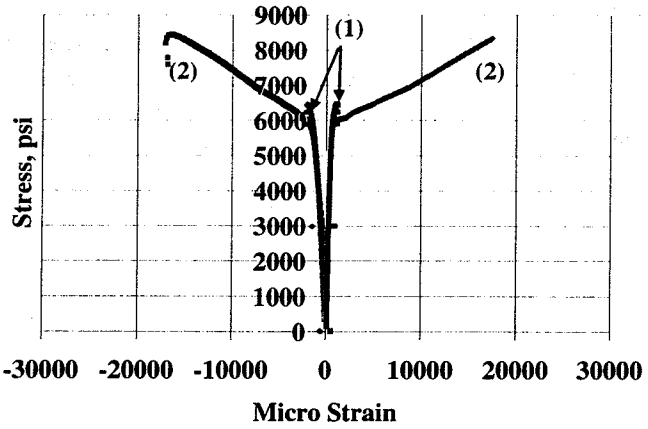

(1) Plain Concrete (2) 1 Layer of Wrap

Figure 4.1 Comparison of Stress-Strain Curves for Plain Concrete and Concrete Cylinder Wrapped with 1 Layer of Wrap

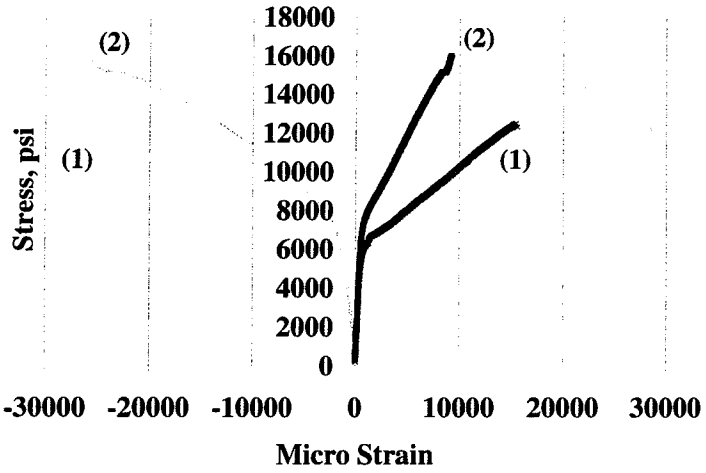

(1) 2 Layers of Wrap (2) 3 Layers of Wrap

Figure 4.2 Comparison of Stress-Strain Curves for Concrete Cylinders Wrapped with 2 and 3 Layers of Wrap

MODELS FOR CONFINED CONCRETE

A number of researchers have conducted fundamental tests examining the axial stress-strain behavior of plain concrete columns externally confined with FRP. The bi-linear nature of the stress-strain curve for the wrapped cylinder has been observed and reported in the literature previously. More recent investigations in this area are as stated. Confining effects of CFRP (Carbon Fiber Reinforced Plastics) sheets on concrete cylinders and the resulting increase in strength and ductility has been evaluated by Kono et al. (1998) by relating this increase to an increase in the Confinement Index. Fyfe et al. (1998) proposed an equation for determining the Fibrwrap^R jacket thickness for a concrete column to allow for a specified amount of axial strain. A condensed written summary about similar studies conducted by other researchers was presented by Harries et al. (1998) who tested the effects of confinement on concrete columns when wrapped with unidirectional glass and carbon fabric. They also studied the confining effects provided by a composite having multi-directional glass fabric as a reinforcement with 50% of weight oriented in the circumferential direction and 25% of its fibers each at $\pm 45^0$. Hoppel et al. (1997) proposed theoretical equations to predict the ultimate strength and axial strain in the wrapped cylinder based on the bi-linear response of the stress-strain curve obtained during the compression tests.

The determination of the mechanistic behavior of confined concrete is important, as it will help in investigating the following issues:

1. Application of the results obtained in the laboratory to an actual field situation where larger dimension piers are employed.
2. Prediction of the strength of the wrapped column accounting for environmental degradation and reduction in the composite properties.

STRESS-STRAIN MODEL

The stress-strain curve obtained for the cylinder wrapped with one layer of FRP is compared with that obtained for a plain concrete cylinder in Fig. 4.1. From this figure it is clear that the initial linear stage of the stress-strain response for the wrapped cylinder closely matches with the stress-strain curve obtained for the plain concrete cylinder. This in turn suggests that most of the load applied in this region is resisted by the concrete. A sudden change in slope is observed at a certain point when the load is continuously applied on the wrapped cylinder. It is understood that the concrete is partially failed at this point and the composite is mainly responsible for maintaining the integrity of the wrapped column thereafter (Kanatharana and Lu, 1998; Hoppel et al., 1997). For the same reason, the second linear region of the stress-strain response can be attributed to the post-cracking stage that identifies the point of change in slope of the curve as the point where the concrete is cracked. The column finally gives way when the strain to failure of the composite (0.0196) is approached, on further application of load.

The proposed model is discussed in two parts. Following the path set by the curve, the first part of the model explains the initial linear region of the bi-linear curve and the next part attempts to explain theoretically the second linear stage. Thus, this model aims to predict the cracking point, where an apparent deviation in the stress-strain curve is observed, and the ultimate failure point of the wrapped column. Therefore, the model includes the estimation of the following:

Cracking Point

Assuming that the cracking points obtained during the compression test are at a same stress level for both axial and the hoop stress-strain curves, the following quantities were estimated:

f'_{cr} = cracking stress for the wrapped cylinder (same in axial as well as hoop direction)

$\varepsilon^c_{\theta,cr}$ = tensile strain in concrete at the cracking point

$\varepsilon^c_{z,cr}$ = axial strain in concrete at the cracking point

Ultimate Failure Point

Similar to the cracking point, the following quantities at the ultimate failure point of the wrapped column were obtained:

f'_{cu} = ultimate failure stress of the wrapped cylinder

$\varepsilon^w_{\theta,u}$ = ultimate failure strain in the wrap in the hoop direction

$\varepsilon^c_{z,u}$ = ultimate failure strain in concrete in the axial direction

Initial Linear Stage of the Stress-Strain Response

In Figure 4.3 is illustratedthe different forces acting on the wrapped cylinder and composite wrap in the presence of an axial compressive load that is indicated by σ_z.

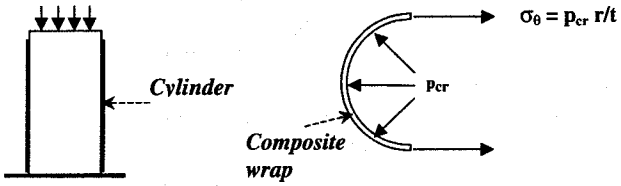

Figure 4.3 Free-body Diagram Illustrating the Forces Acting upon the Cylinder and the Composite Wrap

As a natural consequence of this external load, the cylinder tries to expand in the lateral direction, exerting a pressure on the walls of the composite wrap. This is indicated in the figure as $\mathbf{p_{cr}}$. As the composite wrap tries to hold the cylinder in place preventing the failure of concrete, a tensile stress, σ_θ, is developed in it, which can be obtained by simple force equilibrium and is given by:

$$\sigma_\theta = p_{cr}\, r/t \tag{4.1}$$

where r is the radius of the cylinder and t is the thickness of the composite wrap.

Eq. 4.1 can be used only when the axial load resisted by the composite wrap is negligible compared to that borne by the concrete cylinder. This assumption is reasonable since the thickness of the composite wrap is much smaller than the radius of concrete column (t<<r), so that the following relation is always satisfied

$$E_z^w \cdot A_w / E_c \cdot A_c << 1$$

where, E_z^w = elastic modulus of the wrap in the axial direction

E_c = modulus of elasticity of concrete

A_c and A_w = cross-sectional area fractions of the concrete and composite wrap respectively (see note below).

Cross-sectional area of concrete = πr^2 ; Cross-sectional area of composite wrap = $2\pi r\, t$

$$A_w = \frac{2\pi rt}{2\pi rt + \pi r^2} = \frac{2t}{2t + r}$$

$$A_c = \frac{\pi r^2}{2\pi rt + \pi r^2} = \frac{r}{2t + r}$$

Based on this concept, an equation predicting the axial compressive strength of the concrete cylinder in presence of a confining pressure, p_{cr}, was originally proposed by Richart et al. (1928) as

$$f_{cr}^{'} = f_c^{'} + 4.1 \cdot p_{cr} \tag{4.2}$$

where,

$f_{cr}^{'}$ = axial compressive strength of concrete in the presence of a confining pressure

$f_c^{'}$ = compressive strength of plain concrete without the confining pressure

As Eq. 4.2 can only be used when the confining pressure acting on the concrete is negligible compared to its compressive strength, i.e., $p_{cr} << f_c^{'}$, it is utilized to predict the stress at the cracking point in the bi-linear stress-strain curve. Therefore, p_{cr} could be more accurately recognized as the confining pressure at cracking point. Cracking stress of the wrapped cylinder can be obtained provided the value of p_{cr} is known.

Obtaining the Value of Confining Pressure, p_{cr} at the Cracking Point

In Eq. 4.1, the tensile stress in the composite is substituted as a product of tensile strain and the modulus of elasticity of the composite so that

$$\sigma_\theta = E_\theta^w \cdot \varepsilon_{\theta,cr}^w = p_{cr}(r/t) \tag{4.3}$$

where,

$\varepsilon_{\theta,cr}^w$ = cracking strain in the wrap in hoop direction

E_θ^w = modulus of elasticity of the wrap

Rearranging, Eq. 4.3, a relation for the hoop strain in the composite wrap at the cracking point can be given as

$$\varepsilon_{\theta,cr}^w = \frac{p_{cr} r}{E_\theta^w t} \tag{4.4}$$

Alternatively, applying the laws of mechanics, the hoop strain in concrete, $\varepsilon_{\theta,cr}^c$, at the cracking point is given by

$$\varepsilon_{\theta,cr}^c = \frac{f_{cr}' \nu_c}{E_c} \tag{4.5}$$

where,

ν_c = Poisson's ratio of concrete (normally given and taken here as 0.22)

It has already been mentioned that after the cracking point is reached, the composite wrap takes over the additional load applied preventing the wrapped cylinder from a catastrophic failure. Therefore, strain compatibility between the concrete and the FRP wrap would result in equal strains in both the members at the interface. Even without a perfect bond at the concrete-FRP interface, transfer of interfacial stress may take place. In this case, computations have to be refined to accommodate the slip. However, it should be stated that a no-slip condition or a perfect bond is assumed here. The following equality is therefore satisfied at the cracking point

$$\varepsilon_{\theta,cr}^w = \varepsilon_{\theta,cr}^c \tag{4.6}$$

Equating Eq. 4.4 and Eq. 4.5,

$$p_{cr} = f_{cr}' \nu_c \left(\frac{t}{r}\right)\left(\frac{E_\theta^w}{E_c}\right) \tag{4.7}$$

Since $p_{cr} << f_c'$, the ultimate strength of concrete, f_c', is nearly equal to f_{cr}', so that this quantity can be replaced by f_c' in Eq. 4.7 to obtain the approximate value of p_{cr}. Thus,

$$p_{cr} = f_c' \nu_c \left(\frac{t}{r}\right)\left(\frac{E_\theta^w}{E_c}\right) \tag{4.8}$$

Evaluation of Cracking Stress and Cracking Strain

Once the value of p_{cr} is obtained, it is substituted back in Eq. 4.2 to give the stress at the cracking point, f_{cr}', of the wrapped cylinder. Also, strains in the hoop direction for wrap and concrete at the cracking point given by $\varepsilon_{\theta,cr}^w$ and $\varepsilon_{\theta,cr}^c$ respectively are obtained from Eqs. 4.4 and 4.5.

The only quantity that remains to be estimated is the axial strain in the concrete at the cracking point, $\varepsilon_{z,cr}^c$. Since it was assumed that the concrete resists most of the load in the initial linear region of the stress-strain curve, the axial strain in concrete at this point can be represented by the following equation

$$\varepsilon_{z,cr}^{c} = \frac{f_{cr}^{'}}{E_c} \tag{4.9}$$

Post Cracking Stage of the Stress-Strain Response

Evaluation of the Ultimate Confining Pressure, p_{cu}

Assuming that the composite is in contact with the concrete throughout the second linear region of the curve until failure is reached, an equation that is similar to Eq. 4.4 is proposed to determine the ultimate tensile strain in the wrap. Consequently,

$$\varepsilon_{\theta,u}^{w} = \frac{p_{cu} r}{E_{\theta}^{w} t} \tag{4.10}$$

where,

$\varepsilon_{\theta,u}^{w}$ = ultimate failure strain in the wrap in the hoop direction

p_{cu} = confining pressure at failure of the wrapped cylinder

Normally for any composite material, the ultimate strain to failure in hoop direction, $\varepsilon_{\theta,u}^{w}$, is a known value or it could be obtained by conducting separate tensile tests to failure and measuring the ultimate tensile strain. Therefore, the only unknown quantity in Eq. 4.10 is the confining pressure at the ultimate point, p_{cu}, which can be easily obtained in the following way

$$p_{cu} = E_{\theta}^{w} \cdot \varepsilon_{\theta,u}^{w} \cdot \left(t/r\right) \tag{4.11}$$

Evaluation of the Ultimate Compressive Strength and Axial Strain

It can be easily understood from the post cracking response of the wrapped cylinder that the lateral confining pressure increases after the cracking point and this is responsible for a build up in the tensile stress within the composite wrap. The cylinder fails when the tensile strain in the wrap reaches the critical value. It was also stated earlier that after the cracking point, the composite wrap is solely responsible for an increase in the compressive strength of the cylinder. Therefore, the ultimate failure stress of the wrapped cylinder can be determined by assuming a direct proportionality between the increase in the stress after the cracking point to a similar increase in the lateral confining pressure. This results in the following equation

$$f_{cu}^{'} = f_{cr}^{'} + \alpha\left(p_{cu} - p_{cr}\right) \tag{4.12}$$

where,

$f_{cu}^{'}$ = ultimate stress of the wrapped cylinder

α = constant of proportionality (unknown)

Eq. 4.12 can be rewritten by substituting the values of p_{cr} and p_{cu} from Eqs. 4.8 and 4.11 respectively. This results in

$$f_{cu}^{'} = f_{cr}^{'} + \alpha \cdot \left(\varepsilon_{\theta,u}^{w} - \frac{f_c^{'} \nu_c}{E_c}\right) \cdot \left(\frac{t}{r}\right) \cdot E_{\theta}^{w} \tag{4.13}$$

The ultimate axial strain in the concrete, $\varepsilon_{z,u}^{c}$, is proposed as a sum of axial strain at cracking point to the amount of strain gained in the post-cracking stage.

$$\varepsilon_{z,u}^{c} = \varepsilon_{z,cr}^{c} + \frac{\left(f_{cu}^{'} - f_{cr}^{'}\right)}{E_c^{cr}} \tag{4.14}$$

Eq. 4.14 when rearranged using Eq. 4.13 gives:

$$\varepsilon_{z,u}^{c} = \varepsilon_{z,cr}^{c} + \alpha \cdot \left(\varepsilon_{\theta,u}^{w} - \frac{f_c' \nu_c}{E_c} \right) \cdot \left(\frac{t}{r} \right) \cdot \frac{E_\theta^w}{E_c^{cr}} \tag{4.15}$$

where,

E_c^{cr} = elastic modulus of the concrete in the post-cracking stage (unknown)

The model is complete when the values for f_{cu}' and $\varepsilon_{z,u}^{c}$ are estimated. This is possible when the numerical values for α and E_c^{cr} are obtained.

Determination of E_c^{cr} and α

At this stage since it was not possible to obtain independent expressions for α and E_c^{cr} .They were however evaluated from the experimental data as follows. Subsequently, these values were in turn used to estimate the ultimate failure stress and axial strain for the wrapped cylinder that in turn were compared with the experimental results.

Since the slope of the stress-strain curve signifies the modulus, E_c^{cr} is obtained experimentally by equating the ratio of the slopes of the two linear regions to the ratio of modulus of concrete in the respective stages. This results in:

$$\frac{E_c^{cr}}{E_c} = \left(\frac{m_2}{m_1} \right)_{exp} \tag{4.16}$$

where m_2 and m_1 are the slopes of the post cracking stage and the initial linear region of the experimental bi-linear curve in the axial direction obtained by simple linear regression on each of the two regions separately (see Chapter 3).
To obtain the ultimate axial strain and failure stress, the value of α needs to be determined. With successive iterations and a proximity test with the theoretical model and experimental values, the quantity α was determined. Therefore, the theoretical ultimate strength and axial strain values predicted by the model corresponds to the estimated value of α.

Variation of m_2/m_1 with Increase in Thickness of Composite Wrap

Similar tests when conducted on the wrapped cylinders with 2 and 3 layers of FRP revealed that the ratio between the cracked and un-cracked concrete modulus increases as the thickness to radius ratio (t/r) of the wrapped cylinder is increased. The ratio of m_2/m_1 for 1, 2 and 3 layers of FRP wrap were already listed in Chapter 3. It was observed that the numerical value of the parameter α was independent of the number of layers of wrap around the concrete cylinder. This value was approximately equal to 2.90. It should be noted that a different value of α may result in the case of confinement provided by the wrap for concrete cylinders of varying diameters. In such case, proper scaling procedures would have to be adopted besides an experimental verification. Value of α may also vary for a different type of composite wrap and it has to be obtained experimentally.

The model is thus a useful tool to relate the ultimate strength of the concrete column to the amount of confinement.. The stress and strain values at the cracking and the ultimate point obtained from the experiments and those predicted by the model are compared in Table 4.1. The applicability of this model is discussed in the following section.

Discussion of the Model

A fairly good agreement is observed between the ultimate strength and ultimate axial strain values predicted by the model and those obtained experimentally for cylinders wrapped with 1, 2 and 3 layers of wrap. Also, estimated values of the cracking stress and cracking strains for cylinders wrapped with one layer of FRP were consistent with the experimental results. However, it is apparent that the increase in cracking stress and cracking strains suggested by the theoretical model is not in proportion to the experimental observations. This difference could be attributed to a variation in the modulus of the composite for 2 and 3 layers of wrap. It should be noted that, in all the computations, the modulus of elasticity of the composite was assumed equal irrespective of the thickness of the wrap. To justify this difference further, an assumption stating that the stiffness of wrap in the axial direction is negligible compared to that of the concrete, is more precise for 1 layer than it is for 3 layers.

Table 4.1 Correlation between Bi-Linear Stress-Strain Model and Experimental Data

	1 LAYER		2 LAYERS		3 LAYERS	
	Model	Experimental (range)	Model	Experimental (range)	Model	Experimental (range)
t/r	0.0197		0.0439		0.0705	
Cracking Stage						
p_{cr} , psi	18.15		40.48		65.01	
f'_{cr} , psi	5579	4550 - 5600	5671	5800 – 6600	5771	6500
$\varepsilon^c_{z,cr}$	0.0014	0.0011 - 0.0015	0.0014	0.0023 -0.0026	0.0014	0.0021
E^{cr}_c	0.0003	0.0002 - 0.0004	0.0003	0.0005 - 0.0001	0.0003	0.000601
m_2/m_1		0.0438		0.0908		0.100
α	2.9		2.9		2.9	
Ultimate Stage						
p_{cu} , psi	1181.10		2633.8		4230.0	
f'_{cu} , psi	8952	8100 - 8500	13192	12455 – 13200	17850	16910
$\varepsilon^c_{z,u}$	0.0209	0.020 - 0.027	0.0224	0.023 - 0.027	0.0321	0.025

DAMAGE MODEL FOR AGED CONCRETE CYLINDERS

As seen in the previous sections, FRP wrapped concrete cylinders exposed to a combination of high temperature and liquid media experienced maximum reduction in the ultimate strength after 1000 hrs of aging; the reduction in strength continued upon continual exposure. On the other hand, samples exposed to an extended freeze-thaw cycles had a considerable change in their compressive strength after 3000 hrs of aging. One can clearly observe a progressive damage process as the wrapped cylinder is exposed to severe environment with time. An important objective is to model this degradation process taking place in the FRP wrapped cylinders. It was also seen that the aged cylinders exhibit a bi-linear stress-strain relationship similar to the control samples when subjected to an axial load. In this chapter, the bi-linear stress-strain model derived in the previous sections is extended to incorporate changes in the properties of the composite to predict the extent of damage.

Derivation of the Damage Model

Concept

Since exposure to accelerated aging conditions for as many as 3000 hrs did not alter the strength of the plain concrete cylinder, it is confirmed that degradation of concrete is not an important factor responsible for a change in compressive strength of the wrapped cylinder. Therefore, in this case, possible elements that could deteriorate after exposure to aging conditions are (i) the composite wrap and, (ii) interfacial bond between the concrete and the FRP. Results from DMTA experiments indicated a noticeable change in the property of the composite specimens aged in liquid media. But the major challenge in this set of experiments is to estimate the damage caused by different aging conditions.

Properties of the composite wrap can be altered in three ways:

1. Change in the modulus of the composite
2. Reduction in the ultimate tensile strain to failure, indicating that the composite has become brittle upon aging
3. Combination of the above two possibilities

For an assumption that the reduction in the modulus of FRP is a factor in reducing the ultimate strength of the cylinder after aging, the reduced modulus of the wrap is accounted by the following expression

$$E_{\theta}^{w}(t) = E_{\theta}^{w}\left(1 - d_1(t)\right) \tag{4.17}$$

where,

$E_{\theta}^{w}(t)$ = Modulus of the composite after exposure to aging for a time period of "t"

$d_1(t)$ = Damage parameter associated with the modulus of FRP after an aging time of "t"

Similarly, the reduced ultimate strain of the composite can be expressed as

$$\varepsilon_{\theta,u}^{w}(t) = \varepsilon_{\theta,u}^{w}\left(1 - d_2(t)\right) \tag{4.18}$$

where,

$\varepsilon_{\theta,u}^{w}(t)$ = Ultimate strain of the aged composite after a time period of "t"

$d_2(t)$ = Damage parameter associated with the ultimate strain to failure after aging time "t"

For the initial undamaged state of the cylinder, i.e., at time equal to zero, $d_i(0) = 0$. For the limiting stage which represents the situation where there is complete damage to the wrap, $d_i(t_{lim}) = 1$. When the numerical values of "d" are monitored over a period of time, the rate of damage can be obtained for a particular composite and a given accelerated aging condition. Thus a kinetic law for the degradation process can be obtained for determining the residual strength of the wrapped cylinder after any given time.

Theoretical Evaluation of the Reduction in Cracked Strength and Strain

Stress and strain values at the cracking point of the wrapped cylinder are altered if there is any change in the modulus of the composite. A reduction in modulus results in an equivalent reduction in the confining pressure at the cracking point. This value is obtained by substituting Eq. 4.17 into Eq. 4.8 and can be given as follows

$$p_{cr,d} = f_c^{'} \nu_c \left(\frac{t}{r}\right)\left(\frac{E_{\theta}^{w}\left(1 - d_1(t)\right)}{E_c}\right) \tag{4.19}$$

where,

$p_{cr,d}$ = value of confining pressure at cracking point for damaged specimen

Once an estimate of $p_{cr,d}$ is obtained, it is substituted in Eq. 4.2 to obtain cracking stress of the aged cylinder. This is given by the following relation:

$$f_{cr,d}^{'} = f_c^{'} + 4.1 \cdot p_{cr,d} \tag{4.20}$$

Hoop and axial strains in concrete for the damaged cylinder follow. These are calculated using Eq. 4.21 and Eq. 4.22, respectively.

$$\varepsilon_{\theta,cr,d}^{c} = \frac{f_{cr,d}^{'} \cdot \nu_c}{E_c} \tag{4.21}$$

$$\varepsilon_{z,cr,d}^{c} = \frac{f_{cr,d}^{'}}{E_c} \tag{4.22}$$

where,

$\varepsilon_{\theta,cr,d}^{c}$ = cracked strain in hoop direction for the damaged cylinder

$\varepsilon_{z,cr,d}^{c}$ = cracked strain in axial direction for the damaged cylinder

Confining Pressure at the Ultimate Failure Point of the Cylinder

Ultimate pressure at the confining point depends on the modulus and ultimate strain to failure of the composite. Hence, the ultimate pressure at the confining point for the aged cylinder can be given by the following equation that is analogous to Eq. 4.11.

$$p_{cu,d} = E_{\theta}^{w}\left(1-d_1(t)\right)\cdot\varepsilon_{\theta,u}^{w}\left(1-d_2(t)\right)\cdot\left(t/r\right) \tag{4.23}$$

Theoretical Evaluation of Reduction in the Ultimate Strength and Strain

An equation for the ultimate strength of the cylinder is obtained by modifying Eq. 4.13. This modification involves substituting Eqs. 4.17, 4.18 and 4.20 in Eq. 4.13. The result is

$$f'_{cu,d} = f'_{cr,d} + \alpha\cdot\left(\varepsilon_{\theta,u}^{w}\left(1-d_2(t)\right)-\frac{f'_c\nu_c}{E_c}\right)\cdot\left(\frac{t}{r}\right)\cdot E_{\theta}^{w}\left(1-d_1(t)\right) \tag{4.24}$$

The ultimate axial strain of the aged concrete specimen follows similar substitution of Eqs. 4.17, 4.18 and 4.22 in Eq. 4.15. This results in Eq. 4.25

$$\varepsilon_{z,u,d}^{c} = \varepsilon_{z,cr,d}^{c} + \alpha\cdot\left(\varepsilon_{\theta,u}^{w}\left(1-d_2(t)\right)-\frac{f'_c\nu_c}{E_c}\right)\cdot\left(\frac{t}{r}\right)\cdot\left(\frac{E_{\theta}^{w}\left(1-d_1(t)\right)}{E_{c,d}^{cr}}\right) \tag{4.25}$$

where,

$f'_{cu,d}$ = Ultimate strength of the cylinder after aging

$\varepsilon_{z,u,d}^{c}$ = Ultimate axial strain in concrete after aging

$E_{c,d}^{cr}$ = Damaged cracked modulus of the concrete

To estimate $f'_{cu,d}$ and $\varepsilon_{z,u,d}^{c}$ for the damaged cylinder, ultimate hoop strain in the wrap after aging (value of d_2), the modulus of FRP wrap after aging (value of d_1), the modulus of the cracked concrete after aging, $E_{c,d}^{cr}$, and the value of α need to be known. The values of d_1 and d_2 are computed from the modulus and ultimate strain obtained from the tensile test experiments on the FRP samples. Since independent equations for obtaining $E_{c,d}^{cr}$ and α could not be formulated, they have to be determined from the experiments alone. Different assumptions involved in obtaining these quantities are given below.

On the basis of the result that the parameter α is independent of the confinement that was provided when different layers of wrap were used, it was assumed that the value of α remains the same in the case of aged specimens also.

The second linear region of the bi-linear curve for the aged specimen was almost parallel to that obtained for the control specimen. Since the value of the cracked concrete modulus is defined as the ratio between the slopes of the two linear regions of the curve (Eq. 4.14), this value can be considered to be the same for the control specimen and the aged cylinder.

Estimates of d_1 and d_2 are obtained from the tensile tests on aged FRP samples.

Predictions from the Damage Model

Table 4.2 gives the values for d_1 and d_2 for the given aging conditions using the results obtained from the tension tests on the FRP samples (Table 3.6). Since the tensile tests were conducted only for an aging time of about 1500 hrs, estimates of damage parameter could not be obtained for higher periods of aging. From this table it is evident that changes in the elastic modulus and the ultimate tensile strain of the FRP are indeed responsible for the reduction in the ultimate strength of the cylinder.

Table 4.2 Comparison of Predicted Values from the Model with Experimental Results

AGING CONDITIONS	d_1	d_2	PREDICTED VALUES FROM MODEL		EXPERIMENTAL RESULTS	
			$f'_{cu,d}$ (psi)	$\varepsilon^c_{z,u,d}$	$f'_{cu,d}$ (psi)	$\varepsilon^c_{z,u,d}$
Dry Heat, 150 ^{0}F	0.038	-0.102	8953	0.0210	8077	0.0196
pH 12.4, 73 ^{0}F	0.048	0.00	8602	0.0189	8411	0.0206
pH 12.4, 150 ^{0}F	0.055	0.423	7284	0.0113	6150	0.0088
Freeze-thaw	0.141	0.078	8086	0.0160	8051	0.0159

As shown in Table 4.3, reasonable predictions of ultimate strength and strain for the aged cylinders were obtained (within 10%) for the aging conditions mentioned except for pH 12.4 and 150 ^{0}F where, the model overestimated the residual compressive strength of the cylinder (20% error). This could be because the damage model discussed above identifies the damage caused to the FRP only considering a change in its modulus of elasticity and the ultimate tensile strain to failure. It is noted that another major factor that may have caused the reduction in the strength of the cylinder is the interfacial debonding between the FRP wrap and the concrete surface or a weakening of fiber-matrix bond. Since the model assumes that at all load points the FRP wrap is bonded to the concrete cylinder, it actually fails to recognize debonding between the two members. Therefore, in the case where the actual reduction in the strength of the cylinder was more than that predicted by the model, it is apparent that other factors like debonding at the FRP-concrete interface or even a similar effect at the fiber-matrix interface could have had a partial contribution in reducing the compressive strength of the cylinders. Thus, this model with the aid of separate experiments can closely determine the causes for the reduction in ultimate strength and ultimate strain of the wrapped cylinder.

Table 4.3 Difference Between Experimental Ultimate Strength And Axial Strain Values And Model Predictions

AGING CONDITIONS	% ERROR IN ULTIMATE STRENGTH	% ERROR IN ULTIMATE STRAIN
Dry Heat, 150 ^{0}F	-10.9	-7.1
pH 12.4, 73 ^{0}F	-2.3	8.2
pH 12.4, 150 ^{0}F	-18.4	-28.4
Freeze-thaw	-0.4	-0.6

Comparison of Ultimate Tensile Strains: Compression Test vs. Tension Test

For the aging conditions mentioned, Table 4.4 compares the ultimate hoop strain recorded in the composite wrap during the compression tests with the ultimate tensile strain recorded in the FRP during the tension test. In this table the reported values of d_2 are estimated using the data from the compression test instead of tension tests.

Table 4.4 Comparison of Ultimate Failure Strain (Tensile) From The Compression Tests and The Tensile Tests

AGING CONDITIONS	ULTIMATE TENSILE STRAIN		d_2 (Based on Compression Tests)	d_2 (Based on Tension Tests, Table 4.2)
	Tension Test	Compression Test		
Control	0.0196	0.0174	-	-
Dry Heat, 150 ^{0}F	0.0216	0.0163	0.063	-0.102
pH 12.4, 73 ^{0}F	0.0196	0.0183	-0.052	0.00
pH 12.4, 150 ^{0}F	0.0113	0.0089	0.489	0.423
Freeze-thaw	0.0181	0.0144	0.172	0.078

The estimated values of d_2 based on the compression tests (Table 4.4) were substituted in the damage model to predict the ultimate failure strength and the ultimate axial strain of the aged cylinder. In Table 4.5 are reported the predicted values of the ultimate strength and the ultimate axial strain by the model. These values are compared with the experimental results and a percentage error is evaluated. It is observed that the error in predicting the values of ultimate strength was thereby reduced (compared to error analysis reported in Table 4.3). At the same time, it is also observed that with this operation, the error in predicting the ultimate axial strain was more than that reported previously.

Table 4.5 Error between the Experimental and Predicted Values Based on Modified Estimates of Parameter d_2

AGING CONDITIONS	PREDICTED VALUES FROM MODEL		EXPERIMENTAL RESULTS		% ERROR	
	$f'_{cu,d}$ (psi)	$\varepsilon^c_{z,u,d}$	$f'_{cu,d}$ (psi)	$\varepsilon^c_{z,u,d}$	Stress	Strain
Dry Heat, 150 ^{0}F	8112	0.0161	8077	0.0196	-0.43	17.85
pH 12.4, 73 ^{0}F	8398	0.0178	8411	0.0206	0.15	13.59
pH 12.4, 150 ^{0}F	6912	0.0092	6150	0.0088	12.39	4.55
Freeze-thaw	7564	0.0130	8051	0.0159	6.05	18.24

It should be noted that this computation was attempted only to investigate the capabilities of the damage model in order to furnish a reason for its substantial error in predicting the ultimate strength of cylinder for the aging condition pH 12.4 at 150 ^{0}F. The purpose of these computations was to show that if the "actual strain to failure measurements" from wrapped concrete cylinders were adopted, the damage model prediction for ultimate strength ($f'_{cu,d}$) would be more accurate.

Although the error in predicting the axial strain was significant, prediction of the ultimate strength was considered to be more accurate for the validation of the damage model. This is because, from a structural point of view the prediction in ultimate strength is more important than the prediction of axial strain to failure. Besides, the experimental measurement of ultimate strength is "accurately" computed as load/area. On the other hand the axial strain is measured with the gages bonded on to the FRP wrap but not on the concrete core. Also, the model disregards axial stresses in the FRP wrap.

Stress in Composite Wrap vs. Stress in FRP Tensile Coupons

The stresses experienced by the FRP wrap on the concrete cylinder are not the same as in the FRP tensile coupons. This is a common concern related to the use of fiber reinforced composites for seismic retrofit that questions an accurate determination of the composite properties under loading conditions replicating the actual situation of a confined column. Coupon level tension, flexure and shear tests conducted routinely for composite characterization do not address this issue adequately. To determine the composite properties which simulate those in a field wrap, a Naval Ordinance Loading (NOL) ring or "burst" test is conducted. In this test a 20" diameter ring of the composite material used as a jacket is placed in an apparatus that is hydraulically pressurized internally to simulate confinement and impart only circumferential stresses to the ring. Unlike tension tests, NOL ring tests give a true indication of structural performance, and failure mode including replicating failure initiation. This test is also used to accurately assess the effect of environmental exposure on the behavior of the retrofit system itself including that induced by premature softening or plasticization of the adhesive, if any (Seible and Karbhari, 1996).

CHAPTER 5 -ULTRASONIC NONDESTRUCTIVE EVALUATION

Introduction

Nondestructive techniques have played an important role in military and aerospace applications during the past few decades. Their importance in the infrastructure industry has increased significantly in recent years because of the increasing cost of rehabilitation in major structures such as bridges. Early detection of loss in structural integrity would facilitate the rehabilitation work and enhance the life of a structure. The objectives of nondestructive testing in civil engineering are to classify and quantify flaws, monitor structural integrity, predict performance of structural members, etc. Refinement of existing methods and development of new quantitative analysis tools are necessary to increase the capability and reliability of the testing methods.

Ultrasonic nondestructive testing is a very popular and versatile technique where useful information can be obtained using innovative signal processing techniques. The recent advancements in electronics and computers have made it possible to develop very powerful testing procedures and analysis methodology. Research efforts are also being directed at developing ultrasonic testing that can monitor material integrity and rate of degradation during service. Ultrasonic testing is conducted by transmitting a beam of ultrasonic energy into the material and measuring one or more of the following (Bar-Cohen et al., 1992; Halabe and Franklin, 1998):

(1) Travel time of received ultrasonic waves.
(2) Attenuation and reflection measurements
(3) Features in spectral response of the received signal.

Because ultrasonic waves are mechanical phenomena, they are most adaptable for detecting the structural integrity of engineering materials. Their primary applications are: (1) discontinuity detection, (2) thickness measurements, (3) determination of elastic constants, (4) evaluation of stresses, (5) study of metallurgical structure. However, in recent years its potential to detect anomalies in composite materials is vastly explored.

Advantages and Disadvantages of Ultrasonics

The advantages of ultrasonic techniques are: (1) high sensitivity, allowing detection of minute discontinuities; (2) good penetrating power, allowing examination of thick sections, (3) accuracy in measurement of position and size of discontinuity, (4) fast response, allowing rapid measurement by automated testing, (5) capability of measurement with access from only one surface of the test object. The test conditions that may limit the application of ultrasonic testing are: (1) unfavorable test object geometries such as irregular size, surface roughness, (2) undesirable internal structure such as grain size, structure porosity. The most common method of ultrasonic testing is by using piezoelectric transducers to transmit and receive longitudinal waves, shear waves or surface waves. Ultrasonic testing poses no hazard to the operator or any nearby personnel, which makes it a suitable method for on-site testing. Moreover, only simple training to the user or the operator is needed for applications in which the problem is clearly defined and the technique is well established.

Research Objectives

The objectives of this study on ultrasonic nondestructive testing are as follows:

(a) To develop an ultrasonic testing methodology capable of assessing the structural integrity of FRP wrapped concrete compression members. The methodology developed here should be suitable for testing and evaluation of field members.

(b) To correlate ultrasonic data with ultimate compressive stress and axial/hoop strains of FRP wrapped concrete cylinders, so that material properties and structural integrity of such members can be predicted using ultrasonic measurements.

Ultrasonic Testing Equipment

Ultrasonic testing is performed using the state-of-the-art equipment. Tektronics TDS 460 four channel digitizing oscilloscope was used in this study to acquire and display the ultrasonic waves. The oscilloscope had a bandwidth of 350 MHz at -3 dB attenuation and a maximum sampling rate of 100 MS/s for digitizing the signal. The digitizing rate adopted for this study was 2.5 MHz for broadband piezoelectric transducers at 250 kHz central frequency. The oscilloscope was self calibrating and adjusted to operate at ambient temperatures between +20° C and +30° C. The oscilloscope was compatible with GPIB-PCII/IIA which was a half size IEEE-488 interface board used for data transfer

into a computer. The receiver used in this study was RITEC BR-640. This is a broadband receiver (10 kHz to 10 MHz at -3dB) which was equipped with an amplifier. The bandwidth control was available through adjustable high pass and low pass filters. The experimental settings used in this research was 100 kHz and 1 MHz for the high pass and low pass filters, respectively. The amplification gain provided by the receiver box had a range of -12 dB to 64 dB in gain steps of 4 dB. The receiver gain used in this study was + 36 dB. Ultran broadband piezoelectric transducers producing longitudinal waves were used in this study. The transducers were 0.5" in diameter and had a central frequency of 250 kHz. The transducers were equipped with flexible delay tips to provide better contact and grip on the FRP wrap. Crystal excitations in the transducers were performed using electronic instruments called pulse generators. For applications that require narrow band signals, sinusoidal bursts can be used to excite the transducers. Ritec Advanced Measurement System (RAM - 10000) was used to generate sine wave pulses. This pulser had a very high power option which is up to 2400 volts peak-to-peak. When operating at high frequencies and high voltages, significant heat can be generated internally in the transducers which can damage the transducers. Hence when operating at high frequencies, using few cycles at low voltages is desirable. All controls to this sine wave pulser were through a computer. Figure 5.1 shows the computer menu for producing 10 cycle sine pulse of 400 volts peak-to-peak at 250 kHz frequency by RAM-10000 which was used to excite the transducers. Typical experimental setup for ultrasonic testing used in this study is shown in Figure 5.2.

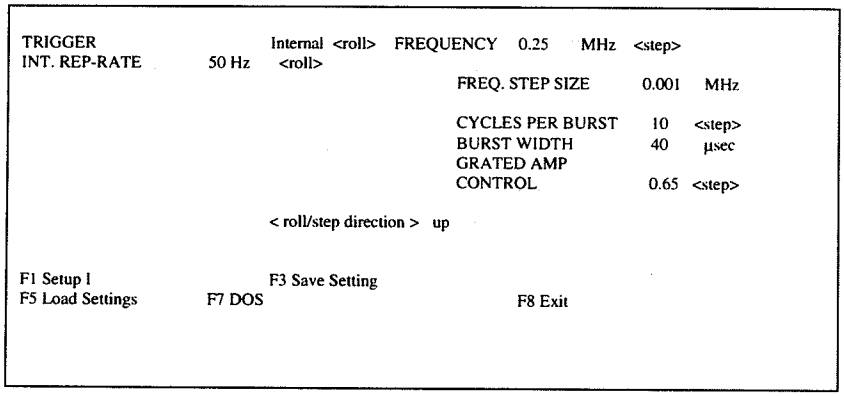

Figure 5.1. Computer menu for control of RAM-10000

Data Acquisition and Signal Processing

Data acquisition in ultrasonic testing is achieved by transducers that transform the mechanical vibrations into an electrical signal. The signals are continuous, and conversion of analog signals to digital signals is required for using the processing software in computers. Sampling a signal at discrete intervals and digitizing the amplitudes results in conversion of an analog signal to digital numbers. The process that converts the series of sample amplitudes into a series of discrete numbers is known as digitization. The time interval at which the analog signal is digitized should be small enough to reproduce the waveform without any distortion. Halabe et al. (1996) had adopted a sampling frequency that is ten times the central frequency of the transmitter. Sufficient number of points should be used during the acquisition, to acquire the required length of the signal for analysis. When continuous signals are received, averaging the signals will improve the received time domain signal because it reinforces the significant signal while smoothing the random noise.

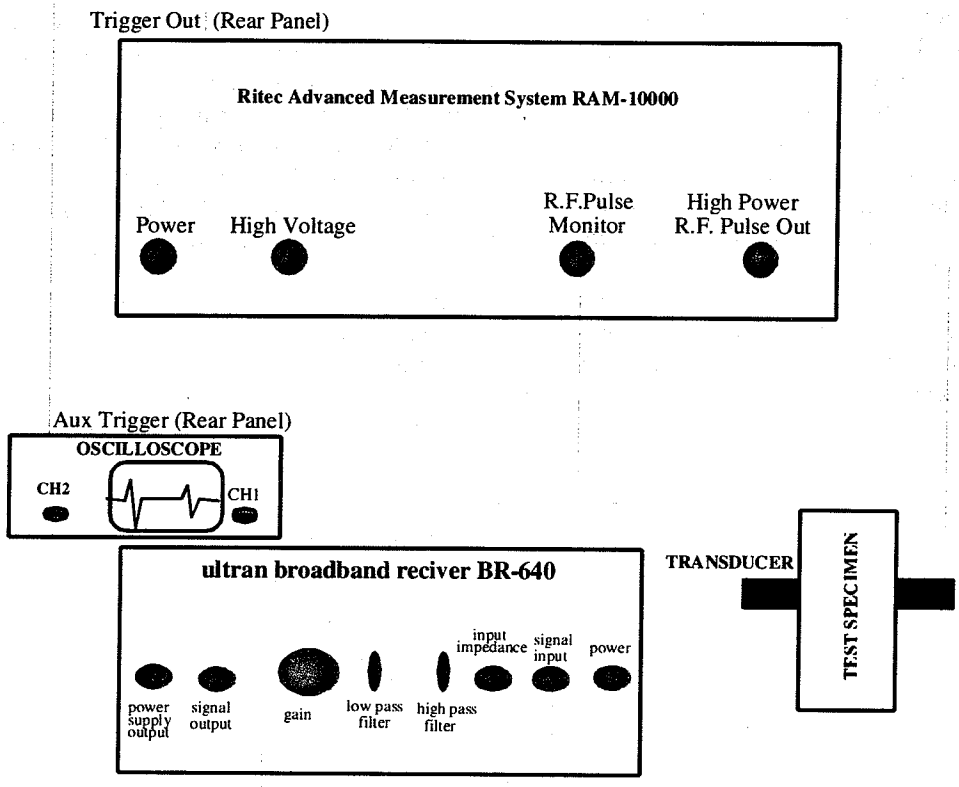

Figure 5.2 Experimental Setup

Interpretation of time domain ultrasonic signals can involve (a) wave arrival time and (b) signal amplitude. A time delay of the ultrasonic wave can be noticed when the wave travels around a defect. Loss in amplitude can also be related to the presence of flaws. Root mean square (*RMS*) amplitude of the time domain signal is a popular tool since it gives a direct measure of the strength of the signal received. *RMS* amplitude can be mathematically expressed as:

$$RMS = \sqrt{\frac{\sum_{i=1}^{N} X_i^2}{N}} \tag{5.1}$$

where N is the number of discrete ordinates measured on the signal, and X_i is the ordinate of the signal at the i^{th} discrete point on the signal.

Analysis of ultrasonic signals in the time domain using methods such as time of flight or amplitude parameters often results in ambiguity, errors, and limited information. On the other hand, analysis of the frequency response can offer the much required additional information (Halabe and Franklin, 1998). Therefore, the current study uses innovative ultrasonic measurement and data analysis methodology developed by CFC researchers (Halabe and Franklin, 1998) to increase the sensitivity and reliability of the ultrasonic technique by measuring signal energy in frequency domain. This approach makes use of Fast Fourier Transforms (FFT), a popular tool for analyzing digitized waveforms. Squaring the FFT amplitudes, $|FS(f)|$, gives the power spectral density (PSD) curve. The area under the power spectral density curve, P, can be used to quantify the total energy in a waveform. This parameter is also called the zeroth moment of PSD and can be mathematically represented as (Halabe and Franklin, 1998):

$$P = \sum_{i=1}^{N/2} \frac{1}{2} |FS(f_i)|^2 \, \Delta f \tag{5.2}$$

Here N represents the total number of points in the time domain signal to be analyzed in the frequency domain, and f denotes the frequency. The total energy in an ultrasonic signal is very sensitive to loss of material integrity, and is a more reliable parameter compared to peak magnitude of PSD (Halabe and Franklin, 1998). Skewness of the PSD curve could also be used to characterize defects, specially if frequency changes are expected in case of ultrasonic signals through defects. Several past studies have used third moment (a measure of skewness) of the spectral response curve. The third moment of the PSD curve is given by (Horne and Duke, 1993):

$$M_3 = \sum_{i=1}^{N/2} \frac{1}{2} |FS(f_i)|^2 f_i^3 \Delta f \tag{5.3}$$

Another important parameter of the power spectral density curve is its central frequency (*C.F.*). This parameter is also called the location parameter and can be mathematically represented as (Halabe and Franklin, 1998):

$$C.F. = \frac{\sum_{i=1}^{N/2} \frac{1}{2} |FS(f_i)|^2 f_i}{\sum_{i=1}^{N/2} \frac{1}{2} |FS(f_i)|^2} \tag{5.4}$$

This study makes use of the peak magnitude of PSD, the zeroth moment or area under PSD (P), the third moment (M_3) and the Central Frequency (*C.F.*) of the power spectral density curve. The use of these parameters on PSD curves instead of FFT curves is advantageous because by squaring the FFT magnitudes the emphasis is placed on high amplitude signals and the effect of small amplitude signals such as noise is minimized (Halabe and Franklin, 1998).

Measurement Conditions for Making Consistent Amplitude Measurements

It is important to note that the amplitude $|FS(f)|$ which influence the parameters used to define the PSD curve is affected by some experimental factors (Halabe and Franklin, 1998). Therefore, it is important that these factors be identified and carefully standardized for a specific application. Only then repeatable measurements and meaningful comparisons can be made. The type of ultrasonic couplant used has significant effect on the amplitude of the signal. The application of the couplant should always be a uniform thin layer. Adopting the right couplant for an application will greatly be influenced by the surface characteristics of the material. UT-X couplant manufactured by Sonotech, Inc. is a general purpose couplant which produces signals with high signal-to-noise ratio. Therefore, this couplant was adopted in this study.

Yet another important factor influencing the signal amplitude is the clamping force used on the transducers (Halabe et al., 1996, 1998). Use of constant clamping force on the transducers is necessary to obtain good repeatability in the measurement conditions. The contact area between the transducer and the material generally dictates the amount of clamping force. One has to obtain the optimal clamping force for a given application. Too small a clamping force will result in poor contact between the transducer and the material while too large a clamping force will cause the couplant to dry rapidly or hinder the sensor crystal vibration. These factors will lead to inconsistent signal measurements. Optimum clamping force for the 0.5" diameter transducers used in this study was obtained as 20 lb.

One can also use a domain window, such as Hanning or Hamming windows, on time domain signals to force it to decay. However, the signal should not be very dispersive and the characteristic shape of the wave should not change much as it propagates. If the signal is of dispersive nature, use of Finite Impulse Response (FIR) filters such as Kaiser or Remez windows are recommended. These techniques will help suppress noise and enhance signal detection. This study uses Kaiser bandpass filter in the range of 225 kHz to 275 kHz with a central frequency of 250 kHz.

Experimental Procedure and Preliminary Investigation

Preliminary tests were conducted to observe if ultrasonics could be effectively used for detecting failure of structural integrity in FRP wrapped concrete cylinders. Plain concrete cylinder, concrete cylinder wrapped with one layer of SEH51, concrete cylinder wrapped with two layers of SEH51, and concrete cylinder wrapped with two layers of SEH51 with artificial debonding (induced by a Teflon sheet) were used in this study. The specimens were tested in this study using 250 kHz transducers (12.7 mm or 0.5" diameter) excited by ten cycle sine pulse with peak-to-peak amplitude of 400 volts. UT-X general purpose couplant and 20 lb clamping force on the transducer was used for obtaining consistent amplitude measurements. 100 waveforms were averaged to remove the effect of random noise. The signals were

acquired at 40 dB receiver gain and digitized at 2.5 MHz. Typical through-transmission signals received from plain concrete, single wrap, double wrap, and debonded (between double wrap and concrete) specimens are shown in Figure 5.3. The vertical scale adopted for the signal received from the debonded specimen is different because of the very low amplitude. The region between two vertical broken lines in Figure 5.3 is the window extracted for spectral analysis which consisted of 512 points. The corresponding energy (Integral of PSD) curves are shown in Figure 5.4. The experimental values are tabulated in Table 5.1.

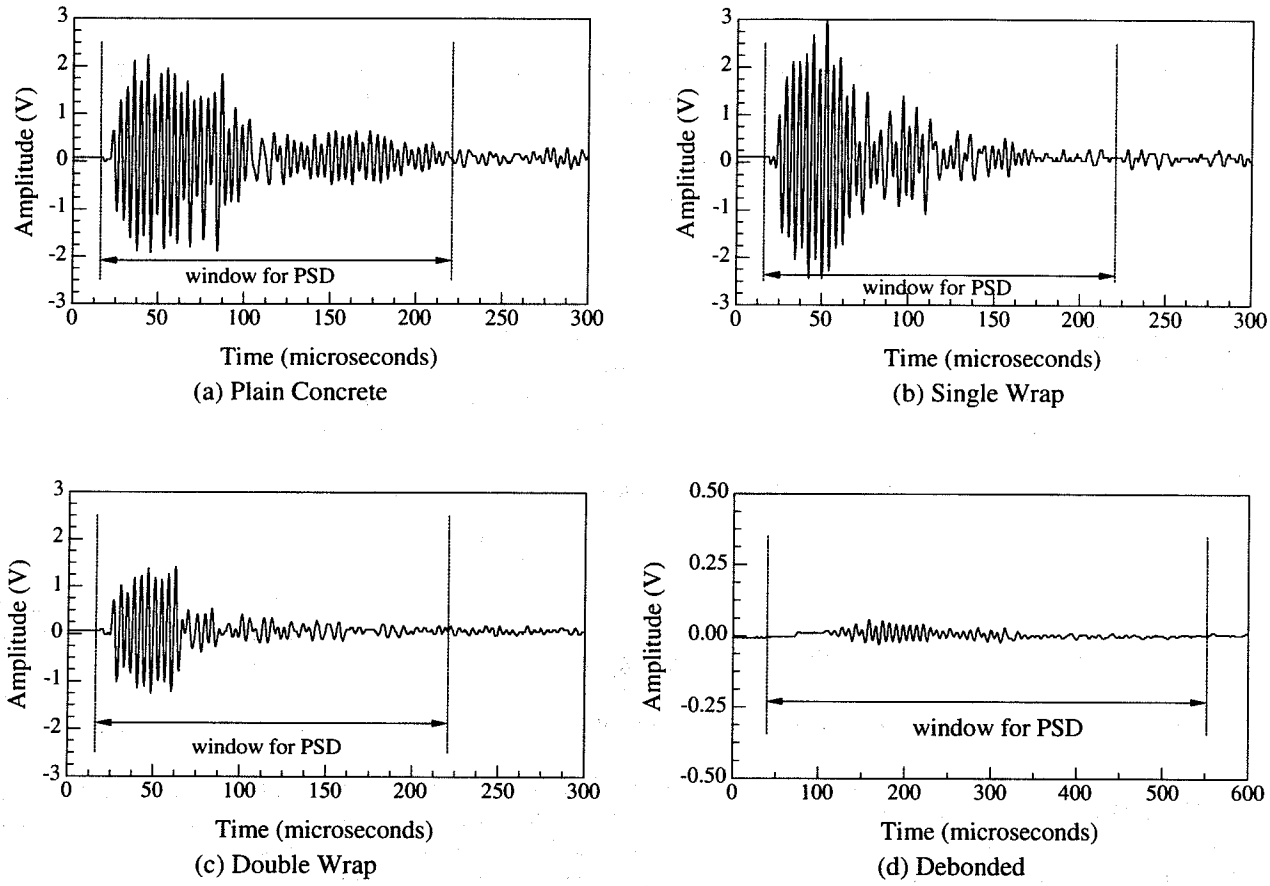

Figure 5.3. Time domain signals obtained from sound and debonded specimens for preliminary investigation

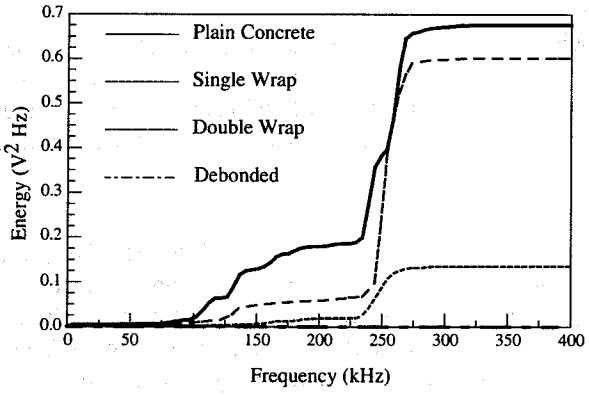

Figure 5.4. Cumulative PSD plots for the time domain signals shown in Figure 5.3

Table 5.1. Experimental Results Obtained from FRP Wrapped Concrete Specimens Using 250 kHz Central Frequency Transducers

Region	Arrival Time (μs)	Peak-to-peak Amplitude (V)	PSD Curve Parameters		
			Area (V^2 Hz)	Third Moment (V^2 Hz^4)	Central Frequency (kHz)
Plain Concrete	23.2	4.16	67.72×10^{-2}	9.3×10^{15}	239
Single Wrap	23.6	5.28	60.20×10^{-2}	9.3×10^{15}	241
Double Wrap	26.0	2.68	13.49×10^{-2}	2.0×10^{15}	235
Debonding	36.4	0.01	4.07×10^{-5}	0.4×10^{12}	176

As shown in Table 5.1, the arrival time increases in case of FRP wrapped members because the wrap thickness provides additional travel distance. Moreover, travel velocity is significantly lower in composite material (in transverse direction) compared to concrete. Peak-to-peak amplitude in the time domain was not found to be a reliable parameter. In fact, the amplitude obtained from the single wrap specimen is higher than the amplitude from plain concrete. The loss in signal energy due to increases in the travel distance and the additional interfaces in wrapped members is indicated by the area and third moment of the PSD curve (see Table 5.1). When one wrap is used, the bond is very good and only a small loss in the energy is observed. In case of double wrap the presence of bond or glue between the wraps as well as the bond between the concrete and wrap has a much greater influence on the transmitted energy. This indicates that the bond between the two individual composite wraps is not as strong as that between the concrete and wrap. In case of the debonded specimen, the arrival time increased significantly (since the wave had to travel in the circumferential direction around the debonded specimen). Also, there is drastic reduction in the area, third moment and central frequency parameters. The significant decrease in the central frequency is consistent with the wave travel in the circumferential direction through the composite wrap (a dispersive medium) in case of debonded specimens. The loss in energy and the frequency shift between the double wrap and the double wrap with debonding is very significant. This indicates that the proposed methodology using area under PSD (energy parameter) can be successfully used to detect debonding between concrete and composite wrap in rehabilitated field members. Hence, for further testing and evaluation of FRP wrapped concrete members subjected to degradation due to environmental aging, spectral analysis was employed.

Ultrasonic Testing Of Specimens Subjected To 1000 Hours of Accelerated Environmental Aging

Concrete cylinders were wrapped with one layer of SEH 51 woven fabric and subjected to various accelerated environmental aging for 1000 hours. One specimen for each aging condition was used for ultrasonic testing. The specimens were tested using 250 kHz transducers (12.7 mm or 0.5" diameter) excited by ten cycle sine pulse with peak-to-peak amplitude of 400 volts. UT-X general purpose couplant and clamping force of 20 lb was used for obtaining consistent amplitude measurements. 100 waveforms were averaged to remove the effect of random noise. The through-transmission signals were acquired at 40 dB receiver gain and digitized at 2.5 MHz. Ultrasonic signals were received from six different locations for each specimen to obtain the overall condition of the structural integrity between concrete and FRP wrap. The experimental results obtained from specimens subjected to 1000 hours of accelerated aging further indicate that ultrasonics can be used to detect degradation of FRP wrapped concrete members. The analytical procedure for detecting degradation in structural integrity is illustrated with an example. Time domain signals received from a control sample (under room temperature) and a specimen subjected to aging environment (pH = 7; Temperature, T = 150 °F; and Relative Humidity, RH = 100%) are shown in Figure 5.5. Very small change is noticed in the arrival time. A much greater change is observed in the time domain amplitude of the signals as shown in Figure 5.5. This change between the two signals is magnified in the spectral analysis which also provides additional information. Spectral analysis was conducted on the extracted region (512 points long, between the two broken vertical lines shown in Figure 5.5. The obtained power spectral Density (PSD) curves and their cumulative plots for the two signals are shown in Figure 5.6. The PSD curves shows a big difference indicating that the energy in the received signal has been significantly affected. The cumulative plot indicates a loss of 66% in the energy for the specimen subjected to accelerated aging. The third moment

of the PSD curve also showed a loss of 62% in the energy. Such a huge drop in energy is an indication of degradation in the specimen. Central frequency of the PSD curve did not decrease indicating that the environmental aging conditions did not affect the wave attenuation properties of the FRP wrapped specimens.

Experimental results obtained for the various specimens subjected to 1000 hours of environmental aging are shown in Table 5.2. A close relationship is observed between the ultrasonic signal energy (area under the PSD curve) and the ultimate compressive strength of specimens within the same batch (i.e., same type of environmental aging). In order to study this relationship further and develop correlation equations, ultrasonic and static compression tests were conducted on the same specimen and the results studied on a one-to-one basis using specimens subjected to 3000 hours of environmental aging, as described in the next section.

Table 5.2. Experimental Results Obtained from Concrete Cylinders Wrapped with FRP and Subjected to Various Accelerated Aging Conditions for 1000 Hours

Environmental Conditioning	Arrival Time (μs)	Peak-to-Peak Amplitude (V)	PSD Curve Parameters				Ultimate Compressive Strength (psi)
			Peak Magnitude (V^2)	Area (V^2 Hz)	T. M. (V^2 Hz^4)	C. F. (kHz)	
Control Sample T = 73 °F	24.0	5.44	3.61×10^{-5}	60.20×10^{-2}	9.33×10^{15}	242	8445
pH=7; T=150 °F RH = 100%	24.8	3.20	0.98×10^{-5}	20.28×10^{-2}	3.54×10^{15}	252	5990
pH=9.4; T=73 °F RH = 100%	24.0	4.52	2.56×10^{-5}	46.40×10^{-2}	7.83×10^{15}	253	8316
pH=12.4;T=73 °F RH = 100%	24.4	4.90	3.63×10^{-5}	58.16×10^{-2}	8.83×10^{15}	247	8356
pH=12.4; T=150 °F RH = 100%	25.2	2.54	1.24×10^{-5}	18.25×10^{-2}	3.04×10^{15}	235	6104
Dry Heat T = 150 °F	26.0	4.70	4.45×10^{-5}	53.59×10^{-2}	8.86×10^{15}	253	8045
Freeze-Thaw, RH=100% T_{min}= -20 °F; T_{max}=120 °F	25.6	4.16	2.04×10^{-5}	38.95×10^{-2}	5.56×10^{15}	230	7913

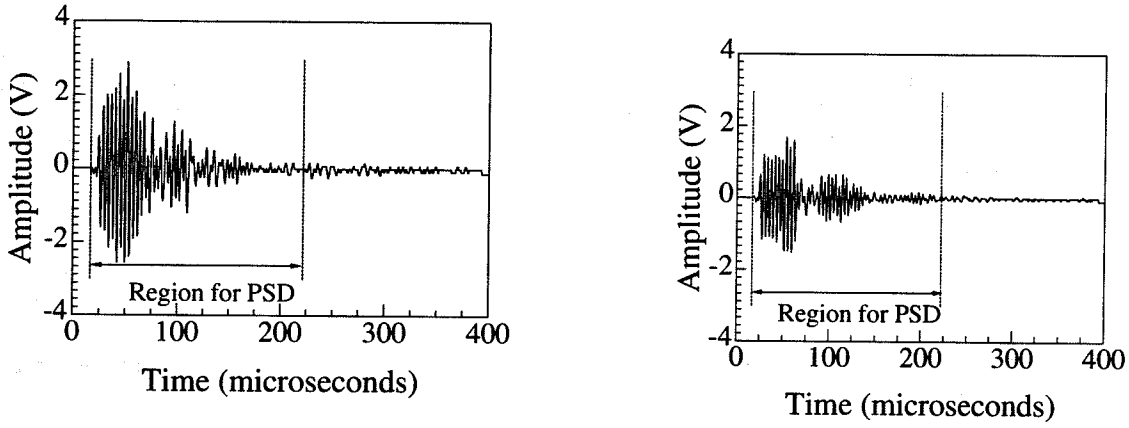

(a) Control Sample (b) Specimen with Accelerated Aging

Figure 5.5. Through-transmission signals obtained from control sample and 1000 hours aged specimen (ph =7, T = 150 °F, and RH = 100%) using 250 kHz central frequency transducers

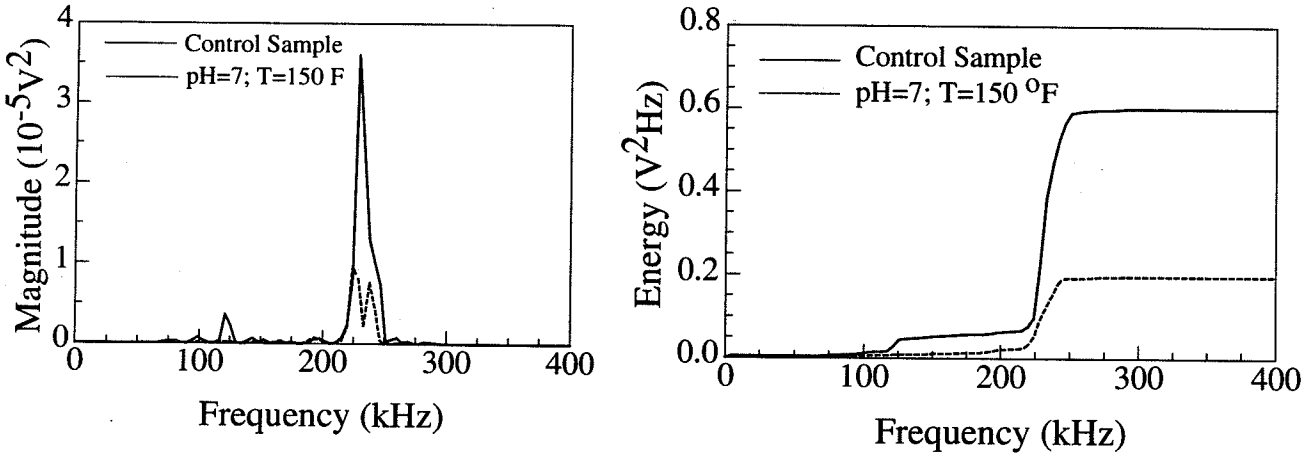

(a) PSD Plots (b) Cumulative PSD Plots

Figure 5.6. Spectral analysis of the time domain signals shown in Figure 5.5

Ultrasonic Testing of Specimens Subjected to 3000 Hours of Accelerated Environmental Aging

Concrete cylinders were wrapped with one layer of SEH 51 woven fabric and subjected to various accelerated environmental aging for 3000 hours. One specimen per aging condition was used for testing using ultrasonics. The specimens were tested using 250 kHz transducers (12.7 mm or 0.5" diameter) excited by ten cycle sine pulse with peak-to-peak amplitude of 400 volts. UT-X general purpose couplant and clamping force of 20 lb was used for obtaining consistent amplitude measurements. 100 waveforms were averaged to remove the effect of random noise. The through-transmission signals were acquired at 40 dB receiver gain and digitized at 2.5 MHz. The signals were passed through a Kaiser bandpass filter in the frequency range 225 kHz to 375 kHz to remove frequency dependent noise. Ultrasonic signals were received from fifteen different locations for each specimen to obtain the overall condition of the FRP wrapped concrete cylinders. While specimens with 1000 hours of aging showed a close pattern between the ultimate compressive strength and the average ultrasonic signal energy with ultrasonic testing at six locations per specimen, a higher number of signals were acquired for 3000 hours specimens in order to achieve a better correlation leading to mathematical equations. Since ultrasonic testing is highly localized, a large number of signals are required for obtaining

the condition of the specimen. The advantage of acquiring large number of signals will be seen in the next section where the regression analysis is discussed. The experimental results obtained from specimens subjected to 3000 hours of accelerated aging indicate affirmatively that ultrasonics can be used to detect degradation of FRP wrapped concrete members. The advantage of using spectral analysis is illustrated next using two signals. Typical signals received from the control sample and specimen subjected to freeze-thaw aging (T_{min} = -20 °F, T_{max} = 120 °F, and RH = 100%) are shown in Figure 5.7. No change is observed in the arrival time or the peak-to-peak amplitude in the time domain. The window of 512 points extracted for PSD analysis is shown in Figure 5.7 by the two vertical broken lines. The resulting PSD curves are shown in Figure 5.8(a). The cumulative PSD plot represents the total energy in an ultrasonic signal. The difference between the signals is very clear from the cumulative PSD plots shown in Figure 5.8(b). The experimental results obtained for the various specimens are shown in Table 5.3. These results represent the average value of the parameters for each specimen. The statistical method used to remove outliers and obtain these averages is described in the next section.

Table 5.3. Ultrasonic Test Results Obtained from Concrete Cylinders Wrapped with FRP and Subjected to Various Accelerated Aging Conditions for 3000 Hours

Aging Condition	Arrival Time (μs)	Peak-to-Peak Amplitude (V)	PSD Curve Parameters			
			Peak Magnitude (V^2)	Area (V^2 Hz)	Third Moment (V^2 Hz^4)	Central Frequency (kHz)
T = 73 °F	24.1	6.21	9.60×10^{-5}	142.9×10^{-2}	23.1×10^{15}	253
pH=7; T=150 °F RH = 100%	25.3	5.97	6.35×10^{-5}	103.8×10^{-2}	16.5×10^{15}	251
pH=9.4; T=73 °F RH = 100%	24.7	6.12	8.86×10^{-5}	129.5×10^{-2}	21.0×10^{15}	252
pH=12.4; T=73 °F RH = 100%	24.7	6.07	9.68×10^{-5}	132.3×10^{-2}	21.6×10^{15}	253
pH=12.4; T=150 °F RH = 100%	25.5	5.85	5.99×10^{-5}	101.1×10^{-2}	16.3×10^{15}	252
T = 150 °F	25.2	6.13	9.38×10^{-5}	130.7×10^{-2}	21.6×10^{15}	254
T_{min}= -20 °F; T_{max}=120 °F RH=100%	25.2	6.04	7.85×10^{-5}	110.6×10^{-2}	17.8×10^{15}	252

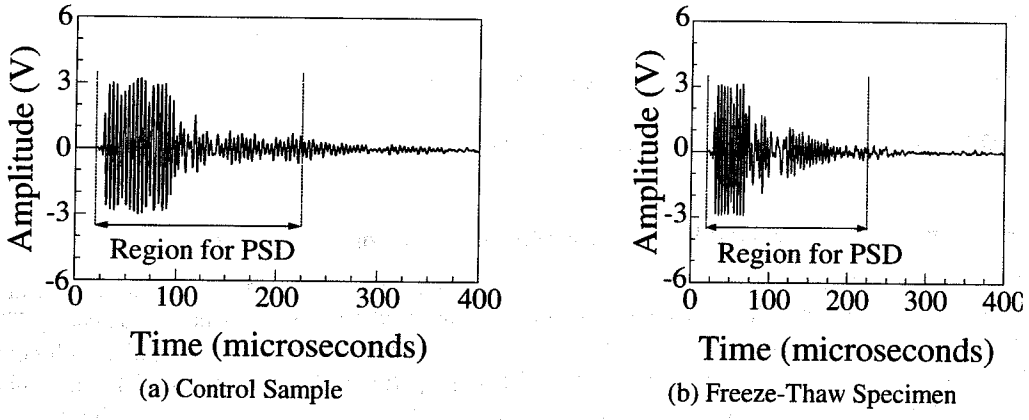

(a) Control Sample

(b) Freeze-Thaw Specimen

Figure 5.7. Through-transmission signals obtained from control sample and 3000 hours aged specimen (T_{min} = - 20 °F, T_{max} = 120 °F, and RH = 100%) using 250 kHz central frequency transducers

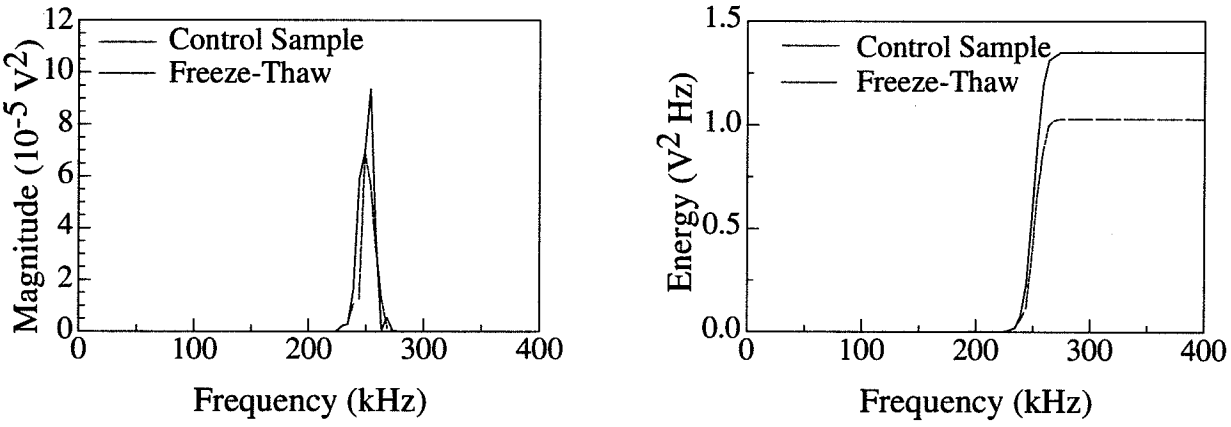

(a) PSD Plots

(b) Cumulative PSD Plots

Figure 5.8. Spectral analysis of the time domain signals shown in Figure 5.7

Nonlinear Regression Analysis

A regression analysis was performed based on the ultrasonic signal energy received from the specimens subjected to 3000 hours of aging. The large number of signals (n = 15) received from each specimen at different locations enabled a statistical analysis and obtain signals that truly represent the specimen. This statistical analysis was performed for each specimen based on the energy parameter (area under PSD curve). The outliers were removed for each specimen data by rejecting values that fell outside the probability range of 95% (i.e., average $\pm$ $t_{0.025,14}$ x standard deviation), where $t_{0.025,14}$ is equal to 2.1448 and corresponds to 14 degrees of freedom (n - 1). The parameters for the remaining signals from each specimen were averaged to obtain representative parameters for each specimen. The representative parameters for each specimen are shown in Table 5.3. The arrival time of the signals showed a very small change (up to 1 ms or 4 %) between environmentally aged specimens and the control specimen (the first specimen in Table 5.3. Loss in peak-to-peak amplitude in the time domain is also very small. This illustrates the need for frequency domain analysis for these signals. The peak magnitude, area and third moment of the PSD curves showed significant changes which helped in distinguishing the signals. The central frequency did not show any appreciable change.

Results of the static compression test on the specimens were obtained from the experimental results in Chapter 3. The ultimate compressive strength, ultimate axial strain, ultimate hoop strain and ultrasonic signal energy for each specimen are shown in Table 5.4. Loss of integrity in FRP wrap or FRP-concrete bond has a direct bearing on the ultimate compressive strength. Also, the loss in integrity has a direct influence on the ultrasonic signal energy (area under PSD) in through-transmission, as shown by the data in Table 5.4. Hence, the ultrasonic signal energy should be very closely related to the ultimate compressive strength. Different correlation analysis was conducted between the signal energy and the stress and strains obtained from each specimen. A logarithmic-logarithmic fit was found to provide good correlation. Coefficient of determination (R^2) of 0.93 was obtained between ultimate compressive strength (f_{cu}') and ultrasonic signal energy as shown in Figure 5.9. Logarithmic regression analysis between ultimate axial strain ($\varepsilon_{z,u}^{c}$) and ultrasonic signal energy resulted in a poor R^2 value of 0.41 as shown in Figure 5.10. However, the ultimate hoop strain ($\varepsilon_{\theta,u}^{c}$) showed a good logarithmic correlation with ultrasonic signal energy resulting in a R^2 of 0.95 as shown in Figure 5.11. This is because the ultimate hoop strain and the ultimate compressive strength are closely related. The high R^2 value obtained between the ultrasonic signal energy and the ultimate compressive stress or the ultimate hoop strain encouraged development of a predictive model for condition assessment of FRP wrapped compression members, which is described next.

Table 5.4. Static Test and Ultrasonic Signal Energy Results Obtained from FRP Wrapped Concrete Cylinders Subjected to 3000 Hours of Accelerated Environmental Aging

Aging Condition	Ultimate Compressive Strength, f_{cu}' (MPa)	Ultimate Axial Strain, $\varepsilon_{z,u}^{c}$	Ultimate Hoop Strain, $\varepsilon_{\theta,u}^{c}$	Ultrasonic Signal Energy (V^2Hz)
T = 73 °F	62.82	0.0184	0.0238	142.9×10^{-2}
pH=7; T=150 ° F RH = 100%	42.23	0.0123	0.0071	103.8×10^{-2}
pH=9.4; T=73 ° F RH = 100%	61.19	0.0132	0.0203	129.5×10^{-2}
pH=12.4; T=73 ° F RH = 100%	61.51	0.0220	0.0194	132.3×10^{-2}
pH=12.4; T=150 ° F RH = 100%	44.96	0.0151	0.0086	101.1×10^{-2}
T = 150 ° F	57.00	0.0169	0.0176	130.7×10^{-2}
T_{min}= -20 ° F; T_{max}=120 ° F RH=100%	49.57	0.0113	0.0091	110.6×10^{-2}

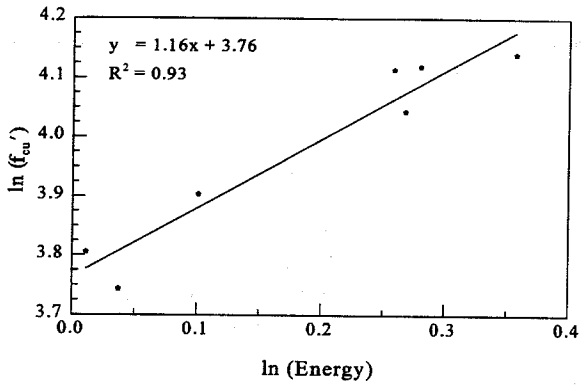

Figure 5.9. Regression plot between ultrasonic signal energy and ultimate compressive strength

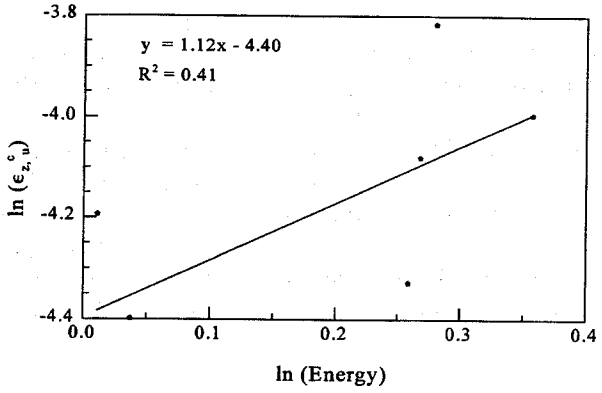

Figure 5.10. Regression plot between ultrasonic signal energy and axial strain

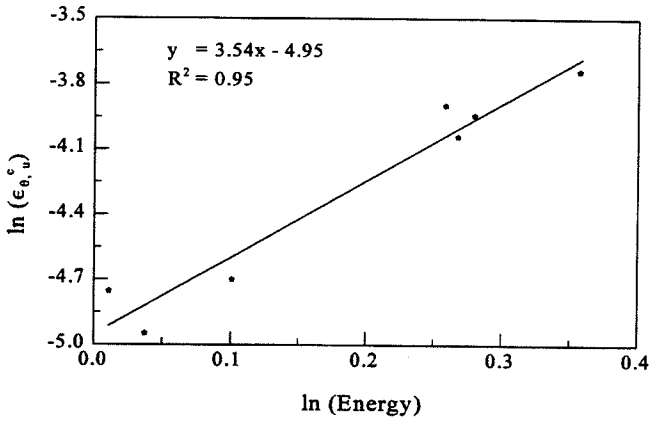

Figure 5.11. Regression plot between ultrasonic signal energy and hoop strain

Predictive Model for Condition Assessment

This section presents a generalized model and calibration procedure for prediction of ultimate compressive strength and hoop strain for FRP wrapped compression members. Based on logarithmic regression analysis, the generalized equations relating the ultrasonic signal energy (P) and the ultimate compressive strength (f) or ultimate hoop strain (ε) can be written as:

$$\ln(f) = a\ln(P) + b \tag{5.5a}$$

$$\ln(\varepsilon) = c\ln(P) + d \tag{5.5b}$$

The constants in the above equations depend on the size of the concrete member, the mechanical properties of the concrete and composite wrap, and also the properties of the ultrasonic transducers and measurement system. The constants can be evaluated if known sets of values for f, ε and P for two specimens are available. Based on Equation 5.5b, the ultimate hoop strain was predicted for each specimen for 3000 hours of accelerated environmental aging as shown in Table 5.4. The constants were obtained using ε and P for the first two specimens in Table 5.4. The discrepancy between the predicted values and the actual values for the remaining specimens are within 25%, which is acceptable for ultimate strains in materials such as concrete. Experimental errors associated with ultimate strain measurements, which are highly dependent on strain gage locations, could have contributed to this variation.

For field prediction, it may not always be possible to have two known sets of values for f, ε and P to obtain the constants in Equations (5.5a) and (5.5b). Therefore, this study proposes an alternative procedure using two cases: (a) a control specimen and, (b) a hypothetical case of total loss in structural integrity between FRP and concrete. In the latter case, the specimen will have strength (f) equivalent to that of the core concrete, and the corresponding value of P can be obtained using the procedure described later in this paper. The subscript 'o' is used for the control specimen with no loss in structural integrity between FRP wrap and concrete, and the subscript 'c' represents the condition where there is total loss in structural integrity between FRP wrap and concrete. Using the two boundary conditions in Equation (5.5a), we obtain:

$$\ln(f_o) = a\ln(P_o) + b \tag{5.6a}$$

$$\ln(f_c) = a\ln(P_c) + b \tag{5.6b}$$

Solving for the constants 'a' and 'b' and substituting in Equation (5.5a), we obtain:

$$\ln(f) = \ln(f_o) - \frac{\ln\left(\frac{f_o}{f_c}\right)}{\ln\left(\frac{P_o}{P_c}\right)} \times \ln\left(\frac{P_o}{P}\right) \tag{5.7}$$

Similarly, the equation for predicting the ultimate hoop strain (ε) can be written as:

$$\ln(\varepsilon) = \ln(\varepsilon_o) - \frac{\ln\left(\frac{\varepsilon_o}{\varepsilon_c}\right)}{\ln\left(\frac{P_o}{P_c}\right)} \times \ln\left(\frac{P_o}{P}\right) \tag{5.8}$$

Based on Equations (5.7) and (5.8), ultrasonic signal energy measurement can be used to assess the condition of FRP wrapped concrete compression members in the field. Specimen characteristics such as f_o, f_c, ε_o, and ε_c can be obtained from cast specimens or standard values based on engineer's discretion. The values of ultrasonic signal energy parameters P_o and P_c in Equations (5.7) and (5.8) are dependent upon several factors such as concrete and FRP mechanical properties, size of the compression member, spectral response of the transducers, frequency-amplitude response of the equipment used, clamping force, couplant type, etc. Therefore, it is essential to standardize the test procedure and use the same equipment and transducers for field testing. The following paragraph describes a method to estimate P_c from mean and standard deviation of the measurements for P_o. The applicability of this procedure is shown by predicting the ultimate compressive strength for the laboratory specimens at 3000 hours of accelerated environmental aging.

Static compression test provided the ultimate compressive strength of plain concrete (f_c = 40.9 MPa at 3000 hours) and control specimen (f_o = 62.8 MPa at 3000 hours). The ratio of the signal energy P_o/P_c for 3000 hours can be obtained based on the mean (P_o = 1.43 V^2Hz) and standard deviation (0.28 V^2Hz) of the signal energy for the wrapped control specimen. The value of ultrasonic signal energy for total loss of structural integrity between the FPR wrap and concrete, P_c, can be obtained using one-sided t-distribution (P_c = 1.43 - 1.771 x 0.28 = 0.93 V^2Hz, where 1.771 = $t_{0.05,13}$). Thus the ratio of the signal energy P_o/P_c is obtained as 1.5 for the 3000 hour case. Using Equation (5.7), the ultimate compressive strength were predicted for all the specimens. As shown in Table 5.5, these predictions are within 7% of the actual values obtained from static compression tests. The close prediction illustrates that the model could be successfully used for monitoring and assessing concrete compression members rehabilitated using FRP wraps. Although the model has been developed using area under PSD curve, the same can be achieved using third moment. Since the central frequency did not change appreciably, the model using third moment will perform identically to that of the model developed using area under the PSD curve.

Table 5.5. Model Prediction for Ultimate Hoop Strain and Ultimate Compressive Strength for FRP Wrapped Concrete Cylinders Subjected to 3000 Hours of Accelerated Environmental Aging

Aging Condition	Signal Energy (V^2Hz)	$\varepsilon_{\theta,u}^{c}$		f_{cu}'(MPa)	
		Predicted	Actual	Predicted	Actual
T = 73 °F	1.43	0.0237	0.0238	62.82	62.82
pH=7; T=150 °F RH = 100%	1.04	0.0071	0.0071	44.70	42.23
pH=9.4; T=73 °F RH = 100%	1.30	0.0165	0.0203	56.75	61.19
pH=12.4; T=73 °F RH = 100%	1.32	0.0175	0.0194	57.68	61.50
pH=12.4; T=150 °F RH = 100%	1.01	0.0063	0.0086	43.38	44.96
T = 150 °F	1.31	0.0170	0.0176	57.21	57.00
T_{min}= -20 °F; T_{max}=120 °F RH = 100%	1.11	0.0091	0.0091	47.94	49.57

CHAPTER 6 –IMPLEMENTATION

DEMONSTRATION PROJECT

A bridge in need of column repair was selected by West Virginia Department of Transportation, Division of Highways (WVDOT-DOH) to demonstrate the IDEA Product. The subject bridge is the Pond Creek Road Overpass Bridge carrying Interstate Route 77 in Wood County, West Virginia.

Pond Creek Road Overpass Bridge

According to the WVDOT-DOH Condition Report, six columns of two piers had vertical hairline cracking. These cracks resulted from a previous unsuccessful repair with a concrete layer after the columns were subjected to fire and the original concrete cover was lost.

A Special Provision for "Repair and Environmental Protection of Concrete Columns with Fiber Composite Wrap System (Wet Lay Up)" was drafted in collaboration with the West Virginia Department of Transportation. The Special Provision includes the following items: Materials, Handling of Materials, Design, Installation Procedure, Quality Control and Qualification Tests. The Special Provision was utilized by WVDOT-DOH for bidding the repair project.

FIELD APPLICATION OF THE FRP COMPOSITE WRAP

Three columns of the Pier 2 of the Bridge Northbound were repaired in July 1998 with the fiber composite wrap system evaluated through the IDEA Project. The other three columns were repaired with an alternative rehabilitation method using prefabricated composite cylindrical shells.

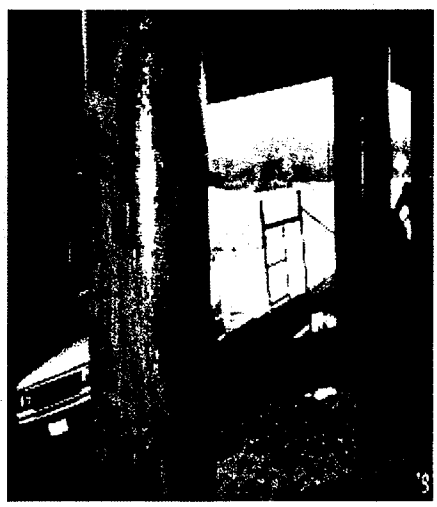

Column prior to the application of the FRP wrap

Wrap being applied to the column

Wrapped Column

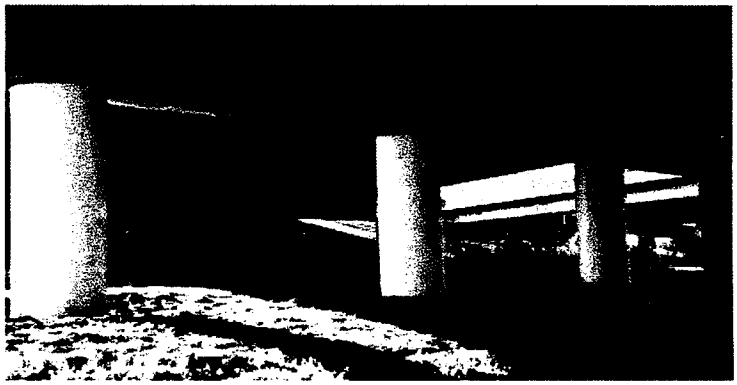

Project Completed

The field performance of the repaired concrete columns was monitored during the first year after installation and the results were satisfactory.

CHAPTER 7 – CONCLUSIONS

Conclusions of the IDEA Project

An important objective of this IDEA Project was to study the efficiency and durability of a fiber-reinforced composite wrap system for the rehabilitation of concrete structures. The composite material employed for this study was E-glass fabric reinforcement (with a small percentage of aramid in the axial direction) embedded in an epoxy resin matrix. From the experimental results obtained, several conclusions were drawn.

Efficiency of the Wrap

- Use of a composite wrap definitely enhances the strength and ductility of the plain concrete cylinder.
- Higher ultimate strength and axial strain values are obtained for concrete cylinders wrapped with more than one layer of FRP suggesting that considerable increase in strength and ductility could be achieved with an increase in jacket thickness around the column but at a higher cost.
- Visual inspection of the failed wrapped cylinders suggested that the epoxy resin used in the preparation of the composite wrap exhibited excellent bonding characteristics and served as a very good adhesive with the concrete substrate.

Effects of Environmental Conditioning on Mechanical Properties

- From the compression test results obtained on aged cylinders, it can be inferred that the composite wrap exhibits appreciable durability when exposed to liquids at ambient temperatures or dry heat. However, a considerable reduction in the strength and the ultimate strain to failure of the wrapped cylinders was observed when they were aged in liquid media at elevated temperature. This effect was independent of the pH of the liquid medium.
- Since there was no reduction in the ultimate strength of plain concrete cylinder after aging, deterioration of concrete was not responsible for the reduction in strength of the wrapped cylinder.
- It can be concluded from the tensile tests that the aging conditions affected the properties of the composite wrap by reducing its tensile strength. Exposure to high temperature and alkaline solution had a serious impact on the tensile strength of the composite. FRP specimens subjected to pH 12.4 at 73 ^{0}F or dry heat at 150 ^{0}F did not result in any significant change in their properties. A significant reduction in the modulus, though, was observed only in the case of extended freeze-thaw cycles.
- Therefore it is understood that a combined exposure to high temperature and liquid media rendered a reduction in FRP tensile strength, which was in turn responsible for lowering the compressive strength of the wrapped cylinders exposed to similar conditions.
- Results from the DMTA temperature sweep experiments suggested a possible deterioration of the epoxy polymer properties; this was indicated by a split in the tan δ curve. On the other hand, composite strips aged in alkaline solution (pH 12.4) at 150 F failed earlier when tested in tension. This suggested that the fiber composite exhibited strength reduction upon aging. Therefore, it can be concluded that degradation in the aged fiber composite is an important cause for reduction in the ultimate strength and strain of the wrapped cylinder.

Stress-Strain Response and Bi-Linear Model

- The stress-strain curve for wrapped cylinders tested under compression follow a bi-linear relationship, with the second linear region being related to the post-cracking stage i.e., after the concrete begins to fail.
- A bi-linear stress-strain model that was developed helped in evaluating the mechanistic behavior of the wrapped cylinder in terms of fundamental equations. This model predicted the ultimate strength and strain of the wrapped cylinder given the properties of the composite. The ultimate values predicted by the model were in good agreement with those obtained experimentally.

Damage Mechanics Model for Aging

- Tensile test results of aged FRP specimens were employed in a damage model to describe the damage caused due to exposure to aging conditions. This model could predict the residual strength and strain of the wrapped cylinders after 1000 hrs of aging. Damage in the FRP wrap was related to damage parameters d_1 and d_2 to identify changes in the

modulus and the ultimate strain to failure of the composite. For samples exposed to freeze-thaw, dry heat at 150 ^{0}F and alkaline solution of pH 12.4 at 73 ^{0}F, the values predicted by the model were in close conformity (within 10%) with the experimental results.

- Prediction of the ultimate strength by the model resulted in an error that was more than 10% for the aged cylinders exposed to alkaline solution of pH 12.4 at 150 ^{0}F. This suggests a possibility of another mode of failure. For example, a difference in hygrothermal expansion of the concrete and the composite may have resulted in a loss of contact between the two members at some locations. For the damage model to determine precisely the residual strength of aged wrapped cylinder, the calculations have to be modified to account for this mode of failure.

Ultrasonics Non-Destructive Evaluation Method

- The ultrasonic testing methodology proposed in this study can be successfully used for detecting degradation of structural integrity in FRP wrapped concrete compression members. The study illustrated the usefulness and reliability of spectral analysis for quantitative prediction, even though time domain analysis was not successful in characterizing the specimen degradation. The proposed methodology identifies regions of degradation based on simple parameters such as peak magnitude, area, and third moment of the Power Spectral Density curve.
- Logarithmic regression analysis showed that the area under PSD curve (i.e., ultrasonic signal energy) has a good logarithmic correlation with the ultimate compressive strength and hoop strain. However, the correlation between the ultrasonic signal energy and axial strain is poor. A model has been proposed in this study to predict the ultimate compressive stress and ultimate hoop strain from the received ultrasonic signal energy.
- The proposed methodology can be used for long-term performance monitoring of FRP bonded systems in the field. It should be noted that uniformity in testing condition and equipment is of utmost importance for consistent ultrasonic signal energy measurements. Also, field monitoring may impose additional difficulties such as larger dimensions and presence of steel reinforcement.

Recommendations

Since the reason for failure of the wrapped cylinder after aging was attributed to the degradation of the composite wrap, it would be useful to investigate the causes for failure of the composite itself. To this end, individual aging effects on the resin, fiber and fiber-matrix bond need to be further investigated. In addition, effects of aging on the concrete-matrix interface and its role in reducing the quality of the wrapped cylinder needs to be examined. Experimental results obtained and the bi-linear model derived in the present study in conjunction with future investigations in the stated issues should help recognize and further understand the deterioration problem. This would in turn assist in improving the properties of the composite wrap for rehabilitation purposes.

GLOSSARY AND REFERENCES

GLOSSARY

A_c	Cross-sectional area fraction of the concrete
A_w	Cross-sectional area fraction of the composite wrap
$d_1(t)$	Damage parameter associated with the modulus of FRP after an aging time of "t"
$d_2(t)$	Damage parameter associated with the ultimate strain to failure after aging time "t"
E_c	Modulus of elasticity of concrete
E_c^{cr}	Elastic modulus of the concrete in the post-cracking stage
$E_{c,d}^{cr}$	Damaged cracked modulus of the concrete
E_z^w	Elastic modulus of the wrap in the axial direction
E_θ^w	Modulus of elasticity of the wrap
$E_\theta^w(t)$	Modulus of the composite after exposure to aging for a time period of "t"
$f_c^{'}$	Compressive strength of plain concrete in the absence of confining pressure
$f_{cr}^{'}$	Cracking stress for the wrapped cylinder (same in axial as well as hoop direction)
$f_{cu}^{'}$	Ultimate failure stress of the wrapped cylinder
$f'_{cr,d}$	Cracking stress of the aged cylinder
$f_{cu,d}^{'}$	Ultimate strength of the cylinder after aging
G'	Storage modulus
G''	Loss modulus
m_1	Slope of the initial linear region of the bi-linear curve in the axial direction
m_2	Slope of the second linear region of the bi-linear curve in the axial direction
p_{cr}	Confining pressure at the cracking point
p_{cu}	Confining pressure at the ultimate point
$p_{cr,d}$	Value of confining pressure at cracking point for damaged specimen
$p_{cu,d}$	Confining pressure at the ultimate point for the aged cylinder

r	Radius of the concrete cylinder
t	Thickness of the composite wrap
T_g	Glass transition temperature
Tan δ	Numerical value of G''/G'
V_f	Fiber volume fraction
W_f	Fiber weight fraction
z	Axial direction
α	Proportionality parameter
$\varepsilon^c_{z,cr}$	Axial strain in concrete at the cracking point
$\varepsilon^c_{\theta,cr}$	Tensile strain in concrete at the cracking point
$\varepsilon^w_{\theta,cr}$	Cracking strain in the wrap in hoop direction
$\varepsilon^c_{z,u}$	Ultimate failure strain in concrete in the axial direction
$\varepsilon^w_{\theta,u}$	Ultimate failure strain in the wrap in the hoop direction
$\varepsilon^w_{\theta,u}(t)$	Ultimate strain of the aged composite after a time period of "t"
$\varepsilon^c_{\theta,cr,d}$	Cracked strain in hoop direction for the damaged cylinder
$\varepsilon^c_{z,cr,d}$	Cracked strain in axial direction for the damaged cylinder
$\varepsilon^c_{z,u,d}$	Ultimate axial strain in concrete after aging
ν_c	Poisson's ratio of concrete
θ	Hoop direction
σ_z	Axial compressive load on the wrapped cylinder
σ_θ	Hoop stress developed in the composite wrap due to external load on the cylinder

REFERENCES

Aminabhavi, T.M., *"Liquid Diffusion into Epoxy-Resin Composites"*, Journal of Applied Polymer Science, **35**, 1988, p.1251-1256.

Bar-Cohen, Y., Mal, A. K., and ASM Committee on Ultrasonic Inspection (1992). Ultrasonic Inspection,@ *ASM Handbook - Nondestructive Evaluation and Quality Control*, 17, 231-277.

Bavarian, B., J. Shirely, R. Ehrgott and R. Di Julio, "External Support of Concrete Structures using Composite Materials", *Fiber Composites in Infrastructure: Proceedings of the First International Conference on Composites in Infrastructure,* Tuscon, AZ, Jan 1996, p. 917-928.

Buck, S.E., D.W. Lischer and S. Nemat-Nasser, "The Combined Effects of Load, Temperature and Moisture on the Durability of E-Glass/Vinyl Ester Composite Materials", *42nd International SAMPE Symposium*, May 1997, p. 444-454.

Busel, J.P. and D. Barno, "Composites Extend the Life of Concrete Structures", 1996. http://iti.acns.nwu.edu/clear/infr/busel.html

Cheremisinoff N.P. and P.N.Cheremisinoff, Fiberglass-Reinforced Plastics Deskbook, Ann Arbor Science, Ann Arbor, MI, 1978, p. 327-328.

De Neve, B. and M.E.R. Shanahan, "Effects of Humidity on an Epoxy Adhesive", *Chemtracts-Macromolecular Chemistry*, 4, Jan/Feb 1993, p. 31-38.

Fyfe, E.R., D.J. Gee and P.B. Milligan, "Composite Materials for Rehabilitation of Civil Structures and Seismic Applications", *Second International Conference on Composites in Infrastructure*, Tuscon, AZ, Jan 1998, p. 760-771.

Halabe, U. B., and Franklin, R. (1998). Ultrasonic Signal Amplitude Measurement and Analysis Techniques for Nondestructive Evaluation of Structural Members, *Proceedings of International Symposium on Nondestructive Evaluation Techniques for Aging Infrastructure and Manufacturing*, Vol. 3396, sponsored by SPIE - The International Society for Optical Engineering, San Antonio, TX, March 30-April 2, pp. 84-94.

Halabe, U. B., GangaRao, H. V. S., Petro, S. H., and Hota, V. R. (1996). Assessment of Defects and Mechanical Properties of Wood Members Using Ultrasonic Frequency Analysis,@ *Materials Evaluation*, 54(2), 314-322.
Harper, C.A., Handbook of Plastics, Elastomers, and Composites, 3rd edn, Mc-GrawHill, New York, 1996, p. 4.30-4.31.

Harries, K.A., J. Kestner, S. Pessiki, R. Sause and J. Ricles, "Axial Behavior of Reinforced Concrete Columns Retrofit with FRPC Jackets", *Second International Conference on Composites in Infrastructure*, Tuscon, AZ, Jan 1998, p. 411-425.

Hawkins, G.F., G.L. Steckel, J.L. Bauer Jr. and M. Sultan, "Qualification of Composites for Seismic Retrofit of Bridge Columns", In Durability of Fiber Reinforced Polymer (FRP) Composites for Construction, Eds. B. Benmokrane and H. Rahman, Sherbrooke, Canada, 1998, p. 25-36.

Hobbs, D.W., Alkali-Silica Reaction in Concrete, Thomas Telford Ltd., London, 1988, p. 6.

Horne, M. R., and Duke Jr., J. C. (1993). Methods for Implementation of the AU Method/Approach,@ *Second International Conference on Acousto-Ultrasonics*, Atlanta, GA, June 24-25, 13-20.

Hollaway, L., Polymers and Polymer Composites in Construction, Thomas Telford Ltd., London 1990, p. 18-21.

Hoppel, C.P.R., T.A. Bogetti and J W. Gillespie, "Design and Analysis of Composite Wraps for Concrete Columns, *Journal of Reinforced Plastics and Composites*, 16, No. 7, 1997, p. 588-602.

Jenny, Y. J., J. M. Kennedy and D. D. Edie, "Modelling the Dynamic Response of the Continuous Fiber Composite Materials", *Fiber, Matrix and Interfaces Properties : ASTM STP 1290*, 1996, p. 67-71.

Kanatharana, J. and L.W. Lu, " Strength and Ductility of Concrete Columns Reinforced by FRP Tubes", *Second International Conference on Composites in Infrastructure*, Tuscon, Arizona, Jan 1998, p. 370-379.

Karbhari, V.M. and F. Seible, "Seismic Retrofit of Bridge Columns Using Advanced Composite Materials", *Private Communication with Dr. R. Lopez-Anido*, 1997.

Karbhari, V.M. and M. Engineer, "Effect of Environmental exposure on the External Strengthening of Concrete with Composites - Short Term Bond Durability", *Journal of Reinforced Plastics and Composites*, **15**, Dec 1996, p. 1194-1216.

Karbhari, V.M., M. Engineer and D.A. Eckel, " On the Durability of Composite Rehabilitation Schemes for Concrete: Use of Peel Test", *J. of Material Science*, **32**, Jan 1997, p. 147-156.

Kono, S., M. Inazumi and T. Kaku, "Evaluation of Confining Effects of CFRP Sheets on Reinforced Concrete Members", *Second International Conference on Composites in Infrastructure*, Tuscon, Arizona, Jan 1998, p. 343-355.

Lopez-Anido, R "Analysis and Design of Orthotropic Plates Stiffened by Laminated Beams for Bridge Superstructures," Doctoral Dissertation, Dept. of Civil and Environmental Engineering, West Virginia University, Morgantown, WV, 1995.

Lopez-Anido, R., D.T. Troutman and J.P. Busel, "Fabrication and Installation of Modular FRP Composite Bridge Deck", *Paper Submitted for ICE'98, Nashville, TN*, 1998.

Mallick, P.K., Fiber -Reinforced Composites: Materials, Manufacturing and Design, Marcel Dekker Inc., NY, 1993, p. 22-37, 50-64.

Marzi, T., U. Schroder, M. Heb and R. Kosfeld, "The Influence of Water on the Epoxy Reisn-Glass Interphases", *Materials Research Society Symposium Proceedings: Interfaces in Composites*, **170**, Nov 1989, p. 123-127.

Mirmiran, A., M. Kargahi, M. Samaan and M. Shahawy, "Composite FRP-Concrete Column with Bi-Directional External Reinforcement", *Fiber Composites in Infrastructure: Proceedings of the First International Conference on Composites in Infrastructure*, Tuscon, AZ, Jan 1996, p. 888-902.

Richart, F.E., A. Brandtzaeg and R.L. Brown (1928), "A Study of Failure of Concrete Under Combined Compressive Stresses", University of Illinois Engineering Experimental Station, Bulletin No. 185, p. 1-102.

Saadatmanesh, H., M.R. Ehsani and J. Limin, "Repair of Earthquake -Damaged RC Columns with FRP Wraps", *ACI Structural Journal*, **94**, no.2, Mar/Apr 1997, p. 206-215.

Saadatmanesh, H., M.R. Ehsani and M.W. Li, "Strength and Ductility of Concrete Columns Externally Reinforced with Fiber Composite Straps", *ACI Structural Journal*, **91**, no.4, Jul/Aug 1994, p. 434-447.

Seible, F., and V.M. Karbhari, "Seismic Retrofit of Bridge Columns Using Advanced Composite Materials," FHWA Report, 1996.

Soulier, J.P., R. Berruet, A. Chateauminois, B. Chabert and R. Gauthier, "Interactions of Fiber-Reinforced epoxy Composites with Different Salt Water Solutions Including Isotonic Liquid", *Polymer Communications*, **29**, Aug 1988, p. 243-246.

Troxell, G.E., H.E. Davis and J.W. Kelly, Composition and Properties of Concrete, 2nd edn, McGraw-Hill, NY, 1968, p. 268-288.

Wang, J. Z. and D. F. Socie, " Failure Strength and Damage Mechanisms of E-Glass/Epoxy Laminates Under In Plane Biaxial Compressive Deformation", *J. of Composite Materials*, **27**, no.1, 1993, p. 40-58.

APPENDIX A - EVALUATION OF FIBER AND COMPOSITE PROPERTIES FOR THE FIBER WRAP

The glass fabric used for wrapping of cylinders consisted of the following

G1 = vertical direction glass fibers
A = vertical direction aramid fibers
G2 = hoop direction glass fibers

Table A1. Measurements on Individual Fiber Strands Constituting the Fabric

FIBER STRANDS	Wt. per unit length g/ft.	No. of strands in 1sq. ft. area (0.0929 sq.m.)of fabric	Density of fiber material (g/cc)
G1	0.1517 (0.498g/m)	24	2.56
G2	0.6210 (2.037g/m)	133	2.56
A	0.1065 (0.349g/m)	24	1.44

Basis of calculation for the following table is an area 1 sq.ft. of the fabric.

Table A2. Specifications for the Fabric

FABRIC PROPERTIES	**G1**	**G2**	**A**	**TOTAL**
TEX	498	2038	349	
Yield,yd/lb	997	243		
Denier			3145	
Spacing, cm.	1.27	0.23	1.27	
Wt. per unit area, g/sq.m.	39.19	889.07	27.51	955.77
Vol. per unit area, cc/sq.m	15.31	347.29	19.11	381.71
Weight fr.	0.04	0.93	0.03	1
Volume fr.	0.040	0.91	0.050	1

The quantities in Table A2 are defined in the following manner:

- The nominal linear weight of the bare glass strand is expressed as *TEX.*
- TEX number is calculated as the mass in g. per 1000 m of the fibers
- Yield is a unit to measure the size of the roving. Given in linear yards per pound, yd/lb
- *1 yd/lb. = 496055 / TEX*
- Aramid fiber uses the metric measurement of Denier. It is g. per 9000m of yarn.
- *Denier = TEX * 9.0*
- The spacing is calculated as width/no of strands.
- Weight per unit area is calculated as *0.1x {TEX(g/km) /spacing (cm)}*

Calculation of fiber volume fraction for the composite wrap:

- Fiber volume fraction for 1 layer composite wrap can be calculated as follows:
- Thickness of 1 layer of = 0.039 in. (0.099 cm.)
- Volume of laminate = 990.6 cc/sq. cm
- Volume of Resin = 990.6 - 381.71 = 608.894 cc/sq. cm (where, volume of fibers per unit area of fabric is 381.71cc/sq. m. from table given above)
- Weight of Resin = 669.783 g/sq. cm
- From the above data, volume fraction for various components can be easily calculated

Components	Volume fraction
G1	0.015
G2	0.351
A	0.019
Resin	0.615
Total	1.000

Therefore in the composite considered:

- Volume fraction of the fibers (G1+G2+A) = 0.385
- Weight fraction of fibers (G1+G2+A) = 0.588

Table A3. Estimate of Fiber Volume Fraction (V_f) and Fiber Weight Fraction (W_f) in the Composite Wrap for Different Layers of Fabric

No. of layers	Effective thk. of each layer (in)	V_f	W_f
1	0.039	0.385	0.588
2	0.044	0.342	0.541
3	0.047	0.320	0.517

APPENDIX B - EXPERIMENTAL SETUP AND TEST SPECIMENS

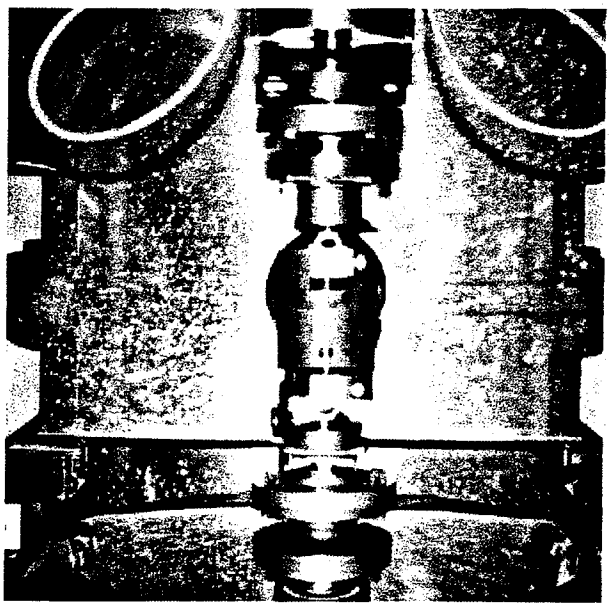

Figure B1. DMTA Test Set-Up

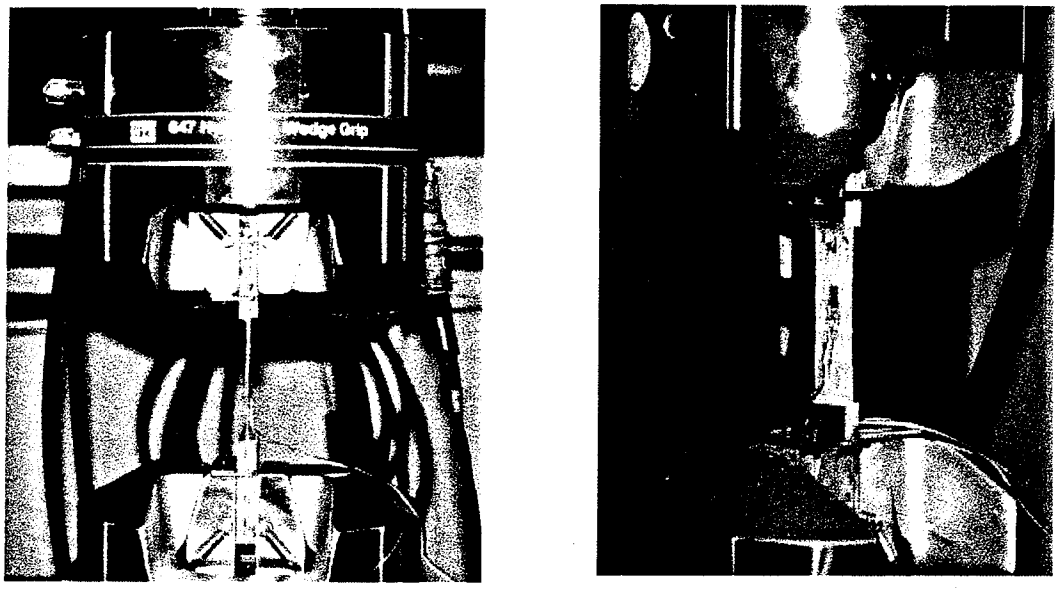

Figure B2. Tensile Test Set-Up

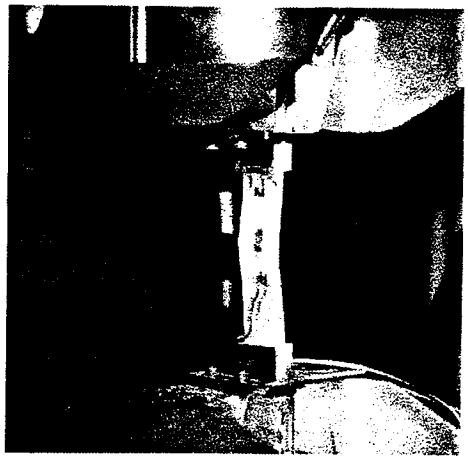

Figure B3. FRP Specimen Failed in Tension

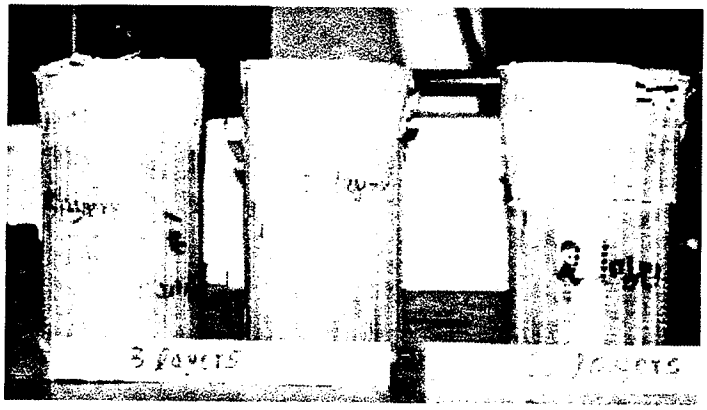

Figure B4. Failed Concrete Cylinders (2 and 3 Layers of Wrap)

APPENDIX C - EXPERIMENTAL DATA

Table C1. Compressive Strength of Control Cylinders (psi)

4" x 8" Cylinders (Plain Concrete)	6" x 12" Cylinders (Plain Concrete)	1 Layer of Wrap	2 Layers of Wrap	3 Layers of Wrap
5730	4810	8064	12781	17269
5411	4722	8445	12455	16552
5356		8300	12669	
5570				
5459				
Ave: 5505	Ave: 4766	Ave: 8270	Ave: 12635	Ave: 16910

Table C2. Aged Concrete Cylinders Without Wrap (1000 hrs)

AGING CONDITION	ULTIMATE STRENGTH, psi
pH 12.4, 73 ^{0}F	
#1	5952
#2	5586
#3	5650
Average	5729
pH 12.4, 150 ^{0}F	
#1	5586
#2	5538
Average	5562
Freeze-thaw	
#1	5904
#2	6000
#3	5459
Average	5788

Table C3. Aged Concrete Cylinders with 1 Layer of Wrap (1000 hrs)

CONDITION	f'_{cr}, psi	$\varepsilon^{c}_{z,cr}$	$\varepsilon^{w}_{\theta,cr}$	f'_{cu}, psi	$\varepsilon^{c}_{z,u}$	$\varepsilon^{w}_{\theta,u}$
pH 9.4, 73 ^{0}F						
A2	5407	0.0015	0.0003	8571	0.0255	0.0180
A3	4710	0.0016	0.0003	8169	0.0286	0.0180
Average	5059	0.0016	0.0003	8370	0.0271	0.0180
pH 12.4, 73 ^{0}F						
A9	4973	0.0011	0.0003	8230	0.0208	0.0171
A10	4846	0.0014	0.0004	8591	0.0203	0.0195
Average	4910	0.0013	0.0004	8411	0.0206	0.0183
pH 12.4, 150 ^{0}F						
A19	4896	0.0013	0.0004	5966	0.0087	0.0079
A20	4784	0.0011	0.0003	6333	0.0089	0.0099
Average	4840	0.0012	0.0004	6150	0.0088	0.0089
pH 7.0, 150 ^{0}F						
W2	4532	0.0012	0.0003	6548	0.0130	0.0103
W3	4287	0.0013	0.0003	5570	0.0091	0.0081
W4	4830	0.0015	0.0003	6142	0.0133	0.0085
Average	4550	0.0013	0.0003	6087	0.0118	0.0090
Dry Heat, 150 ^{0}F						
D2	4852	0.0015	0.0006	8174	0.0199	0.0161
D3	4709	0.0015	0.0004	7979	0.0192	0.0164
Average	4781	0.0015	0.0005	8077	0.0196	0.0163
Freeze-thaw						
Ft2	6062	0.0014	-	7913	0.0123	0.0140
Ft3	5621	0.0014	0.0002	8189	0.0195	0.0147
Average	5842	0.0014	0.0002	8051	0.0159	0.0144

Table C4. Aged Concrete Cylinders with 1 Layer of Wrap (3000 hrs)

CONDITION	f'_{cr}, psi	$\varepsilon^{c}_{z,cr}$	$\varepsilon^{w}_{\theta,cr}$	f'_{cu}, psi	$\varepsilon^{c}_{z,u}$	$\varepsilon^{w}_{\theta,u}$
Control						
C1	5943	0.0150	-	9107	0.0130	-
C2	5817	0.0160	0.0005	9418	0.0184	0.0239
C3	5826	0.0130	0.0003	8927	0.0165	0.0174
Average	5862	0.0147	0.0004	9151	0.0160	0.0207
pH 9.4, 73 ^{0}F						
A1	5979	0.0013	0.0004	8872	0.0137	0.0203
A4	5983	0.0015	0.0004	8917	0.0148	0.0194
Average	5981	0.0014	0.0004	8895	0.0143	0.0199
pH 12.4, 73 ^{0}F						
A8	5947	0.0015	0.0004	8917	0.0220	0.0194
Average	5947	0.0015	0.0004	8917	0.0220	0.0194
pH 12.4, 150 ^{0}F						
A21	4755	0.0022	0.0005	6518	0.0151	0.0086
A23	4750	0.0015	0.0004	5951	0.0073	0.0067
Average	4753	0.0019	0.0005	6235	0.0112	0.0077
pH 7.0, 150 ^{0}F						
W1	4576	0.0015	0.0003	6122	0.0123	0.0071
W5	5026	0.0014	0.0003	5981	0.0059	0.0055
Average	4801	0.0015	0.0003	6052	0.0091	0.0063
Dry Heat, 150 ^{0}F						
D1	4685	0.0013	0.0003	8264	0.0169	0.0176
D4	4534	0.0014	0.0004	8054	0.0164	0.0163
Average	4610	0.0014	0.0004	8159	0.0167	0.0169
Freeze-thaw						
Ft4	5626	0.0016	0.0004	7171	0.0138	0.0104
Ft5	5727	0.0016	0.0004	7186	0.0113	0.0091
Average	5677	0.0016	0.0004	7179	0.0126	0.0098

Table C5. Aged Concrete Cylinders with Without Wrap (3000 hrs)

AGING CONDITION	ULTIMATE STRENGTH, psi
Control	
#1	5761
#2	5554
#3	5829
Average	5715
pH 12.4, 73 ^{0}F	
#1	5825
#2	5443
#3	5554
Average	5607
pH 12.4, 150 ^{0}F	
#1	5777
#2	5523
#3	5889
Average	5730
Freeze-thaw	
#1	5825
#2	5729
#3	5506
Average	5687

Table C6. Aged Concrete Cylinders with 1 Layer of Wrap (8000 hrs)

CONTROL							
	f'_{cu}, psi		$\varepsilon^{w}_{\theta,u}$		$\varepsilon^{c}_{z,u}$		
C1	8560		0.0187		-		
C2	8786		0.0193		0.0198		
C3	8952		0.0187		0.0160		
Average	8766		0.0189		0.0179		
AGING CONDITIONS							
	f'_{cu}, psi	$\varepsilon^{w}_{\theta,u}$	$\varepsilon^{c}_{z,u}$		f'_{cu}, psi	$\varepsilon^{w}_{\theta,u}$	$\varepsilon^{c}_{z,u}$
pH 9.4, 73 ^{0}F				Dry Heat, 150 ^{0}F			
A5	8305	0.0130	0.0146	D5	8907	-	0.0195
A6	8435	0.0200	-	D6	8641	-	-
A7	7818	0.0168	0.0137	D7	9223	0.0216	0.0176
Average	8186	0.0166	0.0142	Average	8924	0.0216	0.0186
pH 12.4, 73 ^{0}F				Freeze-thaw			
A12	8044	0.0168	0.0174	Ft1	6754	0.0076	0.012
A14	8194	0.0160	0.0184	Ft7	6839	0.0076	0.011
Average	8119	0.0164	0.0179	Average	6797	0.0076	0.012
pH 12.4, 150 ^{0}F				pH 7.0, 150 ^{0}F			
A24	6227	0.0051	-	W8	5921	0.0062	0.0090
A25	5989	0.0043	0.0068	W5	5580	-	0.0041
Average	6108	0.0047	0.0068	W6	5404	0.0052	0.0045
				Average	5635	0.0057	0.0058

Table C7. Tensile Tests Data

SPECIMEN	thk (in.)	Breaking Stress, psi	Modulus, msi	Ultimate Strain
Control				
C1	0.049	55578	3.23	0.0189
C2	0.061	51787	2.71	0.0202
C3	0.057	52003	2.77	0.0209
C4	0.056	51293	2.84	0.0183
Average	0.056	52665	2.89	0.0196
Control: Load ⊥ fiber direction				
T1	0.061	4402	0.697	0.0085
T2	0.062	4335	0.679	0.0082
Average	0.062	4369	0.688	0.0084
pH 12.4, 150^{0}F				
A1	0.057	27786	2.78	0.0103
A2	0.055	30151	2.91	0.0106
A3	0.061	32284	2.49	0.0129
Average	0.057	30074	2.73	0.0113
pH 12.4, 73 ^{0}F				
L1	0.060	50227	2.82	0.0189
L2	0.059	49512	2.89	0.0183
L3	0.060	49430	2.47	0.0210
L4	0.058	52164	2.81	0.0201
Average	0.059	50333	2.75	0.0196
Dry Heat, 150 ^{0}F				
D1	0.061	54659	2.96	0.0205
D2	0.061	56241	2.68	0.0226
D3	0.061	54651	2.70	0.0217
Average	0.061	55184	2.78	0.0216
Freeze-thaw				
Ft1	0.059	43058	2.45	0.0178
Ft2	0.056	51540	2.58	0.0202
Ft3	0.065	38909	2.42	0.0163
Average	0.060	44502	2.48	0.0181